Sodium Channel *Scn8a* as a Target for Antiepileptic Therapy

by

Sophie F. Hill

A dissertation submitted in partial fulfillment
of the requirements for the degree of
Doctor of Philosophy
(Neuroscience)
in the University of Michigan
2023

Doctoral Committee:

Professor Miriam H. Meisler, Co-Chair
Professor Sally Camper, Co-Chair
Professor Roman Giger
Professor Lori Isom
Associate Professor Kenneth Kwan

Sophie F. Hill

sfhill@umich.edu

ORCID iD: 0000-0002-8331-9812

© Sophie F. Hill 2023

To my dog Jordan,

who helped me through the hardest days of the pandemic. RIP.

ACKNOWLEDGEMENTS

First and foremost, I want to thank Miriam. From the first day of my rotation, you gave me just the right amount of guidance and independence. I've learned a lot about how to design and perform experiments, and especially about the how to present my data in talks and in papers. Now, knowing that I'm going to stay in the sodium channel field, I feel very lucky to have studied with someone who's been there since the very beginning. I look forward to our future collaborations!

My committee members, Sally Camper, Roman Giger, Lori Isom, and Ken Kwan, have all given extremely helpful feedback on my experiments. After each of our meetings, Miriam and I have always said that I'm lucky to have such a great group to guide my progress. I also want to thank our collaborators at the University of Michigan, especially the labs of Tony Antonellis and Jacob Kitzman. As the only grad student in Miriam's lab for the first four years of my PhD, our joint lab meetings helped me feel more at home in the Department of Human Genetics. The administrative teams in the Neuroscience Graduate Program and Human Genetics have also provided me with a lot of support.

I also want to thank the other members of the Meisler lab. Guy, who taught me how to do ICV injections on my first day in the lab and has been a resource in many of my subsequent experiments; Wenxi, my sodium channel buddy; Young, who always knows where to find the reagent I need, even if it's buried among 20-year-old samples;

and Quinn, who has made me NOT the youngest person in the lab! I've been lucky to work closely with two amazing undergrads, Sanjna Chalasani and Aparna Sumanth. Both Sanjna and Aparna contributed to many of the experiments in this dissertation, especially with mouse genotyping. Sanjna also spent two years helping me monitor my mice for seizures, a thankless and boring task!

Finally, I want to thank my friends and family, who have made my PhD much more enjoyable – especially during the early months of the pandemic. To my cohort and other friends I've made while in graduate school, I want to say thank you and good luck! I'm sad to be leaving Michigan after 9 years, but I'm sure we'll stay in touch!

TABLE OF CONTENTS

LIST OF FIGURES

LIST OF TABLES

LIST OF APPENDICES

ABSTRACT

The voltage-gated sodium channel Nav1.6 is a key regulator of neuronal excitability. Gain-of-function variants of *SCN8A*, the gene encoding Nav1.6, cause developmental and epileptic encephalopathy (DEE). *SCN8A*-DEE is characterized by drug-resistant seizures, movement disorders, and intellectual disability.

We hypothesized that reducing expression of *SCN8A* would compensate for gain-of-function mutations. We developed an antisense oligonucleotide (ASO) that reduces expression of mouse *Scn8a* transcript. In *SCN8A*-DEE mice, neonatal administration of the *Scn8a* ASO delayed seizure onset and prolonged lifespan. However, people with *SCN8A*-DEE can only be treated after they begin to have seizures and receive a diagnosis. I therefore also administered the *Scn8a* ASO after the onset of seizures. The ASO reduced seizure frequency and prolonged survival from less than two months to more than one year after seizure onset.

Due to its important role in the generation of action potentials, we hypothesized that reducing *SCN8A* expression could also be therapeutic in epilepsy caused by mutation of other genes. I administered the *Scn8a* ASO to epilepsy models caused by mutation of the sodium channel gene *Scn1a*, the potassium channel genes *Kcna1* and *Kcnq2*, and the synaptic protein LGI1. The *Scn8a* ASO prolonged survival in all four models. Notably, the *Scn1a* mutant mice were completely rescued by a single, neonatal dose. I also tested reduction of potassium channel gene *Kcnt1* in *Scn1a* and *Scn8a*

mutants. The *Kcnt1* ASO significantly prolonged survival of both models, though to a lesser extent than the *Scn8a* ASO. These results suggest that targeting key ion channel genes, including *Scn8a* and *Kcnt1*, may be a generalizable treatment for epilepsies of diverse etiologies.

Despite the prominent role of ion channel genes in causing epilepsy, little is known about the transcriptional consequences of ion channel mutations. I performed single-nucleus RNA-sequencing on the hippocampus of *Scn8a* mutant mice. Before the onset of seizures, I detected few transcriptional changes within any cell type. After ten weeks of chronic seizures, dentate gyrus granule cells exhibited the most transcriptional changes, suggesting that seizures may specifically affect this cell type. I also detected expression of the voltage-gated sodium channels in oligodendrocyte precursor cells and a possible increase in the number of hippocampal oligodendrocytes in the *Scn8a* mutant mice, which may point to a role for sodium channels in oligodendrocyte differentiation. My results suggest that oligodendrocytes and dentate gyrus granule cells may play a role in the pathology of *SCN8A*-DEE.

Chapter I

Introduction[1]

A brief history of *SCN8A*

In 1958, the *med* (motor endplate disease) allele arose as a spontaneous mouse mutation at the University of Edinburgh (Fig. 1-1) (Duchen, 1970; Green *et al.*, 1981). Mice homozygous for the *med* allele develop a progressive paralysis phenotype that is lethal by three weeks of age (Green *et al.*, 1981). The underlying mechanism was not identified until 1995, when the Meisler lab discovered the causative gene, *Scn8a*, and identified its sequence similarity with known voltage-gated sodium channel alpha subunits (Burgess *et al.*, 1995; Kohrman *et al.*, 1996). The human ortholog, *SCN8A*, was cloned three years later (Plummer *et al.*, 1998).

Based on the mouse phenotype, researchers expected that human mutation of *SCN8A* would primarily cause motor dysfunction (Meisler *et al.*, 2001). Indeed, the first human *SCN8A* mutation was discovered in a screen for ataxia (Trudeau *et al.*, 2006). However, the most common phenotype associated with *SCN8A* was not discovered until 2012, when whole-genome sequencing of a family quartet identified a *de novo* mutation in *SCN8A* that caused a severe form of epilepsy (Veeramah *et al.*, 2012). Since then, genetic testing has identified hundreds of *SCN8A* mutations that cause a

[1] This chapter was adapted from: Meisler MH, Hill SF, Yu W. Sodium channelopathies in neurodevelopmental disorders. *Nature Reviews Neuroscience*, 2021.

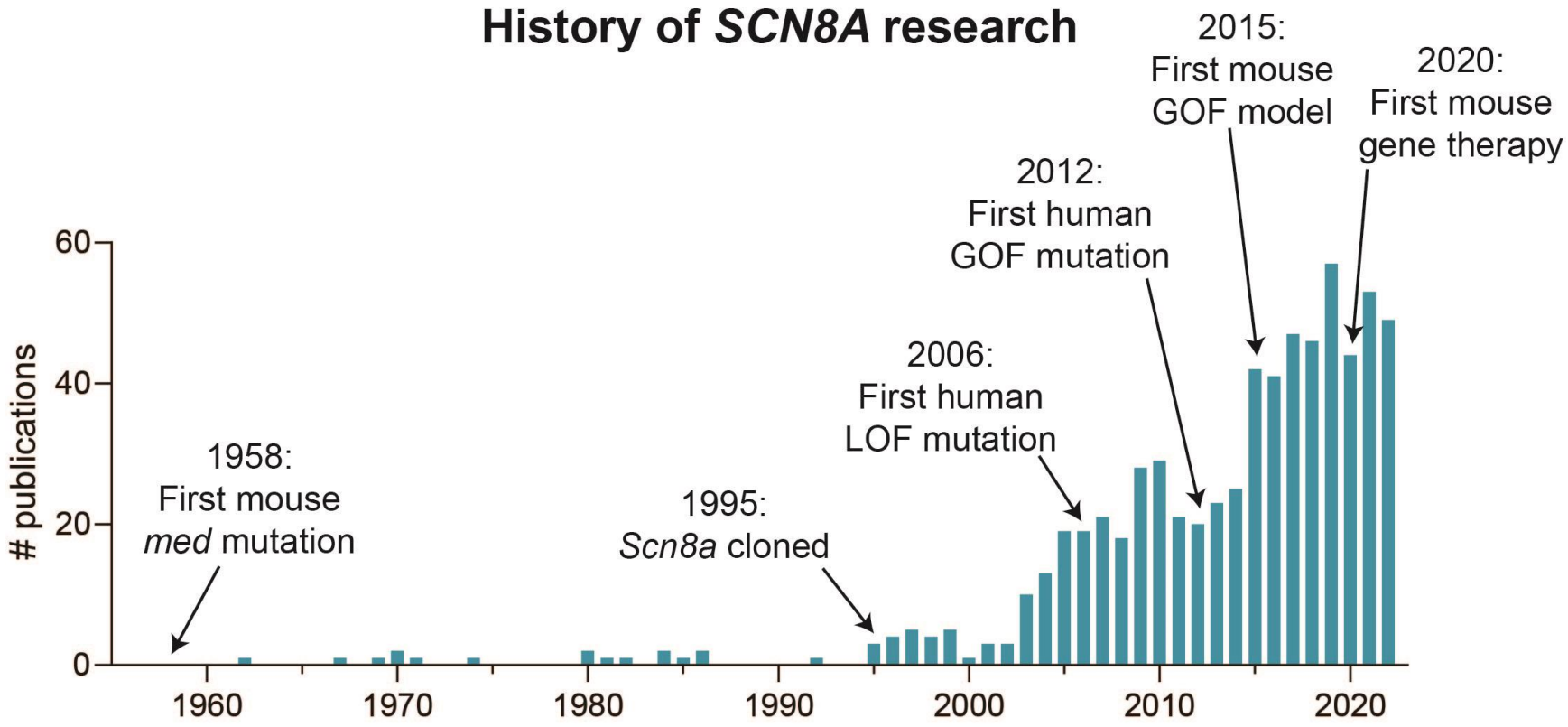

Figure 1-1. History of *SCN8A* research. The first *Scn8a* mouse mutation was discovered in breeding stocks at the University of Edinburgh in 1958. The mouse gene was cloned in 1995. Since then, research related to *SCN8A* has exploded. The annual number of publications in Pubmed with *SCN8A* as a search term is shown. Arrows indicate papers from the Meisler lab, except for the 1958 mouse mutant. GOF, gain of function; LOF, loss of function. Inspired by Figure 2 from (Knowles *et al.*, 2022a).

spectrum of disease ranging from mild intellectual disability to developmental and epileptic encephalopathy (Gardella *et al.*, 2018; Meisler *et al.*, 2021; Johannesen *et al.*, 2022). Now, precision therapies for *SCN8A* epilepsy are on the horizon.

My thesis explores several aspects of *Scn8a* epilepsy in the mouse: the efficacy of reducing *Scn8a* expression to treat *Scn8a* epilepsy (Chapters II & III) and other genetic epilepsies (Chapter IV), the efficacy of reducing *Kcnt1* expression to treat *Scn8a* epilepsy (Chapter V), and the effects of an *Scn8a* mutation on gene expression in the hippocampus (Chapter VI). In this chapter, I introduce the voltage-gated sodium channel genes, their function in neurons, and their associated diseases.

The voltage-gated sodium channel gene family

The voltage-gated sodium channel (VGSC) α-subunit gene family is comprised of ten genes in the human genome (Fig. 1-2A). The three sodium channel genes expressed at a high level in neurons of the central nervous system are shown in blue (Fig. 1-2A). The gene family was generated by whole genome duplication events during early chordate evolution generating four sodium channel loci, followed by tandem gene duplications within the loci on chromosomes 2 and 3 later in vertebrate evolution (Plummer and Meisler, 1999; Zakon, 2012). The channels are key players in the initiation and propagation of action potentials, the unit of electrophysiological activity in neurons. Sodium channels are among the most highly evolutionarily conserved genes in the human genome, and retain regions of significant sequence identity to invertebrate and prokaryotic sodium channels.

Deviations from normal channel function have major clinical consequences that

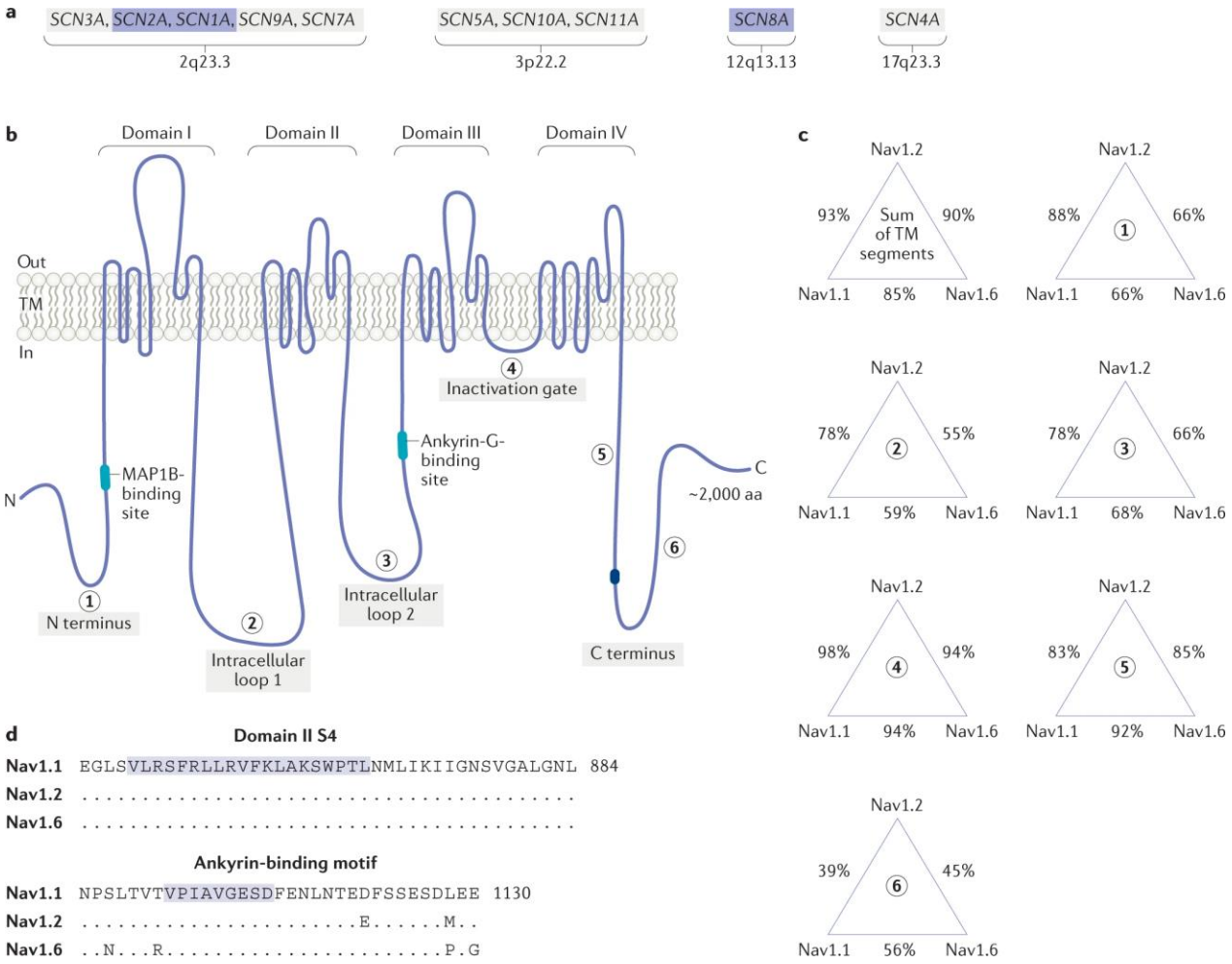

Figure 1-2. Evolutionary conservation of human sodium channel genes. (A) Chromosomal locations (2q23.3, 3p22.2, 2q13.13 and 17q23.3) of human voltage-gated sodium channel genes. The channels with high expression in the adult CNS (blue) are covered in this review. (B) The voltage-gated sodium channel α subunit is composed of four transmembrane (TM) domains separated by intracellular loops: 1, amino terminus (N-terminus); 2, cytoplasmic loop 1; 3, cytoplasmic loop 2; 4, inactivation gate; 5, proximal half of carboxy terminus (C-terminus); 6, distal half of C-terminus. (C) Percent conservation of amino acid (aa) sequence in the protein domains of *SCN1A* (Nav1.1), *SCN2A* (Nav1.2), and *SCN8A* (Nav1.6). Labels refer to domains in panel B. (D). Examples of regions of high sequence conservation in transmembrane segment 4 (S4) of domain II (top, highlighted) and around the nine-residue ankyrin-binding motif (bottom, highlighted) (Lemaillet *et al.*, 2003). Dots represent amino acid identity of Nav1.2 and Nav1.6 to the indicated sequence of Nav1.1. Figure from Meisler *et al*., 2021.

include seizures, intellectual disability, behavioral abnormalities, and movement disorders. The genes *SCN1A* (Nav1.1), *SCN2A* (Nav1.2), and *SCN8A* (Nav1.6) are responsible for most of the known neurological sodium channelopathies. In one survey of 8,565 individuals with epilepsy and neurodevelopmental disorders, 5% carried mutations in one of these three genes (Lindy *et al.*, 2018). *SCN3A* (Nav1.3) has recently been associated with rare neurodevelopmental disorders (Smith *et al.*, 2018; Zaman *et al.*, 2020).

The structure of the VGSC α-subunit is represented in Fig. 1-2B. The protein includes four homologous domains, each containing six transmembrane segments with high sequence conservation, two large cytoplasmic loops with lower sequence conservation, a highly conserved inactivation gate, and cytoplasmic N-terminal and C-terminal domains. Two cryo-EM structures of human Nav1.6 have recently been published (Fan *et al.*, 2023; Li *et al.*, 2023b). The domains assemble in three dimensions with transmembrane segments 5-6 (S5-6) in the center, forming a pore. Within each domain, S4 (also called the voltage sensor) contains three to five positively charged amino acids and responds to changes in transmembrane voltage.

Consistent with their more recent divergence, *SCN1A* and *SCN2A* are more closely related to each other than to *SCN8A* (Fig. 1-2C). The 24 transmembrane (TM) segments exhibit 93% amino acid sequence identity between *SCN1A* and *SCN2A* but only 85% and 90% identity to *SCN8A*. An example of an invariant TM segment is shown in Fig. 1-2D. In the more divergent N-terminus, there is 88% sequence identity between *SCN1A* and *SCN2A* but only 66% identity to *SCN8A*. Despite extensive sequence conservation, the channels have diverged in function and regulation, and each of the

three genes is essential in mammals. Evolutionary conservation offers a clue to functional impact, and variation at residues that are identical in all three channels (e.g., Fig. 1-2D) tend to be more deleterious than variants at residues that have diverged.

Physiology of neuronal VGSCs

During a neuronal action potential, depolarization of the membrane causes the voltage sensors to move towards the extracellular surface, triggering the pore to open (Xu *et al.*, 2019). The resulting influx of sodium ions causes further membrane depolarization: the rising phase of the action potential. After roughly 1-5 milliseconds, the channel undergoes fast inactivation. In this state, the pore remains open, but sodium ions cannot enter the cell because the inactivation gate physically blocks the intracellular side of the pore. When the resting membrane potential is restored, the voltage sensors return to their resting positions and the channel resumes the closed, resting, conformation. Changes in this progression underlie the pathogenesis of sodium channel mutations.

Each α-subunit alone can form a pore (Fan *et al.*, 2023; Li *et al.*, 2023b), but recent evidence suggests that the VGSCs may operate as dimers (Clatot *et al.*, 2017; Clatot *et al.*, 2018). The VGSC complex also includes β-subunits, which function as cell-adhesion molecules and interact with the pore-forming channels to modulate channel activity (Bouza and Isom, 2018).

Electrophysiological measurements used to assess the functional effects of patient mutations are shown in Fig. 1-3. Peak or transient current refers to the maximal inward flow of sodium ions at the beginning of the action potential. The small remaining

current at 100 msec after the peak is defined as ‘persistent current’ (Fig. 1-3A). The voltage dependence of channel activation describes channel opening (Fig. 1-3B), and the voltage dependence of inactivation describes channel closing (Fig. 1-3C); these are altered by many pathogenic mutations. 'Resurgent current’ contributes to repetitive neuronal firing and is generated when channels open during repolarization after an action potential (Fig. 1-3D).

Partial or complete loss of function (LOF) mutations are usually recognized by reduction or elimination of peak current density. Gain-of-function (GOF) mutations cause changes in other parameters. Increased persistent current, due to impaired stability of the closed channel conformation, is frequently associated with seizures. Nav1.6 generates a higher proportion of persistent and resurgent current than Nav1.1 or Nav1.2 in many types of neurons (Raman *et al.*, 1997; Pan and Cummins, 2020). Deletion of *Scn8a* in forebrain excitatory neurons causes Nav1.2 to replace Nav1 at the AIS, resulting in reduced persistent current (Katz *et al.*, 2018).

A hyperpolarizing shift in the voltage dependence of activation leads to premature channel opening and excess neuronal firing. Conversely, depolarizing shifts in the voltage dependence of activation reduce channel activity. Delayed channel inactivation can also contribute to excess neuronal activity.

Categorizing variants as LOF or GOF can be difficult because many variants affect more than one aspect of channel physiology. For example, the *SCN8A* variant p.N1768D causes a decrease in peak current density but a large increase in persistent current and a depolarizing shift in the voltage dependence of inactivation (Veeramah *et al.*, 2012). A more appropriate classification system might be to examine the effect of a

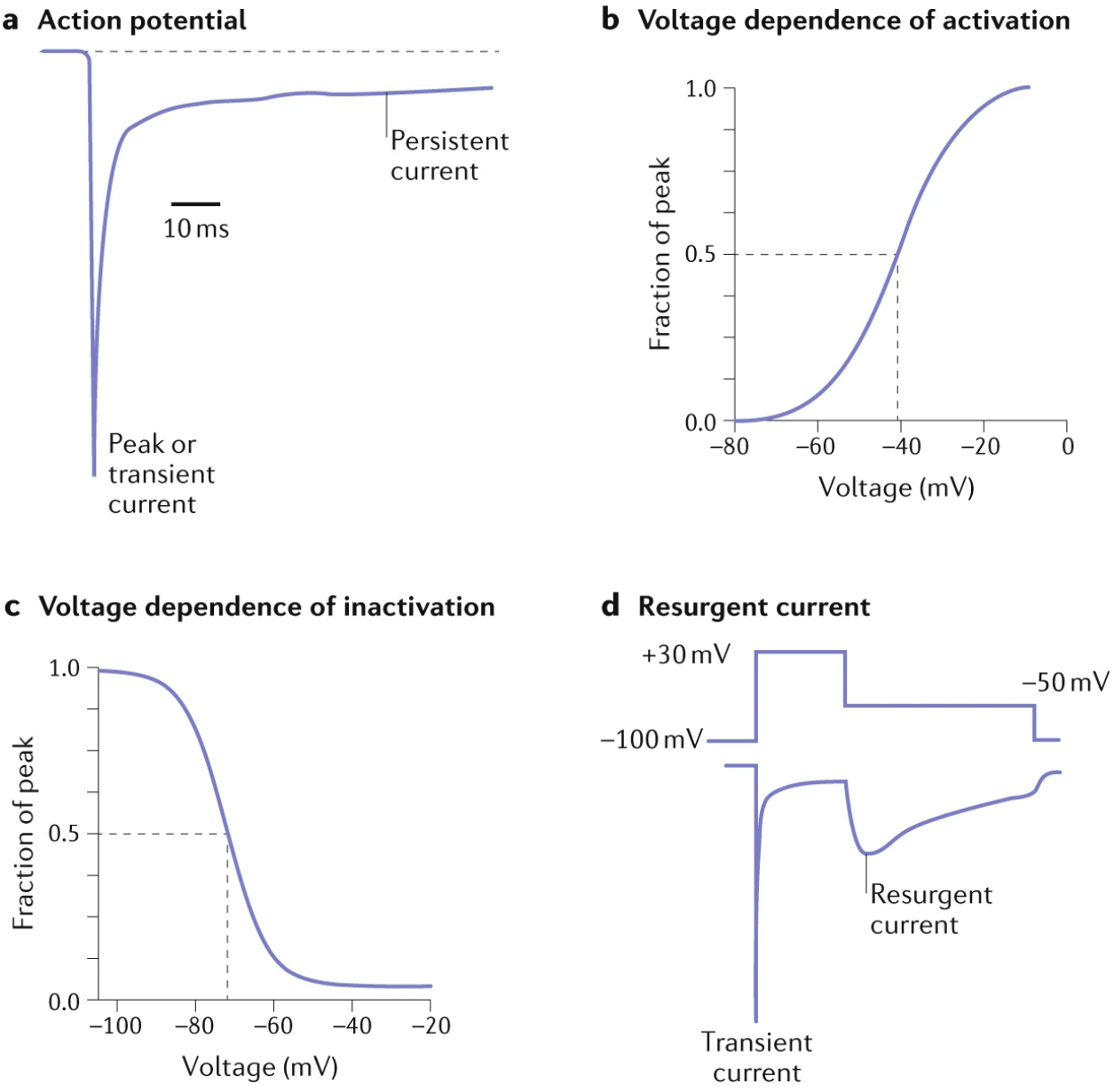

Figure 1-3. Channel properties frequently used to characterize patient mutations. Five parameters used to characterize abnormal function of mutated channels are represented. Typical, wildtype function is depicted. (A) Peak and persistent current. (B) Voltage dependence of channel activation. (C) Voltage dependence of channel inactivation. (D) Resurgent current. Vertical lines in B and C mark the voltage at which 50% of channels are active. Figure from Meisler *et al*., 2021.

mutation on neuronal firing. The *SCN8A* p.N1768D variant causes spontaneous firing of transfected rat hippocampal neurons, suggesting a net GOF effect.

Experimental measurements are usually performed on transfected cells, including kidney-derived HEK cells, neuroblastoma-derived ND7/23 cells, and cultured primary neurons. The choice of cell type can influence variant classification because VGSC activity is modulated by other proteins like the sodium channel β-subunits and calmodulin, many of which are only expressed in neurons (Smith *et al.*, 1998; Rush *et al.*, 2005; Calhoun and Isom, 2014). There is even evidence that the same VGSC may have different electrophysiological properties in different parts of the neuron (Sole *et al.*, 2019). In one recent study of Nav1.6 variants, combined analysis in neuroblastoma and primary neuronal cultures was more consistent than either alone in predicting clinical consequences (Liu *et al.*, 2019). Animal models provide access to the effects of mutations in different types of neurons, but *in vivo* models are limited to a small number of mutations. Recent work in patient-derived iPSCs makes it possible to assess the function of mutant channels in the context of the patient's individual genetic background, and the iPSCs can be differentiated into neuronal subtypes of interest (Tidball *et al.*, 2020).

Subcellular localization of Nav1.6

In neurons, VGSCs are concentrated at the axon initial segment (AIS). Action potentials are initiated at the AIS and propagated in two directions. Forward propagation from the distal AIS (further from the cell body) initiates conduction down the axon to the nerve terminus. Nav1.6 is the major channel in the distal AIS of adult neurons (Whitaker

et al., 2001; Boiko *et al.*, 2003; Van Wart *et al.*, 2007; Royeck *et al.*, 2008; Hu *et al.*, 2009; Lorincz and Nusser, 2010; Tian *et al.*, 2014; Akin *et al.*, 2015; Akin *et al.*, 2016; Sole *et al.*, 2019). One experiment employing electron microscopy with immunogold labeling estimated that the concentration of $Na_v1.6$ is 40-fold higher at the AIS than in the soma and proximal dendrites (Lorincz and Nusser, 2010). The hyperpolarized voltage dependence of Nav1.6 contributes to the initiation of action potentials at the distal AIS; in the absence of Nav1.6, the threshold for initiation of action potentials is increased (Raman *et al.*, 1997; Maurice *et al.*, 2001; Van Wart and Matthews, 2006; Mercer *et al.*, 2007; Royeck *et al.*, 2008; Hu *et al.*, 2009; Osorio *et al.*, 2010; Katz *et al.*, 2018).

The proximal AIS is occupied by Nav1.1 or Nav1.2, depending on cell type and stage of development (Boiko *et al.*, 2003; Hu *et al.*, 2009; Lorincz and Nusser, 2010; Yamagata *et al.*, 2023). Backpropagation from the proximal AIS to the soma and dendrites modulates synaptic strength and mediates learning and memory.

The AIS localization of Nav1.6 is mediated by interaction with structural proteins, including Ankyrin G (AnkG) and MAP1B. AnkG binds a conserved 9-residue motif in intracellular loop 2 of the VGSCs (Fig. 1-2B) (Jenkins and Bennett, 2001; Lemaillet *et al.*, 2003; Gasser *et al.*, 2012). AnkG binding is sufficient to localize proteins to the AIS and nodes of Ranvier (Lemaillet *et al.*, 2003; Gasser *et al.*, 2012). Mutation of the ankyrin binding motif prevents AIS localization (Gasser *et al.*, 2012; Akin *et al.*, 2015; Sole *et al.*, 2019; Liu *et al.*, 2022a).

The cytoplasmic N-terminus of Nav1.6 contains a binding site for the microtubule binding protein MAP1B (Nav1.6: VAVP, residues 77-80, Fig. 1-2B) (O'Brien *et al.*,

2012b). The corresponding region of Nav1.1 differs by two amino acids (Nav1.1: VSEP) and does not interact with MAP1B (O'Brien *et al.*, 2012b). It is unclear whether Nav1.2 is bound by MAP1B; its binding site differs by only one amino acid from Nav1.6 (Nav1.2: VSVP). Interaction with MAP1B is not required for trafficking to the AIS, but stabilizes Nav1.6 in the AIS membrane by preventing rapid endocytosis, (Sole *et al.*, 2019). The low level of Nav1.6 in the somatodendritic compartment is not affected by loss of AnkG or MAP1B binding sites, suggesting that somatodendritic localization is mediated by a different mechanism (Gasser *et al.*, 2012; Akin *et al.*, 2016; Sole *et al.*, 2019).

The concentration of sodium channels at the nodes of Ranvier mediates saltatory conduction in myelinated neurons. Before myelination begins, or in mature unmyelinated axons, Nav1.2 is expressed uniformly along the whole axon (Westenbroek *et al.*, 1989; Boiko *et al.*, 2001; Whitaker *et al.*, 2001; Liu *et al.*, 2022a). As myelination proceeds, Nav1.6 replaces Nav1.2 at the nodes of Ranvier (Boiko *et al.*, 2001; Liu *et al.*, 2022a).

Recent evidence suggests that the localization of Nav1.2 to the unmyelinated axon is driven by a 36-amino acid sequence in intracellular loop 1 (ICL1) (Liu *et al.*, 2022a). A chimeric Nav1.6 protein with Nav1.2 ICL1 localized to the distal axon. Similarly, chimeric Nav1.2 with Nav1.6 ICL1 did not localize to the distal axon (Liu *et al.*, 2022a). The interacting partner or partners driving this effect are unknown.

Alternative splicing of *SCN8A*

The *SCN8A* pre-mRNA undergoes two types of alternative splicing. *SCN8A* encodes two mutually exclusive copies of the fifth coding exon (corresponding to

transmembrane segments 3 and 4 of domain I) that differ by two amino acids (Plummer *et al.*, 1997; Epilepsy Genetics, 2018). The choice between inclusion of exon 5N (neonatal) or exon 5A (adult) is developmentally regulated (Plummer *et al.*, 1997; Liang *et al.*, 2021). Whether the choice of exon 5A/5N affects Nav1.6 physiology is unknown. (Plummer *et al.*, 1997). Nav1.1 and Nav1.2 also undergo mutually exclusive alternative splicing of exon 5. Although Nav1.2 exons 5A and 5N only differ by one amino acid, the voltage dependence of activation of 5N-containing channels is more depolarized than 5A-containing channels (Sanders *et al.*, 2018). Three individuals with mutations in *SCN8A* exon 5A have been identified to date, and their phenotype is broadly consistent with *SCN8A* GOF mutations in other exons (Epilepsy Genetics, 2018).

The region encoding Nav1.6 domain III contains another set of alternatively spliced exons. The mutually exclusive exons 18A and 18N encode segments 3 and 4 of domain III, corresponding to exons 5A and 5N in domain I, and indicating a shared evolutionary origin (Plummer *et al.*, 1998). Exon 18N is a “poison exon” encoding an in-frame stop codon. Transcripts containing exon 18N are subject to nonsense-mediated decay *in vitro* (Plummer *et al.*, 1998; O'Brien *et al.*, 2012a). Inclusion of exon 18A, which encodes the full-length protein, requires neuron-specific splice factors including RBFOX1 and appears to be restricted to neurons (Gehman *et al.*, 2012; O'Brien *et al.*, 2012a; Zubovic *et al.*, 2012). Cultured astrocytes and oligodendrocytes express only exon 18N, so full-length Nav1.6 protein is not expressed (O'Brien *et al.*, 2012a). The function of this alternative splicing mechanism is unknown but may represent a fail-safe mechanism to prevent damage to non-neuronal cells that could result from expression of VGSCs (Plummer *et al.*, 1997).

SCN8A mutations in human disease

SCN8A is an essential gene, and variation in its sequence is not well-tolerated. The Genome Aggregation Database (gnomAD) consists of exomes and genomes from 140,000 healthy adults (Karczewski *et al.*, 2019). Based on the number of individuals and the length of the gene, gnomAD predicts the expected number of LOF mutations (for *SCN8A*, $n_{expected}$ = 81) and compares to the observed mutation rate (for *SCN8A*, $n_{observed}$ = 5). *SCN8A* has a predicted loss of function intolerance (pLI) score of 1, indicating the highest restriction against LOF mutations (Karczewski *et al.*, 2019). *SCN8A* is also intolerant to missense mutations (Karczewski *et al.*, 2019).

The greatest number of *SCN8A* mutations have been identified in individuals with developmental and epileptic encephalopathy (DEE, Table 1-1) (Johannesen *et al.*, 2022). *SCN8A*-DEE has an average age of onset of 3 months, with multiple seizure types, developmental delay, cognitive impairment, movement disorders and elevated risk of SUDEP (Larsen *et al.*, 2015; Meisler *et al.*, 2016; Johannesen *et al.*, 2018; Johannesen *et al.*, 2022). Seizures are often not responsive to treatment, though high doses of sodium channel blockers can be effective (Boerma *et al.*, 2016; Johannesen *et al.*, 2022).

SCN8A-DEE is caused by heterozygous missense mutations that result in GOF effects on the channel (Meisler *et al.*, 2016). Most mutations occur *de novo*, though inheritance from a mosaic parent has been reported (Wagnon and Meisler, 2015). Several recurrent *SCN8A*-DEE mutations have been identified in multiple unrelated patients (Wagnon and Meisler, 2015; Johannesen *et al.*, 2022). Roughly one quarter of known *SCN8A*-DEE mutations occur at arginine residues R850, R1617, or R1872, likely

Table 1-1. *SCN8A* genotype-phenotype correlations in human and mouse. LOF, loss of function; GOF, gain of function; DEE, developmental and epileptic encephalopathy; BFIS, benign familial infantile seizures.

Genotype	Human	Mouse
-/-	**Not observed**	**Progressive paralysis and death by 3 weeks** (Burgess *et al.*, 1995)
+/-	**Neurodevelopmental disorders without epilepsy** (Trudeau *et al.*, 2006; Wagnon *et al.*, 2017; Johannesen *et al.*, 2022) **Generalized epilepsy with absence seizures** (Johannesen *et al.*, 2022) **<100 cases** (Johannesen *et al.*, 2022)	**Anxiety-like behavior** (McKinney *et al.*, 2008) **Absence seizures** (Papale *et al.*, 2009) **Resistant to chemically induced seizures** (Makinson *et al.*, 2014)
+/GOF	**DEE** (Veeramah *et al.*, 2012; Johannesen *et al.*, 2022) **BFIS** (Gardella *et al.*, 2016; Johannesen *et al.*, 2022) **~750 cases** (Johannesen *et al.*, 2022)	**Seizures and premature death** (Wagnon *et al.*, 2015b; Bunton-Stasyshyn *et al.*, 2019)
GOF/GOF	**Not observed**	**Seizures and death by 1 month** (Wagnon *et al.*, 2015b)

due to the presence of CpG dinucleotides in all three codons (Wagnon and Meisler, 2015; Johannesen *et al.*, 2022). Currently, approximately 750 individuals with *SCN8A*-DEE have been discovered.

Rarely, *SCN8A* GOF mutations can cause benign familial infantile seizures (BFIS) (Gardella *et al.*, 2016; Johannesen *et al.*, 2022). Individuals with BFIS have seizure onset before 1 year and respond well to treatment, especially with sodium channel blockers (Gardella *et al.*, 2016; Johannesen *et al.*, 2022). Seizures in BFIS resolve with age and affected individuals have normal cognition (Gardella *et al.*, 2016; Johannesen *et al.*, 2022). Due to the benign phenotype, inheritance from an affected parent is possible (Gardella *et al.*, 2016; Johannesen *et al.*, 2022). Several *de novo* mutations have also been reported (Johannesen *et al.*, 2022). Some patients also exhibit episodes of paroxysmal dyskinesia during puberty (Gardella *et al.*, 2016).

SCN8A LOF mutations are less commonly identified, possibly because the resulting phenotypes are less severe and therefore less likely to be candidates for genetic testing (Wengert *et al.*, 2019b). The first human *SCN8A* mutation was identified in a screen for ataxia (Trudeau *et al.*, 2006). Out of 151 patients, Trudeau *et al* identified one family with four members who were heterozygous for a frameshift mutation in the final coding exon of *SCN8A*. Detailed clinical evaluation of the proband revealed intellectual disability, developmental delay, ataxia, and cerebellar atrophy. The other affected family members had histories of behavioral and intellectual disability (Trudeau *et al.*, 2006).

Since then, approximately 40 individuals with heterozygous loss-of-function mutations in *SCN8A* have been discovered with familial or *de novo* variants

(Johannesen *et al.*, 2022). These patients experience intellectual disability, behavioral disorders including autism spectrum disorder and ADHD, delayed speech, and microcephaly. Some also have generalized epilepsy, characterized by multiple seizure types, including a high prevalence of absence seizures, with median onset at 3.5 years. Movement disorders without seizures have also been described in patients with heterozygous partial or complete loss-of-function mutations (Wagnon *et al.*, 2018; Laliberte and Myers, 2023).

Two families with biallelic mutations of *SCN8A* have been identified (Wengert *et al.*, 2019b). In both families, the heterozygous parents had cognitive impairment and intellectual disability. The children inherited *SCN8A* mutations from both parents and displayed a severe developmental and epileptic encephalopathy (DEE) with onset before 7 months of age (Wengert *et al.*, 2019b). In each family, one of the *SCN8A* mutations (G269R and G822R) causes complete loss of sodium current in neuron-like ND7/23 cells (Baker *et al.*, 2018). The other mutations cause partial loss-of-function (T1360N and R1638C). Thus, all three probands inherited one complete and one partial LOF allele. It is unclear how those mutations cause DEE. No individuals with complete loss of Nav1.6 activity have been identified.

Mutation of *Scn8a* in the mouse

Mice with *Scn8a* mutations recapitulate many aspects of human *SCN8A*-related disease (Table 1-2). Homozygous null mutation of *Scn8a* causes failure of the neuromuscular junction and hind limb paralysis beginning around 2 weeks of age, leading to death by 3 weeks of age (Burgess *et al.*, 1995). The timing of the paralysis

Table 1-2. Phenotypes of *Scn8a* conditional mutant mice.

***Scn8a* genotype**	**Cre** (cell type)	**Phenotype**
Conditional +/-	***CAG-ER-Cre*** (all cells, activated by tamoxifen)	**Resistant to induced seizures** (Makinson *et al.*, 2014)
	Emx1-Cre, Camk2a-Cre, (forebrain excitatory neurons)	**Resistant to induced seizures** (Makinson *et al.*, 2017)
	Dlx5/6-Cre (inhibitory neurons)	**Absence seizures** (Makinson *et al.*, 2017)
	Foxg1-Cre (cortical neurons)	**Resistant to induced seizures** (Makinson *et al.*, 2017)
Conditional -/-	***Pcp2-Cre*** (cerebellar Purkinje cells)	**Impaired motor function** (Levin *et al.*, 2006) **Impaired motor learning and social interaction** (Woodruff-Pak *et al.*, 2006; Yang *et al.*, 2022b)
	Gabra6-Cre (cerebellar granule cells)	**Impaired motor function** (Levin *et al.*, 2006)
	AAV-Cre (injected into dorsal root ganglion)	**Reduced pain sensitivity** (Chen *et al.*, 2018)
Conditional +/GOF	***EIIa-Cre*** (all cells)	**Spontaneous, premature death at P14** (Bunton-Stasyshyn *et al.*, 2019)
	Nestin-Cre (all neurons)	**Spontaneous seizures, premature death** (Bunton-Stasyshyn *et al.*, 2019)
	Emx1-Cre (forebrain excitatory neurons)	**Spontaneous seizures, premature death at P21** (Bunton-Stasyshyn *et al.*, 2019; Yu *et al.*, 2020)
	Gad2-Cre, Dlx5/6-Cre (inhibitory neurons)	**No spontaneous seizures** (Bunton-Stasyshyn *et al.*, 2019)
	CAG-ER-Cre (all cells, activated in adults by tamoxifen)	**Spontaneous seizures, premature death** (Bunton-Stasyshyn *et al.*, 2019)
	Sst-Cre (somatostatin-positive inhibitory neurons)	**Audiogenic seizures** (Wengert *et al.*, 2021)

phenotype correlates with the postnatal increase in *Scn8a* expression and the replacement of Nav1.2 with Nav1.6 at the AIS and nodes of Ranvier. Haploinsufficiency for *Scn8a* results in absence seizures (Papale *et al.*, 2009) and anxiety-like behavior (McKinney *et al.*, 2008) with normal life span (Burgess *et al.*, 1995; Meisler *et al.*, 2001). These mice are also resistant to chemically-induced seizures (Barker *et al.*, 2017) and to epilepsy caused by haploinsufficiency of *Scn1a* (Martin *et al.*, 2007; Hawkins *et al.*, 2011). Mice with 10% of wildtype *Scn8a* expression have reduced muscle mass and perform poorly on tests of motor function (Kearney *et al.*, 2002).

Our lab generated a floxed allele of *Scn8a* with Cre-mediated conditional deletion of the first coding exon (Table 1-2) (Levin and Meisler, 2004). Knockout of *Scn8a* in cerebellar Purkinje cells causes motor deficits, including ataxia and tremor, and subtle behavioral abnormalities (Levin *et al.*, 2006; Woodruff-Pak *et al.*, 2006; Yang *et al.*, 2022b). Knock-out in cerebellar granule cells had a much milder impact on motor function (Levin *et al.*, 2006). Correspondingly, loss of *Scn8a* had a greater impact on the firing rate of Purkinje cells than cerebellar granule cells (Levin *et al.*, 2006; Osorio *et al.*, 2010). Deletion of *Scn8a* in neurons of the dorsal root ganglion may also reduce sensitivity to painful stimuli (Chen *et al.*, 2018).

Crossing the *Scn8a*$^{fl/+}$ mice with Cre transgenes expressed in all cells (*ER-Cre*) or in excitatory neurons (*Emx1-Cre* or *Camk2a-Cre*) increases resistance to chemically-induced seizures, consistent with observations in *Scn8a*$^{+/-}$ mice (Makinson *et al.*, 2014; Makinson *et al.*, 2017). Crossing with a Cre expressed in inhibitory neurons (*Dlx5/6-Cre*) caused absence seizures (Makinson *et al.*, 2017). Further experimentation revealed that

Scn8a expression in inhibitory neurons of the thalamic reticular nucleus regulates susceptibility to absence seizures (Makinson *et al.*, 2017).

Wong *et al* developed a mouse model with knock-in of the loss-of-function mutation p.R1620L (Liu *et al.*, 2019; Wong *et al.*, 2021). The mutation was originally discovered in an individual with autism spectrum disorder and dyskinesia but without epilepsy (Liu *et al.*, 2019). Mice heterozygous for the R1620L mutation exhibit behavioral abnormalities including hyperactivity and social interaction deficits (Wong *et al.*, 2021). Surprisingly, these mice also had increased seizure susceptibility and rare, spontaneous seizures. This is not consistent with studies of *Scn8a*$^{+/-}$ mice, which are less susceptible to seizures than wildtype (Makinson *et al.*, 2014; Barker *et al.*, 2017; Makinson *et al.*, 2017). Homozygous R1620L mutants exhibited tremor beginning at two weeks of age and worsening until death at three weeks (Wong *et al.*, 2021). The mice likely die due to loss of muscle tone, which could impair feeding or respiration, similar to the *Scn8a* homozygous null mice.

To date, two mouse models of *SCN8A* GOF mutations have been published (Wagnon *et al.*, 2015b; Bunton-Stasyshyn *et al.*, 2019). Heterozygous, constitutive knock-in of the GOF mutation p.N1768D causes neuronal hyperexcitability (Ottolini *et al.*, 2017), including spontaneous firing of transfected or endogenous hippocampal pyramidal neurons (Veeramah *et al.*, 2012; Lopez-Santiago *et al.*, 2017). The *Scn8a*$^{N1768D/+}$ mice exhibit spontaneous seizures and 50% penetrance of premature death by 6 months of age (Wagnon *et al.*, 2015b). Mice homozygous for the p.N1768D mutation are more severely affected. Around the third postnatal week, homozygotes develop movement difficulties and die of a single, lethal seizure before one month of

age (Wagnon *et al.*, 2015b). Interestingly, mice with one N1768D and one null allele exhibit an intermediate phenotype with seizure onset at 8 weeks and average survival of 3 months (Wagnon *et al.*, 2015b). Loss of the wildtype *SCN8A* allele is thus likely worsen the phenotype of *SCN8A*-DEE.

The second *Scn8a*-GOF mouse is a floxed knock-in of the recurrent mutation p.R1872W (denoted *Scn8a*^{R1872W}, Table 1-2) (Bunton-Stasyshyn *et al.*, 2019). Activation of the mutation in excitatory neurons, but not inhibitory neurons, causes spontaneous seizures and premature death at 3 weeks of age (Bunton-Stasyshyn *et al.*, 2019; Yu *et al.*, 2020). When the mutant channel was activated in adult mice, lethal seizures began within weeks (Bunton-Stasyshyn *et al.*, 2019).

Wengert *et al* serendipitously discovered that mice expressing the *Scn8a*-R1872W mutation in somatostatin-positive inhibitory neurons exhibit seizures in response to audiogenic stimulation (Wengert *et al.*, 2021). Mice with global expression of the mutation are also sensitive to audiogenic seizures, but expression in only excitatory neurons does not cause audiogenic susceptibility (Wengert *et al.*, 2021). This phenotype is likely driven by depolarization block in somatostatin-positive interneurons. Depolarization block is caused by excessive stimulation and occurs when so many sodium channels are trapped in the inactivated state that firing of action potentials becomes impossible.

Mutation of other neuronal VGSCs in human disease

The three other neuronal VGSC genes (*SCN1A*, *SCN2A*, and *SCN3A*) are also implicated in disease (summarized in Table 1-3). Heterozygous loss of *SCN1A* causes

Table 1-3. Disorders associated with voltage-gated sodium channel mutation. GOF, gain of function; LOF, loss of function; DEE, Developmental and Epileptic Encephalopathy; GEFS+, Generalized Epilepsy with Febrile Seizures Plus; BFIS, Benign Familial Infantile Seizures.

Gene	Protein	Type of mutation	Associated clinical diagnoses
SCN1A	Nav1.1	GOF	DEE Familial hemiplegic migraine type 3
		LOF	DEE (Dravet syndrome) GEFS+
SCN2A	Nav1.2	GOF	DEE BFIS Episodic ataxia
		LOF	Autism spectrum disorder Intellectual disability DEE
SCN3A	Nav1.3	GOF	DEE Cortical malformations
		LOF	None

Dravet Syndrome, the most common DEE (Wu *et al.*, 2015; Lindy *et al.*, 2018). However, the same heterozygous mutations can cause generalized epilepsy with febrile seizures plus (GEFS+), a less severe seizure disorder (Escayg *et al.*, 2000; Kimura *et al.*, 2005). *SCN1A* GOF mutations cause an inherited migraine disease or an extremely severe DEE accompanied by movement disorders or arthrogryposis (Fan *et al.*, 2016; Dhifallah *et al.*, 2018; Shao *et al.*, 2018; Brunklaus *et al.*, 2022; Clatot *et al.*, 2023).

Both GOF and LOF mutations of *SCN2A* cause DEE (Wolff *et al.*, 2017). Early seizure onset, prior to 3 months of age, is associated with GOF mutations of *SCN2A* (Wolff *et al.*, 2017). Seizure onset after 3 months of age is associated with partial or complete LOF mutations (Kamiya *et al.*, 2004; Ogiwara *et al.*, 2009; Lossin *et al.*, 2012; Wolff *et al.*, 2017; Wolff *et al.*, 2019). LOF mutations of *SCN2A* are also strongly associated with autism spectrum disorder (ASD) (Ben-Shalom *et al.*, 2017). Gain of function mutations of *SCN2A* can also cause BFIS (Heron *et al.*, 2002; Wolff *et al.*, 2017) or episodic ataxia (Liao *et al.*, 2010; Schwarz *et al.*, 2019).

To date, LOF mutations of *SCN3A* have not been associated with disease, though the gnomAD pLI score for *SCN3A* is 1 (Karczewski *et al.*, 2019). Paradoxically, *Scn3a* knockout mice are viable and fertile (Nassar *et al.*, 2006). However, a small but growing number of *SCN3A* GOF mutations have been identified in patients with DEE (Zaman *et al.*, 2018) and cortical malformations, including polymicrogyria and microcephaly (Smith *et al.*, 2018; Zaman *et al.*, 2020).

Genetic modifiers and gene interactions in the mouse

Genetic divergence between inbred strains of mice has been used to identify modifier genes that influence disease severity. For example, haploinsufficiency of *Scn1a*, a model of Dravet Syndrome, causes spontaneous seizures in strain C57BL/6J but not in strain 129 (Yu *et al.*, 2006; Miller *et al.*, 2014). This difference was traced to a previously unrecognized splice site variant in the *Gabra2* gene in strain C57BL/6J that causes a three-fold reduction in expression of the α2 subunit of the GABA receptor (Miller *et al.*, 2014; Mulligan *et al.*, 2019). This *Gabra2* variant also accelerates seizure onset in mice with an epileptogenic mutation of *Scn8a* (Yu *et al.*, 2020; Yu *et al.*, 2022).

Interactions between multiple ion channel variants have also been demonstrated by combining mutants in the mouse. For example, heterozygous loss-of-function of *Scn8a* is protective against seizures in *Scn1a* haploinsufficient mice (Martin *et al.*, 2007; Hawkins *et al.*, 2011) and chemically-induced seizures (Makinson *et al.*, 2014; Barker *et al.*, 2017). Variation in the potassium channel *Kcnv2* modifies the severity of seizures caused by a gain-of-function variant of *Scn2a* (Jorge *et al.*, 2011). Conversely, haploinsufficiency of *Scn2a* mitigates seizures in *Kcna1*$^{-/-}$ mice (Mishra *et al.*, 2017). These genetic interactions may suggest new avenues for targeted therapy and may also predict potential pathogenic gene interactions. In a study of patients with monogenic epilepsy due to cation channel variants, the frequency of secondary deleterious variants in other ion channels was higher than in controls, suggesting exacerbation of the primary pathogenic mutation (Epi25k, 2019).

New small molecule drugs to treat *SCN8A*-DEE

Some patients with *SCN8A*-DEE caused by gain-of-function mutations respond to classical sodium channel blockers, but most continue to experience some seizures and undesirable side effects (Johannesen *et al.*, 2022). Channel-specific activators and inhibitors are predicted to have fewer side effects than the currently available non-specific sodium channel blockers, but it has been difficult to develop drugs that distinguish among the closely related sodium channels. Several new drugs are in clinical or preclinical testing, including the Nav1.6-specific channel blocker NBI-921352 (XEN901) and the persistent-current blockers PRAX330 and PRAX562 (Anderson *et al.*, 2014; Anderson *et al.*, 2017; Baker *et al.*, 2018; Wengert *et al.*, 2019a; Kahlig *et al.*, 2022).

The discovery that reduced *Gabra2* exacerbates *SCN1A* and *SCN8A* epilepsies suggests that that positive allosteric modulators of α2 subunit-containing GABA channels could be effective in these disorders (Miller *et al.*, 2014; Mulligan *et al.*, 2019; Yu *et al.*, 2020, 2020). Supporting this prediction, the $GABA_A$ activator clobazam reduces susceptibility to febrile seizures in *Scn1a*$^{+/-}$ mice (Hawkins *et al.*, 2016).

Antisense oligonucleotide therapy for *SCN8A*-DEE[2]

Unlike traditional small molecule drugs, antisense oligonucleotides (ASOs) can achieve target specificity based on DNA sequence differences among the VGSCs. ASOs are short oligonucleotides, ten to thirty nucleotides in length, that bind cellular

[2] The first four paragraphs of this section were published in: Hill SF and Meisler MH. Antisense Oligonucleotide Therapy for Neurodevelopmental Disorders. *Developmental Neuroscience*, 2021.

RNAs via complementary base pairing and alter pre-mRNA splicing, mRNA stability, transcription, or RNA-protein interaction. ASOs can target proteins that have been considered “undruggable” by directly regulating their transcript level and expression.

To confer stability in vivo, ASOs are composed of chemically modified nucleotides with resistance to enzymatic degradation (Fig. 1-4A). In two common modifications, a 2’-O-methoxyethyl (2’-MOE) group provides resistance to digestion by endonucleases (Monia *et al.*, 1993; McKay *et al.*, 1999), while replacement of phosphate along the nucleic acid backbone with phosphorothioate (PS) confers resistance to endonucleases (Khvorova and Watts, 2017). Other chemical modifications improve binding affinity, solubility, and in vivo stability (Shen *et al.*, 2019).

Two major types of ASOs are gap-mers, which target mRNA for degradation by RNAseH1, and ASOs that bind pre-mRNA and alter splicing by steric hindrance. A typical 20-nucleotide gap-mer would contain PS bonds throughout, 2’-MOE modifications at each end, and unmodified deoxyribose nucleotide nucleotides in the middle (Fig. 1-4A&B). When the gap-mer binds to its target mRNA, the central RNA/DNA hybrid can be cleaved by RNaseH1, resulting in reduced levels of mRNA and protein (Fig. 1-4B). Gap-mers can be used to reduce gene expression as an alternative to RNA interference.

Steric block ASOs contain the 2’-MOE and PS modifications throughout and are not substrates for RNaseH1. Binding of these ASOs to nuclear pre-mRNA can block interaction with splice factors, resulting in inclusion or exclusion of nearby exons (Fig. 1-4C).

We collaborated with Ionis Pharmaceuticals to develop a gap-mer ASO that

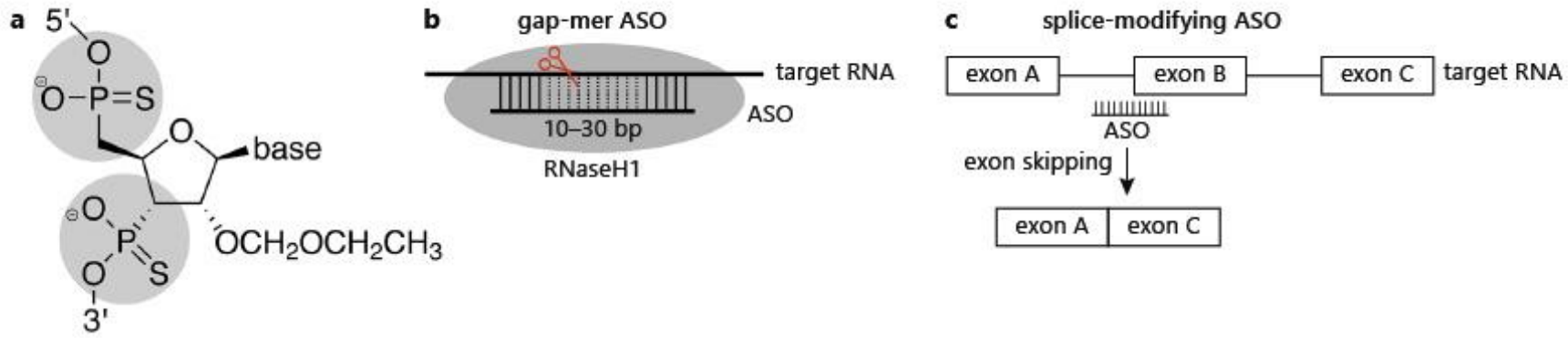

Figure 1-4. Chemical modifications of nucleotides in ASOs. To protect ASOs from enzymatic degradation in vivo, modified nucleotides are incorporated. (A) 2′MOE ribose and phosphorothioate groups. (B) Gap-mer ASOs contain 2′MOE modified bases at their termini (solid lines) and internal unmodified bases (dashed lines) that provide a substrate for degradation by RNaseH1. (C) Binding of steric block ASOs prevents interaction with splice factors, resulting in exon skipping, shown here, or redirection to an alternative splice site. ASOs, antisense oligonucleotides; 2′MOE, 2′-O-methoxy-ethyl. Figure from Hill and Meisler, 2021.

reduces expression of the mouse *Scn8a* transcript (Fig. 1-5) (Lenk *et al.*, 2020). The *Scn8a* ASO binds the 3' untranslated region (UTR) of the mouse *Scn8a* gene (Fig. 1-5A) (Lenk *et al.*, 2020). Administration of the *Scn8a* ASO to cultured neurons reduced *Scn8a* transcript abundance in a dose-dependent manner (Fig. 1-5B) (Lenk *et al.*, 2020). ASOs do not cross the blood-brain barrier, so *in vivo* administration requires intracerebroventricular (ICV) injection of the ASO directly into the lateral ventricles. ICV administration of the *Scn8a* ASO to wildtype mice on postnatal day 2 (P2) caused a 50% reduction in *Scn8a* expression on P21 (Fig. 1-5C) (Lenk *et al.*, 2020).

We tested the efficacy of the *Scn8a* ASO in *Scn8a*$^{cond/+}$ mice carrying the *EIIa-Cre* transgene, which express the p.R1872W mutation in all cells. Mice treated with the control ASO exhibited a single, lethal seizure between P13-P18 (Fig 1-6A) (Lenk *et al.*, 2020). A single dose of *Scn8a* ASO on P2 extended the lifespan of the *Scn8a* mutant mice in a dose-dependent manner (Fig. 1-6A&B). The optimal dose was 45 ug, which extended median survival from 2 weeks to 7 weeks (Fig. 1-6A&B). A second dose of the ASO extended median survival even further (Fig. 1-6A) (Lenk *et al.*, 2020).

ASO therapies for other genetic epilepsies

ASOs targeting specific DNA sequences have been approved for treatment of spinal muscular atrophy (Finkel *et al.*, 2017) and Batten's disease (Kim *et al.*, 2019), and show promise for several types of epilepsy. The *SCN1A* gene contains an alternatively spliced "poison exon" with an in-frame stop codon. Approximately 50% of transcripts in young wildtype mice contain the poison exon (Lim *et al.*, 2020). To treat epilepsy caused by *SCN1A* haploinsufficiency, Stoke Therapeutics developed a steric

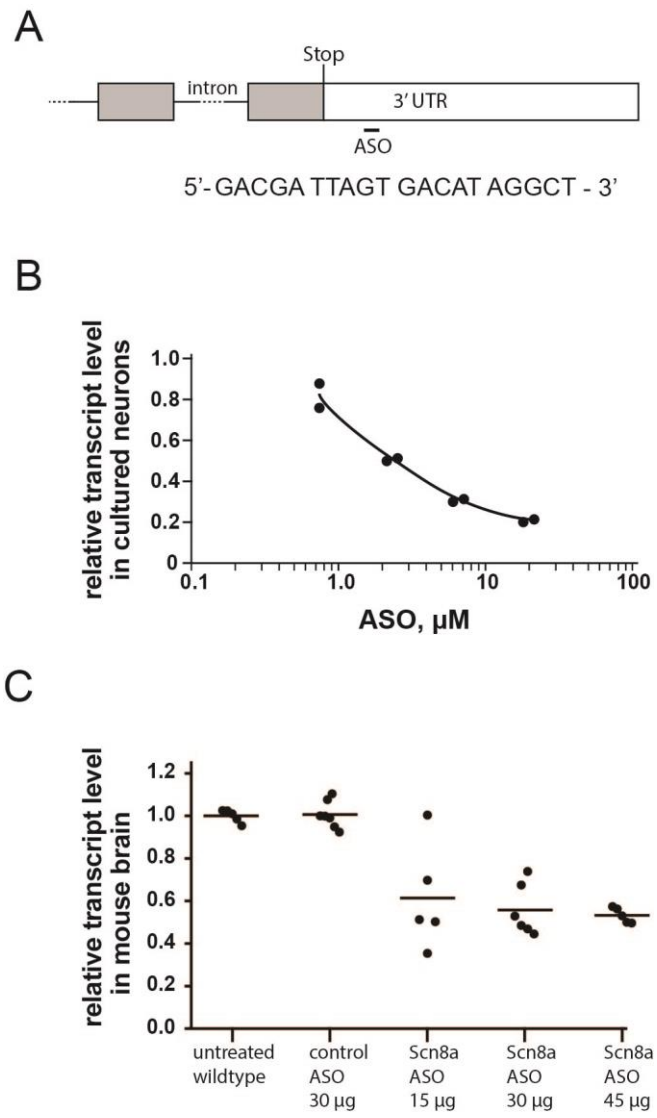

Figure 1-5. *Scn8a* ASO treatment reduces the abundance of *Scn8a* transcript in wild-type neurons and brain. (A) Cartoon of the 3' end of the *Scn8a* gene. The last 2 exons are represented by boxes separated by a line representing the last intron. Coding sequences within the exons are shaded. The position of the stop codon that terminates translation is marked as "stop." The sequence of the 20-base pair (bp) *Scn8a* ASO is shown. The ASO sequence is identical to the genomic sequence of the 30untranslated region (UTR) at a position approximately 500 bp downstream from the translation stop codon within the last exon of the gene. (B) Primary cortical neurons from E14 embryos of strain C57BL/6J were cultured for 3 days with the indicated concentration of *Scn8a* ASO. (C) The indicated dose of ASO was administered to C57BL/6J mice on postnatal day 2, and the abundance of *Scn8a* transcript in brain RNA was measured at postnatal day 21. Five or six animals were treated with each dose; each symbol represents data from 1 animal. Figure from Lenk *et al.*, 2020.

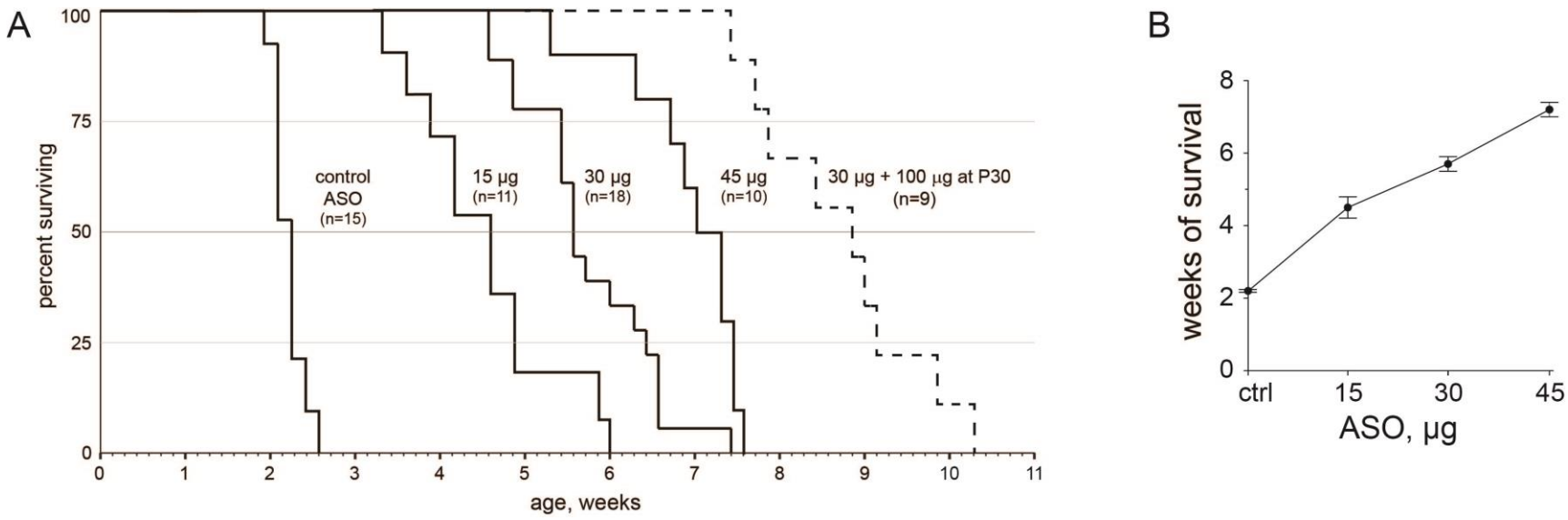

Figure 1-6. *Scn8a* ASO delays seizure onset and prolongs survival of mutant mice expressing the pathogenic mutation *SCN8A*-R1872W. (A) *Scn8a*$^{cond/+}$*,EIIA-Cre* mice were treated on postnatal day 2 by intracerebroventricular injection with the indicated mount of control or *Scn8a* ASO. A second dose of 100 µg of *Scn8a* ASO at postnatal day 35 further extended survival ($p < 0.001$) (dotted line). (B) Dose dependence of mean survival; values are mean ± standard error of the mean. Figure adapted from Lenk *et al*., 2020.

block ASO that prevents inclusion of the poison exon, which increases the abundance of transcripts encoding full-length *SCN1A* (Han *et al.*, 2020). The *SCN1A* ASO extends the lifespan of *Scn1a*$^{+/-}$ mice and is currently in clinical trials to treat Dravet Syndrome (Pong *et al.*, 2022). Gene replacement and CRISPRa methods to upregulate *SCN1A* expression have also been effective in preclinical mouse models of Dravet Syndrome (Colasante *et al.*, 2020a; Yamagata *et al.*, 2020; Fadila *et al.*, 2023).

While the *SCN1A* ASO is the most clinically advanced, additional ASOs are in preclinical development. One ASO is designed to reduce expression of *SCN2A* (Li *et al.*, 2021), and another reduces expression of the potassium channel gene *KCNT1* (Burbano *et al.*, 2022). A different *KCNT1* gap-mer ASO has been used to treat two patients with *KCNT1*-related epilepsy under an FDA Compassionate Use Authorization (Kaiser, 2022). Unfortunately, both patients developed hydrocephalus during treatment, and one died (Kaiser, 2022). There are also rare reports of hydrocephalus in individuals treated with nusinersen, an ASO to treat spinal muscular atrophy, and tominersen, an ASO to treat Huntington's disease (Stoker *et al.*, 2021; Viscidi *et al.*, 2021). The cause of ASO-related hydrocephalus is unclear. However, ASOs and other genetic therapies continue to be promising new therapeutic strategies to treat DEEs.

Conclusion

Since the discovery of *Scn8a* in 1995, enormous progress has been made towards understanding its function in healthy and diseased neurons. We are now at the point of developing precision therapies to treat *SCN8A*-DEE and similar diseases. Because Nav1.6 is a major regulator of overall neuronal excitability, the goal of my

thesis work has been to evaluate its potential as a target for future antiepileptic therapies, which may include genetic therapies and Nav1.6-specific channel blockers.

CHAPTER II

Scn8a Antisense Oligonucleotide Therapy Delays Seizure Onset and Extends Survival in Mouse Models of *SCN8A* Encephalopathy and Dravet Syndrome[1]

ABSTRACT

SCN8A encephalopathy is a developmental and epileptic encephalopathy (DEE) caused by de novo gain-of-function mutations of sodium channel Nav1.6 that result in neuronal hyperactivity. Affected individuals exhibit early-onset drug-resistant seizures, developmental delay, and cognitive impairment. An antisense oligonucleotide (ASO) that reduces expression of *Scn8a* delays seizure onset and prolongs survival in a mouse model of *SCN8A* encephalopathy. In this work, we investigated the kinetics of *Scn8a* knockdown and determined that the effect of the ASO persists approximately 6 weeks after injection. Although haploinsufficiency for *SCN8A* causes movement disorders, reduced *Scn8a* expression did not cause gross motor abnormalities. Finally, we demonstrated that the *Scn8a* ASO completely rescued the seizure and premature lethality phenotypes of an *Scn1a*-DEE mouse model. Our results suggest that reduced *Scn8a* expression could be a safe and effective therapy for *SCN8A* DEE and other epilepsy disorders.

[1] This chapter is excerpted from: Lenk GM, Jafar-Nejad MD, Hill SF, Huffman LD, Smolen CE, Wagnon JL, Petit H, Yu W, Ziobro J, Bhatia K, Parent J, Giger RJ, Rigo F, Meisler MH. *Scn8a* Antisense Oligonucleotide Is Protective in Mouse Models of *SCN8A* Encephalopathy and Dravet Syndrome. *Annals of Neurology*, 2020. Julie Ziobro performed the EEG experiment shown in Figure 2-3C. I performed all the remaining experiments.

INTRODUCTION

Developmental and epileptic encephalopathies (DEEs) are devastating early onset disorders characterized by seizures and developmental delay (Berg *et al.*, 2010; Scheffer *et al.*, 2017). Monogenic causes have been identified for approximately one-third of cases, with voltage-gated neuronal sodium channels accounting for 2% of the total (Meisler and Kearney, 2005; Larsen *et al.*, 2015; Lindy *et al.*, 2018). *SCN8A* encephalopathy (OMIM#614588) is a DEE caused by *de novo* missense mutations in the *SCN8A* gene that encodes the neuronal sodium channel Nav1.6 (Meisler *et al.*, 2016; Gardella *et al.*, 2018; Johannesen *et al.*, 2022). Affected individuals are heterozygous for missense mutations that alter the biophysical properties of the channel, resulting in premature channel opening, delayed channel inactivation, or elevated persistent current (Wagnon *et al.*, 2015a; Meisler *et al.*, 2016). Because Nav1.6 has a major role in excitatory neurons, elevated activity leads directly to increased neuronal excitability (Meisler *et al.*, 2016).

The average age of seizure onset in individuals with *SCN8A* encephalopathy is 4 months. The clinical course is severe, and approximately 50% of affected individuals remain non-ambulatory and nonverbal. Long-term seizure control is rarely achieved with antiepileptic drugs (Gardella *et al.*, 2018; Johannesen *et al.*, 2022). We and others have studied recurrent patient mutations at arginine codon 1872. Substitution of arginine 1872 by the uncharged amino acids leucine, glutamine, or tryptophan impairs inactivation of the Nav1.6 channel (Wagnon *et al.*, 2015a; Wagnon and Meisler, 2015; Liu *et al.*, 2019). We generated a conditional mouse model of p.Arg1972Trp that

recapitulates the early seizure onset and susceptibility to premature death that are characteristic of DEE (Bunton-Stasyshyn *et al.*, 2019).

Because the pathogenic mechanism of *SCN8A* encephalopathy is neuronal hyperexcitability due to gain-of-function mutations, reduction of transcript abundance is a logical therapeutic strategy. Antisense oligonucleotides (ASOs) hybridize by Watson-Crick base pairing to mRNAs, leading to degradation by ribonuclease H, inhibition of translation, or altered splicing. Dominant disorders can be treated with ASOs that reduce both mutant and wild-type transcript (McCampbell *et al.*, 2018; Southwell *et al.*, 2018). The application of ASO therapy to neurological disorders is receiving increasing attention (Roovers *et al.*, 2018; Bennett, 2019; Bennett *et al.*, 2019), and the US Food and Drug Administration has recently approved treatment for spinal muscular atrophy that uses intrathecal administration of an ASO at 6-month intervals (Finkel *et al.*, 2017).

We demonstrated that an ASO targeting the 3'UTR of the mouse *Scn8a* gene reduced expression of *Scn8a* both *in vitro* and *in vivo* (Chapter I, Fig. 1-5). The ASO prolongs the lifespan of *Scn8a*-R1872W mice in a dose-dependent manner (Fig. 1-6) (Lenk *et al.*, 2020). In this chapter, we further characterized the ASO to determine the duration of *Scn8a* knockdown and to identify possible deleterious side effects caused by excessive downregulation of *Scn8a*. We also administered the *Scn8a* ASO to another mouse model of DEE caused by haploinsufficiency of the related sodium channel gene *Scn1a*. These results provide proof of principle that reduction of *Scn8a* transcript is well-tolerated and can reduce the severity of Dravet syndrome (DS), a DEE caused by haploinsufficiency of *SCN1A*.

METHODS

Mutant mice

The conditional allele of *Scn8a* (*Scn8a*^{cond}) on background strain C57BL/6J is activated by Cre recombinase to express the patient mutation R1872W (Bunton-Stasyshyn *et al.*, 2019). The EIIA-Cre transgene on background strain C57BL/6J (JAX 003724) is expressed globally in preimplantation embryos and in mature oocytes. Homozygous male *Scn8a*$^{cond/cond}$ mice were crossed with female EIIA-Cre mice to generate 50% affected animals (*Scn8a*$^{cond/+}$, EIIA-Cre) and 50% unaffected *Scn8a*$^{cond/+}$ controls lacking Cre. Entire litters were randomly assigned to treatment with *Scn8a* ASO or control ASO. Female EIIA-Cre mice were used for breeding to avoid the mosaic Cre expression observed in offspring of male EIIA-Cre mice (Bunton-Stasyshyn *et al.*, 2019).

The *Scn1a* model of DS carries a deletion of exon 1 that is maintained in heterozygous state in strain 129S6/SvEvTac (Miller *et al.*, 2014). Experiments were carried out on affected F1 mice generated by crossing with strain C57BL/6J (Miller *et al.*, 2014). Mice were housed and cared for in accordance with NIH guidelines in a 12/12-hour light/dark cycle with standard mouse chow and water available *ad libitum*. Experiments were approved by the Committee on the Use and Care of Animals at the University of Michigan. Open field activity and wheel running were assayed in the Michigan Mouse Metabolic Phenotyping Center (NIH U2CDK110768).

Antisense oligonucleotides

ASOs were synthesized by Ionis Pharmaceuticals as described (Swayze *et al.*, 2007). The ASOs are 20 base pair (bp) gapmers with 5 2'-*O*-methoxyethyl-modified

ribonucleotides at each end and 10 deoxyribonucleotides in the center. The *Scn8a* ASO 5’ GAACGA TTAGT GACAT AGGCT 3’ is complementary to the 3’ untranslated region (UTR) that does not differ between wild-type and mutant transcript (Fig. 1-5A). The control ASO 5’ CCTAT AGGAC TATTC AGGAA 3’ does not match any transcript encoded by the mouse genome and was shown to be well tolerated in the mouse (Swayze *et al.*, 2007).

Intracerebroventricular administration of ASOs

At postnatal day 2 (P2) mice received 2 µL of ASO in phosphate buffered saline (PBS) injected manually into the cerebral ventricle (Becker *et al.*, 2017).

Quantitative reverse transcription polymerase chain reaction

Scn8a transcripts in mouse brain and cultured neurons were quantified using TaqMan gene expression assays (Applied Biosystems, Foster City, CA) (Bunton-Stasyshyn *et al.*, 2019). Total *Scn8a* transcript was detected with the FAM-labelled assay Mm00488110_m1 using as endogenous control the Tata binding protein mRNA (VIC labeled Mm01277042_m1). Relative transcript quantity was calculated by the ΔΔCT method (Schmittgen and Livak, 2008). Data represent the average result from 2 independent cDNA preparations for each animal.

Western blotting

Purified membrane protein was prepared from whole brain and analyzed by Western blotting essentially as described (Wagnon *et al.*, 2015b). The primary antibodies were rabbit anti-Nav1.6 (Millipore, Billerica, MA #5580, lot 3188705) diluted 1:500 and mouse anti-tubulin (Millipore, #MAB 1637, lot 2080833) diluted 1:1000.

RESULTS

Kinetics of *Scn8a* knockdown by ASO

In *Scn8a*$^{cond+}$, EIIA-Cre mice treated with 45 µg *Scn8a* ASO on P2, seizure onset began at 6 weeks of age (Fig. 1-6A). To determine the duration of the effect of ASO treatment on transcript level and the relationship between transcript level and seizure onset, we measured *Scn8a* transcripts at 3 time points after treatment at P2 with 45 µg ASO. Transcript levels in treated mice at each point were compared with age-matched untreated wild-type controls. The level of transcript at 3 weeks of age was 50% of control (Fig. 1-5C and Fig. 2-1A). At 5 weeks post-treatment, *Scn8a* transcript level was increased to 80% of control, but no seizures were observed. At the time of seizure onset, transcripts in the mice with seizures had reached 100% of the level of untreated controls (Fig. 2-1A). Thus, the reduction of *Scn8a* transcripts by ASO treatment persists for approximately 6 weeks and is correlated with seizure protection. The corresponding reduction of Nav1.6 protein at 3 weeks post-treatment is demonstrated in Fig. 2-1B.

Behavioral phenotyping of *Scn8a* mutant mice treated with ASO

Because *SCN8A* is an essential gene (Burgess *et al.*, 1995), it was important to evaluate potential adverse effects of ASO treatment. From previous work in the mouse, we know that reduction of brain transcripts below 5% of the wild-type level is lethal (Burgess *et al.*, 1995; Kearney *et al.*, 2002) and reduction to 10% of wild-type level results in dystonia, muscle wasting, and reduced body weight (Sprunger *et al.*, 1999; Kearney *et al.*, 2002). In contrast, reduction to 50% of wild-type level is well tolerated in the mouse, with only mild behavioral abnormalities (McKinney *et al.*, 2008) and absence seizures (Papale *et al.*, 2009). Similarly, some haploinsufficient patients with 50% of

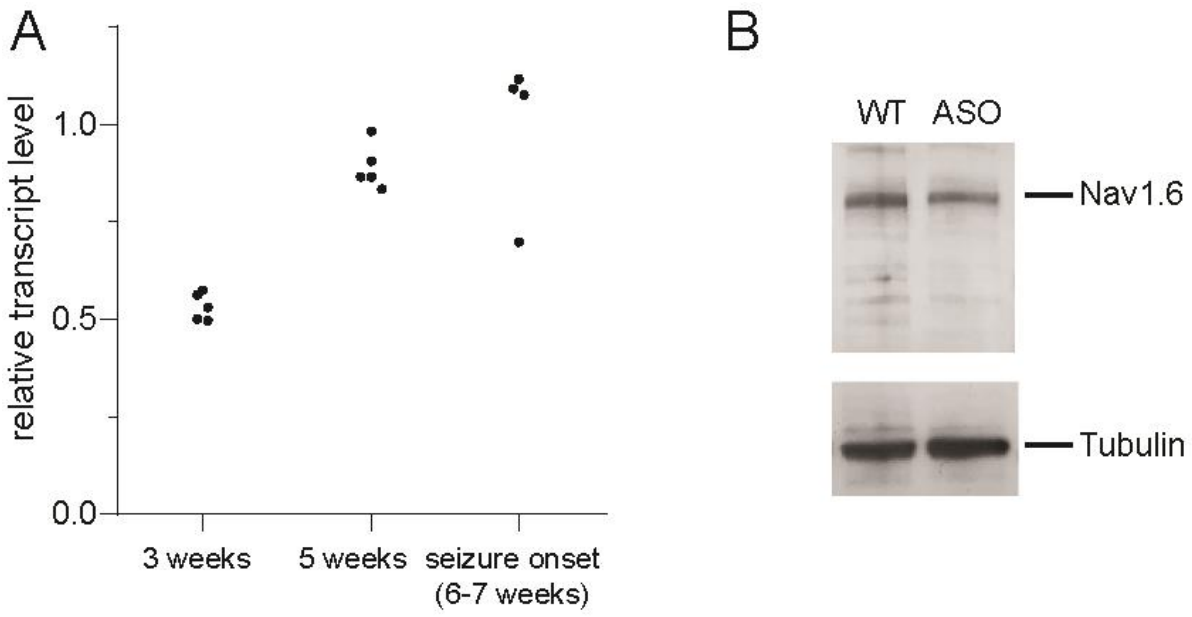

Figure 2-1. Kinetics of *Scn8a* knockdown by ASO. (A) Duration of the effect of *Scn8a* ASO on transcript level. Brain RNA was prepared from *Scn8a*$^{cond/+}$, EIIA-Cre mice treated with 45 µg of ASO on P2 and untreated age-matched wild-type mice and analyzed by quantitative reverse transcription polymerase chain reaction. (B) Reduction of Nav1.6 protein in mouse brain at 3 weeks of age in mice treated with 45 µg of ASO as in (A). ** indicates $p < 0.005$, Student's t-test. Panel A from Lenk *et al*., 2020.

wild-type expression have mild intellectual disability (Wagnon *et al.*, 2017; Wengert *et al.*, 2019b; Johannesen *et al.*, 2022). These earlier observations predicted that the ASO treatment that prevented seizures, with approximately 50% of wild-type expression remaining in brain would have only small effects on movement.

To detect potential impairment of motor function, we compared ASO-treated mutant mice with untreated wild-type littermates. We examined motor activity during the period of extended survival after ASO treatment. In the open field test, mice treated with 45 µg of ASO exhibited normal activity at 6 weeks of age. Total distance travelled, percentage time spent in the center of the open field, and number of rearing events did not differ from wild-type controls (Fig. 2-2A).

In the wheel running test, the ASO-treated mutant mice were slower than the wild-type mice (Fig. 2-2B). There was no difference between the two groups in the time spent running, but the distance covered was reduced by approximately one-third due to a slower average speed of 1.2 km/h for treated mutant mice compared with 2.0 km/h for wild-type controls. Cerebellar function was assessed by analysis of ledge walking, hind limb clasping, gait, and kyphosis (Guyenet *et al.*, 2010). We observed no impairment of cerebellar function in *Scn8a* mutant mice treated with the ASO (Fig. 2-2C-F). Thus, reduction of *Scn8a* transcript to a level sufficient for delay of seizure onset results in only minor effects on movement. Overall, the ASO-treated mice remained alert and active until the onset of seizures.

Scn8a ASO administration in mouse model of *SCN1A* haploinsufficiency

Because Nav1.6 is a major determinant of the firing properties of excitatory neurons, reduction of *Scn8a* expression could have a general ameliorating effect on

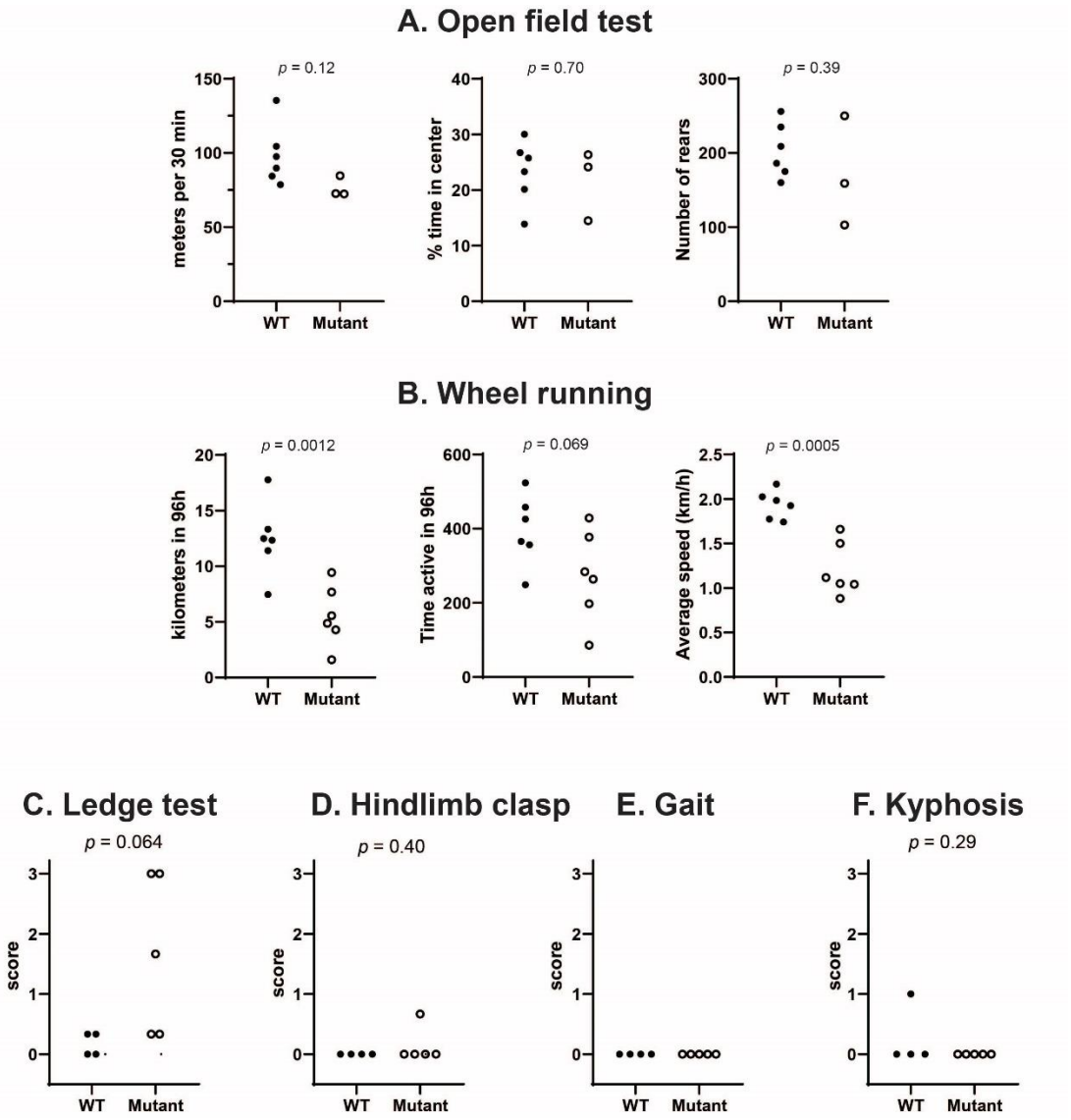

Figure 2-2: Motor activity of ASO-treated mice. *Scn8a*$^{cond/+}$, EIIA-Cre mice were treated with 45 µg *Scn8a* ASO at P2. (A) Activity in an open field was monitored for 30 minutes at 45 days of age. Treated mutant mice did not differ significantly from wild-type mice in average running speed, percentage of time spent in the center of the open field, or number of rears. (B) Wheel running activity was monitored 24 h/day during a 4-day interval between P31 and P39, after habituation to the running cage for 10 days. The distance travelled by the treated mutant mice during the 96 hours of monitoring was significantly smaller than for wild-type mice. There was no significant difference in the time spent running, but the average speed was lower for the mutant mice. (C–F) Cerebellar function was assessed at 5 weeks of age by analysis of ledge walking, hind limb clasping, gait, and kyphosis as described (Guyenet *et al.*, 2010). The only deficit observed was impaired ledge walking in 3 of the 5 treated mutant mice. Each symbol represents 1 animal, and values are the mean of triplicate assays. The p-values are for the comparisons between wild-type and mutant mice (Student's t-test). Figure from Lenk *et al*., 2020.

seizure disorders of various causes (Isom, 2019). To test this possibility, we examined the effect of the *Scn8a* ASO in a mouse model of DS, a DEE caused by loss-of-function mutations of *SCN1A*. Reduction of *Scn8a* by shRNA or genetic deletion was previously shown to be protective against acutely induced seizures in a Dravet mouse (Martin *et al.*, 2007; Wong *et al.*, 2018). We used the Kearney mouse model of DS that is haploinsufficient due to deletion of exon 1 of *Scn1a* (Miller *et al.*, 2014). The untreated DS mice exhibited onset of spontaneous seizures by 4 weeks of age and 50% penetrance of seizures and lethality (Fig. 2-3A), consistent with previous reports (Miller *et al.*, 2014). In contrast, DS mice treated with a single dose of 45 µg of *Scn8a* ASO on P2 survived beyond 5 months of age without behavioral seizures. The *Scn8a* ASO resulted in 50% reduction of *Scn8a* transcript in brain and spinal cord of DS mice with no effect on the *Scn1a* transcript (Fig. 2-3B).

Five consecutive days of EEG recordings of ASO-treated DS mice recorded at 5 months of age did not detect any subthreshold electrographic abnormalities or seizures (Fig. 2-3C). This extended period of protection after a single treatment suggests that ASO administration during a critical period of postnatal development might give long-term seizure control in Dravet patients. A transient developmental window of interneuron dysfunction has been described in Dravet mice (Favero *et al.*, 2018). Expansion of future testing of the *Scn8a* ASO to other seizure models will be of great interest.

DISCUSSION

The experiments described here provide preclinical evidence that therapeutic reduction of *Scn8a* transcript does not result in major adverse effects, suggesting that it

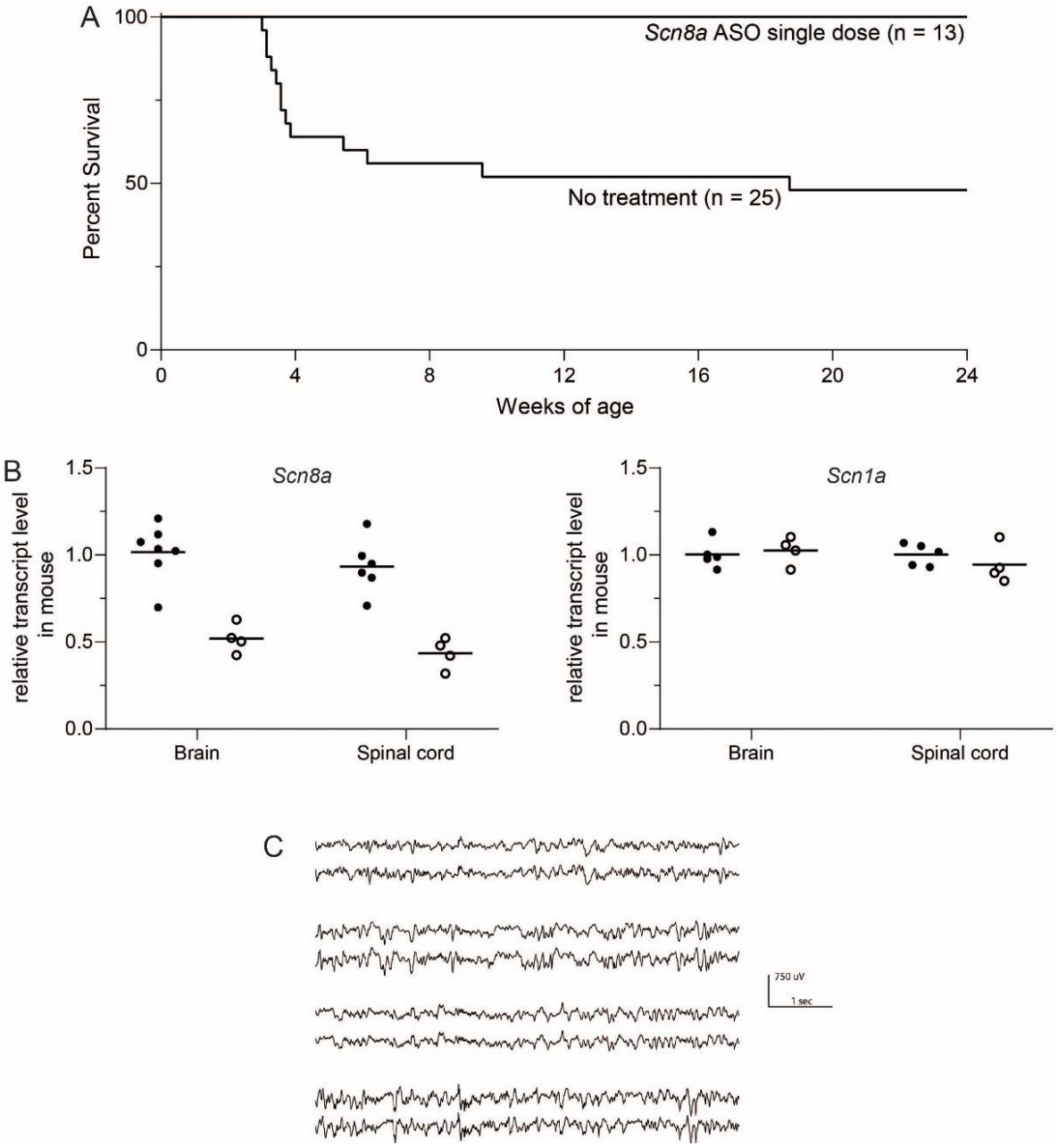

Figure 2-3. *Scn8a* ASO rescues survival of Dravet syndrome mice. *Scn1a*$^{+/-}$ mice were treated on P2 with 45 µg *Scn8a* ASO. (A) For untreated *Scn1a*$^{+/-}$ mice, median survival was 26 days with 50% penetrance of the lethal phenotype. In contrast, all of the ASO-treated mice survived beyond 6 months of age (p = 0.004, Mantel-Cox log-rank test). (B) The *Scn8a* ASO reduces *Scn8a* transcript with no effect on *Scn1a* transcript. Brain and spinal cord RNA was prepared from untreated wild-type P21 (solid symbols) or mice treated with 45 µg *Scn8a* ASO (open symbols). (C) The *Scn8a* ASO protects against electrographic seizures in *Scn1a*$^{+/-}$ mice. Four ASO treated mice at 5 months of age were monitored for 5 successive days with 24-hour electroencephalographic (EEG) recording. No electrographic seizures or other EEG abnormalities were observed (2 traces for each animal, from left and right cortex). Figure from Lenk *et al.*, 2020.

may be well tolerated in patients with *SCN8A* encephalopathy or Dravet Syndrome. Further investigations will be required to determine whether initiation of ASO treatment after seizure onset is also effective. In these animal models, death follows within minutes to days of the first seizure and the resulting inability to evaluate post-onset treatment is a limitation of the present study. However, our results suggest that maintaining reduced *Scn8a* expression is possible and likely to be effective. Clinical application will also require prevention of the deleterious effects associated with more extensive reduction of *SCN8A* expression, for example, by using allele-specific methods, which would limit reduction to 50% of normal expression. Our observations on the DS mouse support the exciting possibility that treatment with *SCN8A* ASO could also be protective in Dravet Syndrome and other seizure disorders with a variety of underlying etiologies.

CHAPTER III

Post-Onset Reduction of *Scn8a* Expression Prolongs Survival and Reduces Seizure Frequency in an *Scn8a* Epilepsy Model[1]

ABSTRACT

De novo mutations of the voltage-gated sodium channel *SCN8A* cause severe developmental and epileptic encephalopathy (DEE). Pathogenic variants result in gain-of-function changes in *SCN8A* activity, poorly controlled seizures, and significant comorbidities. We previously described an antisense oligonucleotide (ASO) that reduces *Scn8a* transcripts. Administration of the ASO on postnatal day 2 (P2) to a mouse model increased survival by three-fold. To investigate the potential effectiveness of post-onset ASO treatment, we evaluated ASO treatment that was initiated after observation of a convulsive seizure and repeated at intervals of 4 to 6 weeks. Repetitive treatment with *Scn8a* ASO initiated after seizure onset provided long-term survival and reduced seizure frequency. These data indicate that reduced *SCN8A* expression in *SCN8A*-DEE patients may be an effective treatment, even when initiated after the onset of seizures.

[1] This chapter is adapted from the submitted manuscript: Hill SF, Yu W, Ziobro J, Chalasani S, Reger F, Meisler MH. Long-term reduction of *SCN8A* after seizure onset is therapeutic in mouse models of epilepsy. *Submitted*, 2023.

INTRODUCTION

SCN8A encodes the neuronal voltage-gated sodium channel Nav1.6, which is concentrated at the distal axon initial segment and is responsible for the initiation of action potentials (Hu *et al.*, 2009; Meisler *et al.*, 2021). Mutations of *SCN8A* are classified as “gain-of-function” or “loss-of-function” depending on their effects on channel activity and neuronal firing (Meisler *et al.*, 2021). Heterozygous, *de novo* gain-of-function variants of *SCN8A* are responsible for a severe form of developmental and epileptic encephalopathy (DEE) (Veeramah *et al.*, 2012; Meisler *et al.*, 2021; Johannesen *et al.*, 2022). *SCN8A*-DEE presents with drug-resistant seizures with median onset at 3 months of age. Additional effects include developmental delay, intellectual disability, movement disorders, sleep disturbance, feeding difficulty and elevated risk of sudden unexpected death in epilepsy (SUDEP). Seizures in *SCN8A*-DEE are not well controlled by available therapies (Johannesen *et al.*, 2022).

We previously generated two mouse models expressing *SCN8A*-DEE mutations: a constitutive knock-in of the mutation p.Asn1768Asp (N1768D) (Wagnon *et al.*, 2015b) and a conditional (floxed) knock-in of the recurrent mutation p.Arg1872Trp (R1872W) (Bunton-Stasyshyn *et al.*, 2019). Both of these mutations cause gain-of-function effects on channel physiology in cell culture experiments and elevated neuronal firing in mouse models (Veeramah *et al.*, 2012; Wagnon *et al.*, 2015a; Lopez-Santiago *et al.*, 2017; Bunton-Stasyshyn *et al.*, 2019).

One proposed therapeutic strategy for treatment of *SCN8A* gain-of-function variants is to reduce *SCN8A* expression. For this purpose, we developed an antisense

oligonucleotide (ASO) that reduces *Scn8a* mRNA abundance (Lenk *et al.*, 2020). A single intracerebroventricular (ICV) injection of the *Scn8a* ASO to R1872W mice at postnatal day 2 (P2) reduced the abundance of the *Scn8a* transcript by 50% and protected against convulsive seizures and lethality for 6 weeks (Lenk *et al.*, 2020). A second dose of ASO extended the protection for five additional weeks, indicating that repetitive treatment would be effective. The *Scn8a* ASO was also therapeutic in mouse models of *Scn1a* haploinsufficiency (Dravet Syndrome) and mutation of the potassium channel genes *Kcna1* and *Kcnq2* (Lenk *et al.*, 2020; Hill *et al.*, 2022).

ASO treatment provided proof-of-principle that reduced *Scn8a* expression was effective when initiated prior to seizure onset. For clinical application, it is important to know whether there are irreversible biological changes during the pre-onset period that could reduce the effectiveness of this treatment. We addressed this question by testing the effectiveness of ASO treatment initiated after the first seizures are observed. This work provides additional support for down-regulation of *SCN8A* as a treatment for DEE.

METHODS

Mice

Scn8a$^{N1768D/+}$ (D/+) mice (Wagnon *et al.*, 2015b) and floxed *Scn8a*$^{R1872W/+}$ mice (Bunton-Stasyshyn *et al.*, 2019) were generated in our laboratory and maintained by backcrossing to strain C57BL/6J (Jax #000664) for more than 15 generations. Both male and female mice were used for experiments. Mice were housed and cared for in accordance with NIH guidelines in a 12/12-hour light/dark cycle with standard mouse chow and water available *ad libitum*. Animal experiments were approved by the

Institutional Animal Care and Use Committee (IACUC) at the University of Michigan in accordance with the National Institute of Health Guide for the Care and Use of Animals (Protocol # PRO00009797). Principles outlined in the ARRIVE guidelines and the Basel declaration (https://www.basel-declaration.org/) including the 3R concept have been considered when planning experiments.

Anti-sense oligonucleotide administration

Scn8a and control ASOs were synthesized by Ionis Pharmaceuticals as previously described (Swayze *et al.*, 2007; Lenk *et al.*, 2020). Mice were anesthetized with isoflurane. ASO was administered within 3 days after the first observed seizure by manual ICV injection into the left lateral ventricle (Kim *et al.*, 2016). Mice received 100 ug of control ASO in 3 uL or 250 ug of *Scn8a* ASO in 5 uL. Injections were repeated at 1-month intervals for the first 6 months and 6 week intervals for the second 6 months of the 12 month treatment period.

Seizure detection

Spontaneous behavioral seizures were detected by visual monitoring of D/+ mice for 8 hours/day, 5 days per week, 9 AM to 5 PM.

RESULTS

Disease progression in the *Scn8a-N1768D* (D/+) mouse model

Mice expressing the N1768D mutation (D/+) (Wagnon *et al.*, 2015b) have seizure onset at 2 to 4 months of age followed by a 6-week progression to lethality (Fig. 3-1). These mice were used to study the effectiveness of post-onset ASO treatment.

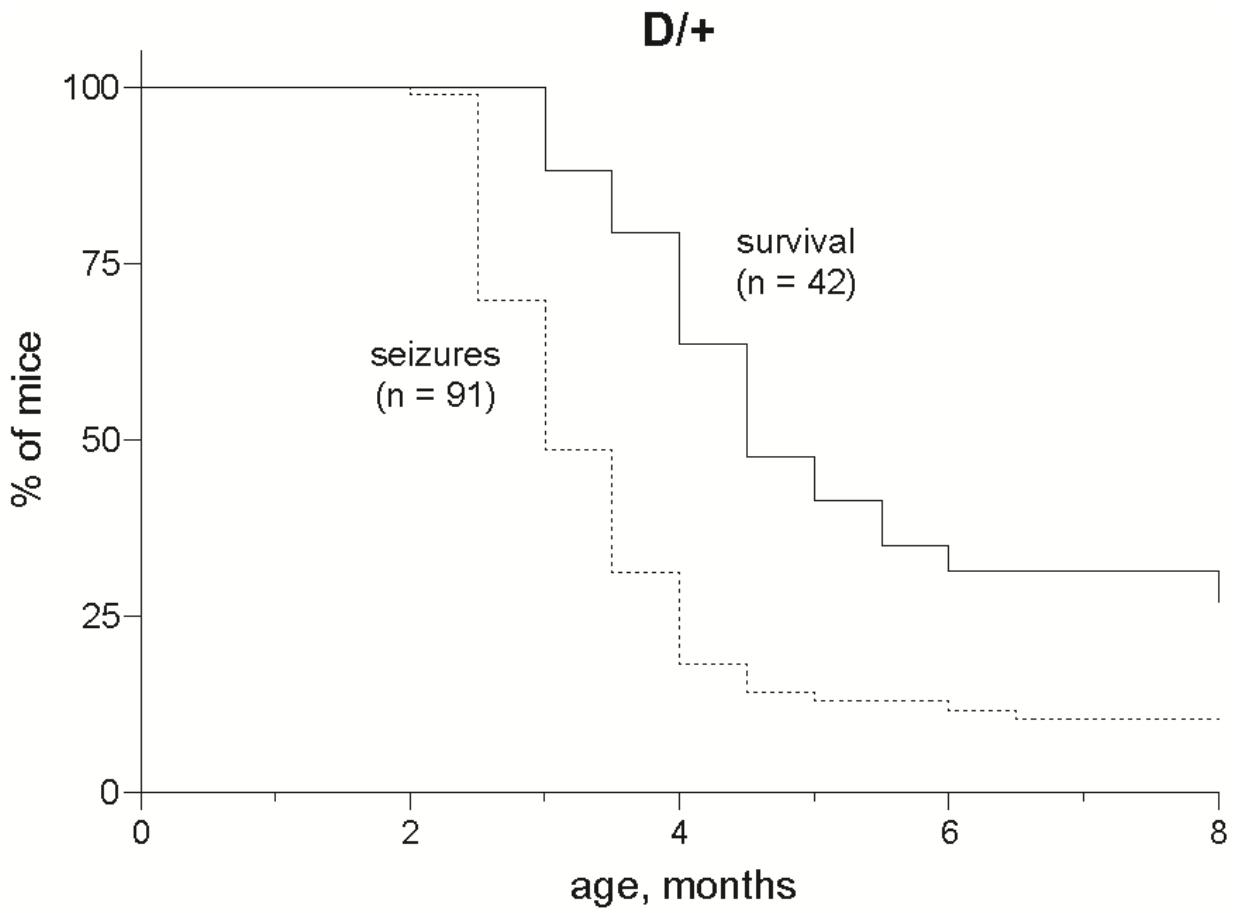

Figure 3-1. Seizure onset and death in the *Scn8a*-N1768D mouse model.
Scn8a$^{N1768D/+}$ constitutive mutant mice exhibit seizure onset at 2 to 3 months of age, followed by a 6-week interval of clustered seizures leading to lethality. Dotted line, percent of mice without seizures; solid line, survival.

Because implantation of EEG electrodes to monitor seizure onset would interfere with subsequent ICV injections of ASO, seizure onset was identified in each D/+ mouse by visual monitoring as described in Methods. Post-onset treatment was initiated 1 to 3 days after the first observation of a convulsive seizure.

Administration of *Scn8a* ASO *after* initiation of seizures is protective in D/+ mice

To evaluate post-onset effectiveness of the *Scn8a* ASO, D/+ mice were treated by intracerebroventricular injection beginning 1 to 3 days after the first observed convulsive seizure. In previous work with administration of the ASO at P2, *Scn8a* transcript level is reduced to 50% of wildtype at 3 weeks and returns to wildtype levels by 6 weeks (Lenk *et al.*, 2020). We therefore administered repeated doses of ASO at one-month intervals for the first 6 months of treatment, and at 1.5-month intervals for the second 6 months. The repeated treatments were well tolerated, without evidence of adverse effects.

Mice receiving control ASO had median survival of 1.7 months after seizure onset (n = 6, Fig. 3-2A, Table 3-1), similar to untreated D/+ mice (Fig. 3-1). In contrast, 5/7 mice treated with *Scn8a* ASO survived for 12 months (p = 0.02, Mantel-Cox log-rank test, Fig. 3-2A). During the 12 months of repeated treatment with *Scn8a* ASO, seizure frequency was reduced from 0.7 seizures / 8 hours in control mice to 0.15 seizures / 8 hours (p = 0.02, Student's t-test, Fig. 3-2B,C). Clusters of seizures occurred near the time of the next ASO administration, when *Scn8a* transcript level returns to wildtype (Lenk *et al.*, 2020). After termination of treatment with the *Scn8a* ASO, seizure frequency increased until death (Fig. 3-2D,E).

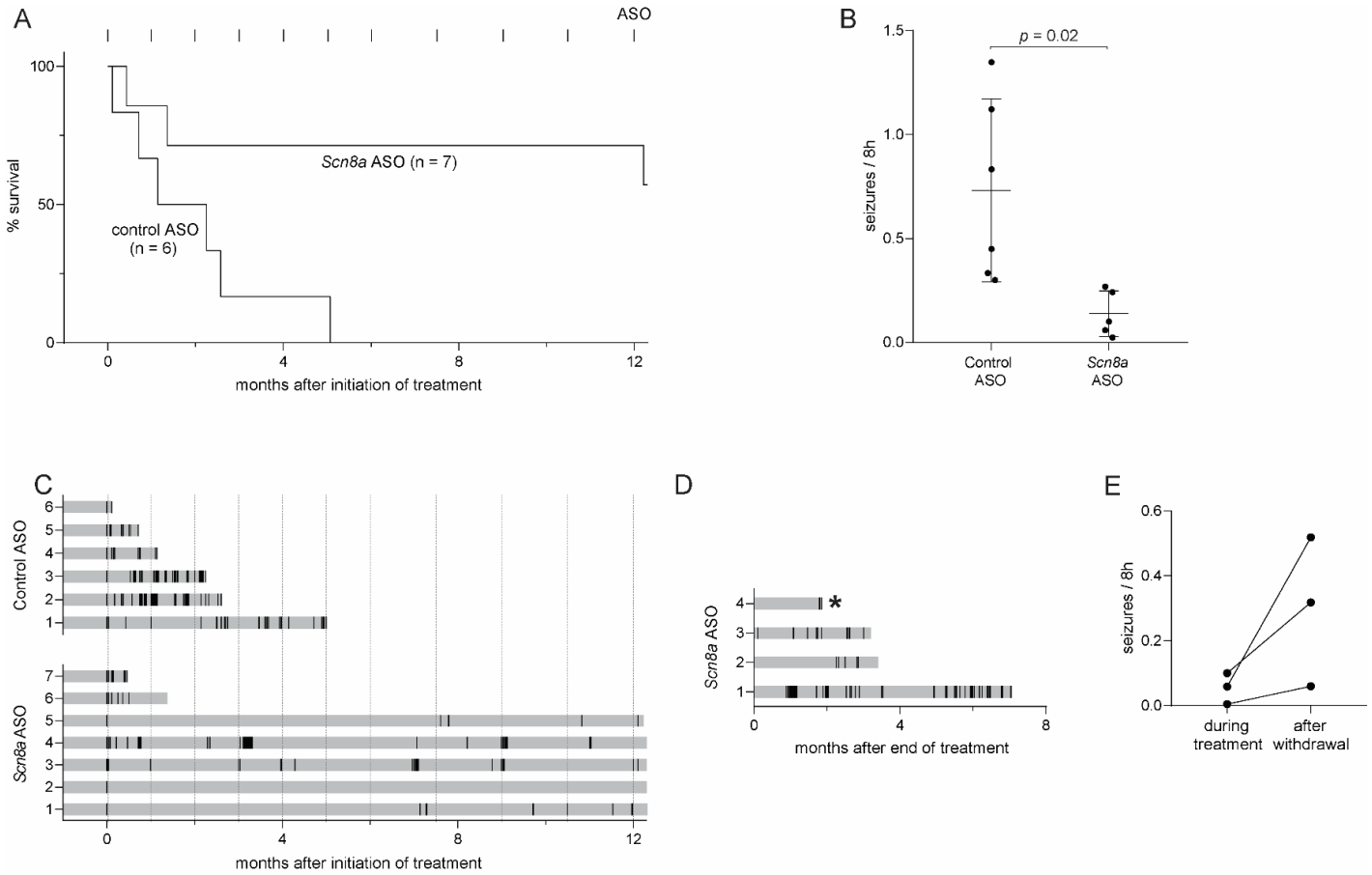

Figure 3-2. Repetitive administration of *Scn8a* ASO, initiated after seizure onset, provides long-term protection against seizures and death in D/+ mice. (A) Post-onset survival of D/+ mice treated with control or *Scn8a* ASO (p = 0.02, Mantel-Cox log-rank test). Vertical lines mark times of administration of ASO. (B) Seizure frequency in mice treated with control or *Scn8a* ASO (p = 0.02, Student's t-test). (C) Raster plot of seizures in D/+ mice treated with control or *Scn8a* ASO. Each row represents one mouse; vertical lines represent seizures. The lifespan of each mouse is indicated in grey. Dotted lines, administrations of ASO. (D) Raster plot of seizures in D/+ mice after discontinuation of ASO treatment. (E) Seizure frequency of individual D/+ mice during and after ASO treatment (p = 0.17, paired t-test). *, alive.

Table 3-1. Survival of D/+ mice treated with *Scn8a* ASO after seizure onset.

ASO	Sex	Onset, months	Death, months	Post-onset survival, months
Control				
1	F	2.6	7.6	5.0
2	M	1.5	4.1	2.6
3	M	2.0	4.3	2.3
4	M	2.4	3.5	1.1
5	F	3.1	3.9	0.7
6	M	5.6	5.7	0.1
Scn8a				
1	F	2.5	21.5	18.9
2	M	2.4	18.0	15.5
3	F	4.9	20.4	15.4
4	M	2.3	>16.1	>13.9
5	F	3.5	15.9	12.2
6	M	2.9	4.3	1.4
7	F	3.8	4.2	0.4

Two of the original seven D/+ mice that received the *Scn8a* ASO died within 2 months of the initial treatment, and did not differ from mice treated with control ASO (Fig. 3-2A). These mice may have had early seizures that were not detected, resulting in longer disease progression before treatment was initiated. These deaths suggest that it will be important to begin ASO treatment as early as possible.

DISCUSSION

DEEs are severe disorders with early onset, drug-resistant seizures as well as behavioral, intellectual, and motor disabilities. We investigated the effects of long-term reduction of *Scn8a* expression in a preclinical model of *SCN8A*-DEE. Initiation of ASO treatment was as effective after seizure onset as previously seen prior to seizure onset (Lenk *et al.*, 2020). Repeated administrations of ASO during a 12-month treatment period were well tolerated and protected most of the D/+ mice from seizures and death. These encouraging preclinical results indicate that reduction of *SCN8A* expression could provide long-term benefits for individuals with *SCN8A*-DEE.

The evaluation of post-onset treatment described here required the ability to identify disease onset and a sufficient 'therapeutic window' for the 2 weeks required for turnover of pre-existing channel protein (Makinson *et al.*, 2014). Both were feasible with the D/+ mice, which have a 6-week interval between seizure onset and death. A convulsive seizure was observed in each D/+ animal prior to initiation of ASO treatment. The lack of response in 2/7 treated mice may be explained if the earliest seizures were missed in those animals, permitting progression to a more advanced stage prior to

initiation of therapy. The effect of delaying the start of treatment will be important to determine.

We have not observed deleterious effects of reducing *Scn8a* expression. *Scn8a*$^{+/-}$ mice with 50% of normal expression exhibit absence seizures (Papale *et al.*, 2009) and anxiety-like behaviors (McKinney *et al.*, 2008). Haploinsufficient patients exhibit absence epilepsy and milder neurodevelopmental abnormalities (Johannesen *et al.*, 2022). These effects of 50% reduction of *SCN8A* may be acceptable in the context of treatment of severe DEE. The consequences of reducing *SCN8A* expression by more than 50% are not well defined. In the mouse, 90% reduction of *Scn8a* causes dystonia (Kearney *et al.*, 2002) and 95% reduction is lethal (Burgess *et al.*, 1995). Allele-specific inactivation of the pathogenic allele could limit down-regulation to a maximum of 50%.

It will be of interest to study *Scn8a* reduction in additional epileptic disorders, beyond mutations in the ion channels studied to date (*Scn1a*, *Scn8a*, *Kcnq2* and *Kcn1a*). Sodium channel blockers with preferential effects on Nav1.6 are currently in clinical trials (NBI-921352, https://clinicaltrials.gov/ct2/show/NCT03467100 and Prax-562 (Kahlig *et al.*, 2022)) and may have broader applications. Our results suggest that long-term reduction of *SCN8A* could become an effective therapy for *SCN8A*-DEE, either by repeated ASO administration or by a single administration of AAV10-shRNA.

Chapter IV

Genetic Interaction Between *Scn8a* and Axon Initial Segment Genes *Kcna1*, *Kcnq2*, and *Lgi1*[1]

ABSTRACT

Voltage-gated sodium and potassium channels regulate the initiation and propagation of neuronal action potentials. Gain-of-function mutations of sodium channel *Scn8a* and loss-of-function mutations of potassium channels *Kcna1* and *Kcnq2* or secreted protein *Lgi1* increase neuronal activity and lead to epilepsy. We tested the hypothesis that reducing expression of *Scn8a* would compensate for loss-of-function mutations of *Kcna1*, *Kcnq2*, or *Lgi1. Scn8a* expression was reduced by administration of an antisense oligonucleotide (ASO). This treatment lengthened survival of the *Kcn1a* and *Kcnq2* mutants, and reduced seizure frequency in the *Kcnq2* mutant mice. The *Scn8a* ASO also prolonged the lifespan of *Lgi1* mutant mice by one week. These observations suggest that reduction of *SCN8A* may be therapeutic for genetic epilepsies resulting from potassium channel mutations.

---

[1] Except for discussion of the *Lgi1* mutant, this work was published as: Hill SF, Ziobro J, Jafar-Nejad P, Rigo F, Meisler M. Genetic interaction between *Scn8a* and potassium channel genes *Kcna1* and *Kcnq2*. *Epilepsia*, 2022.

Julie Ziobro performed the EEG experiments shown in Figures 4-1D and 4-2D. The *Scn8a* ASO was synthesized by Frank Rigo and Paymaan Jafar-Nejad at Ionis Pharmaceuticals (Carlsbad, CA). I performed the remaining experiments.

INTRODUCTION

Sodium and potassium channels concentrated at the axon initial segment (AIS) regulate the generation of neuronal action potentials (Bean, 2007; Huang and Rasband, 2018). Action potentials are initiated by excitatory stimuli that activate voltage-gated sodium channels, permitting influx of sodium ions (Bean, 2007). Subsequent activation of voltage-gated potassium channels permits the exit of potassium ions and repolarizes the neuron (Bean, 2007). Potassium channels encoded by *KCNQ2* modulate subthreshold changes in membrane potential that influence neuronal excitability (Miceli *et al.*, 1993; Weckhuysen *et al.*, 2012). In genetic epilepsies, elevated sodium channel activity or reduced potassium channel activity can result in excess neuronal firing (D'Adamo *et al.*, 2020; Meisler *et al.*, 2021). Emerging genetic therapies for seizure disorders include reduction of sodium channel expression (Lenk *et al.*, 2020) or elevation of potassium channel expression (Snowball *et al.*, 2019; Colasante *et al.*, 2020a). Here, we test the hypothesis that reduced expression of an AIS-concentrated sodium channel can compensate for loss of potassium channel activity.

Loss-of-function mutations of the potassium channel gene *KCNQ2* are a major cause of developmental and epileptic encephalopathy (DEE) (Miceli *et al.*, 1993; Weckhuysen *et al.*, 2012), and loss of function mutations of potassium channel *KCNA1* are responsible for episodic ataxia type 1 and rare cases of DEE (D'Adamo *et al.*, 2020). The secreted protein LGI1 interacts with Kv1 complexes at the synapse (Yamagata *et al.*, 2018). Heterozygous loss-of-function mutations in *LGI1* cause autosomal dominant temporal lobe epilepsy, and autoantibodies against LGI1 also cause seizures (Yamagata *et al.*, 2018).

We used an antisense oligonucleotide (ASO) to reduce expression of the sodium channel gene *Scn8a* in mouse models of *Kcnq2*, *Kcna1*, and *Lgi1* epilepsy. *Scn8a* transcripts were reduced to 50% of wildtype level by administration of the ASO. Transcript levels return to normal 6 weeks after a single injection (Lenk *et al.*, 2020). Our observations suggest that specific reduction of *SCN8A* expression may be a useful therapy for disorders of these potassium channels.

METHODS

Mice

Kcnq2$^{fl/fl}$ mice (Soh *et al.*, 2014) on strain C57BL/6J were provided by Dr. Anastasios Tzingounis, University of Connecticut. *Kcna1*$^{+/-}$ mice (Smart *et al.*, 1998) on a mixed Black Swiss genetic background (Tac:N:NIHS-BC) were provided by Dr. Edward Glasscock, Southern Methodist University. Emx1-Cre mice on strain C57BL/6J were purchased from the Jackson Laboratory (Jax #005628). Both male and female mice were used for the experiments. Mice were housed and cared for in accordance with NIH guidelines in a 12/12-hour light/dark cycle with standard mouse chow and water available ad libitum. All experiments were approved by the Institutional Animal Care and Use Committee (IACUC) at the University of Michigan.

Antisense oligonucleotides

The twenty base-pair *Scn8a* gapmer ASO (5’ GACGA TTAGT GACAT AGGCT 3’), synthesized by Ionis Pharmaceuticals, is complementary to the 3’ UTR of the mouse *Scn8a* transcript (Lenk *et al.*, 2020). The control ASO (5’ CCTAT AGGAC TATCC AGGAA 3’) does not match any mouse transcript and is well tolerated in vivo (Lenk *et al.*, 2020). ASOs were diluted in phosphate-buffered saline

(PBS) for injection. At postnatal day 2 (P2), mutant mice received 45 ug ASO in 2 uL by intracerebroventricular (ICV) injection into the left lateral ventricle. Adult mice were anesthetized with isoflurane and received 100 ug ASO in a 3 uL manual ICV injection into the left lateral ventricle without a guide cannula, as described (Kim *et al.*, 2016).

EEG recording

Screw electrodes were implanted in *Kcnq2*$^{fl/fl}$,*Emx1-Cre* mice at postnatal week 6 (n=2) and in *Kcna1*$^{-/-}$ mice at postnatal week 20 (n=2). For surgery, mice were anesthetized with isoflurane and placed in a stereotaxic adapter. Bilateral screw electrodes were placed in the skull at approximately AP=-2.1, ML= +/-1.7 and a common reference electrode was placed over the cerebellum (approximately AP=-6.0, ML=0). The electrodes were connected to a 6-pin electrode pedestal and the headcap was secured using dental cement. After 1-7 days of recovery, simultaneous EEG recording and video monitoring were performed with a Natus recording system continuously for a minimum of 24 hours and a maximum of 14 days. Signals were acquired at 256 Hz. Data were filtered with a 70Hz low pass filter and 1 Hz high pass filter. Seizures and interictal background were assessed manually by an experienced reader. Seizures were defined as a sudden burst of electrographic activity consisting of rhythmic spike-and-wave discharges lasting >10 seconds and evolving in frequency and amplitude. Interictal epileptiform discharges were not quantified.

Phenotypes

Hindlimb clasping in *Kcnq2* mutant mice was video recorded on P21-23. Mice were suspended by the tail for one minute on three consecutive days. Myoclonic

jerks in *Kcna1* mice were counted during a 5-minute observation period at 11 AM on three successive days by two independent observers blinded to genotype.

RESULTS

Kcnq2 mutant mice

KCNQ2 encodes the AIS-localized potassium channel Kv7.2 which regulates sub-threshold neuronal excitability and resting membrane potential (Miceli *et al.*, 1993; Weckhuysen *et al.*, 2012). Loss-of-function mutations of human *KCNQ2* cause a spectrum of disorders ranging from benign familial neonatal seizures to DEE**,** and it is the second most common gene mutated in DEE (Miceli *et al.*, 1993; Weckhuysen *et al.*, 2012).

Deletion of *Kcnq2* in forebrain excitatory neurons in *Kcnq2$^{fl/fl}$,Emx1-Cre* mice results in neuronal hyperexcitability and spontaneous seizures, as seen in human *KCNQ2* disorders (Soh *et al.*, 2014). The seizures and premature death in these mice provide a useful endpoint for therapeutic intervention. We treated *Kcnq2$^{fl/fl}$,Emx1-Cre* mice with 45 ug of *Scn8a* ASO or control ASO by intracerebroventricular (ICV) injection at postnatal day 2 (P2) (Fig. 4-1A). After treatment with control ASO (n = 12), the first death was observed at 3 weeks of age, and 50% lethality was reached by 8 weeks of age (Fig. 4-1B&C). In mice receiving the *Scn8a* ASO, the first death was delayed to 11 weeks of age, and 50% lethality was not reached until 15 weeks. A second dose of 100 ug ASO at 8 weeks of age further delayed the age of 50% lethality to 19 weeks (Fig. 4-1B&C). Overall, 65% to 75% of mice exhibited premature lethality, regardless of treatment (Chi-square test of proportions, χ^2=0.36, df=2, p=0.83). Reduction of *Scn8a* expression thus extended the lifespan of mice with *Kcnq2* deficiency but did not prevent premature lethality.

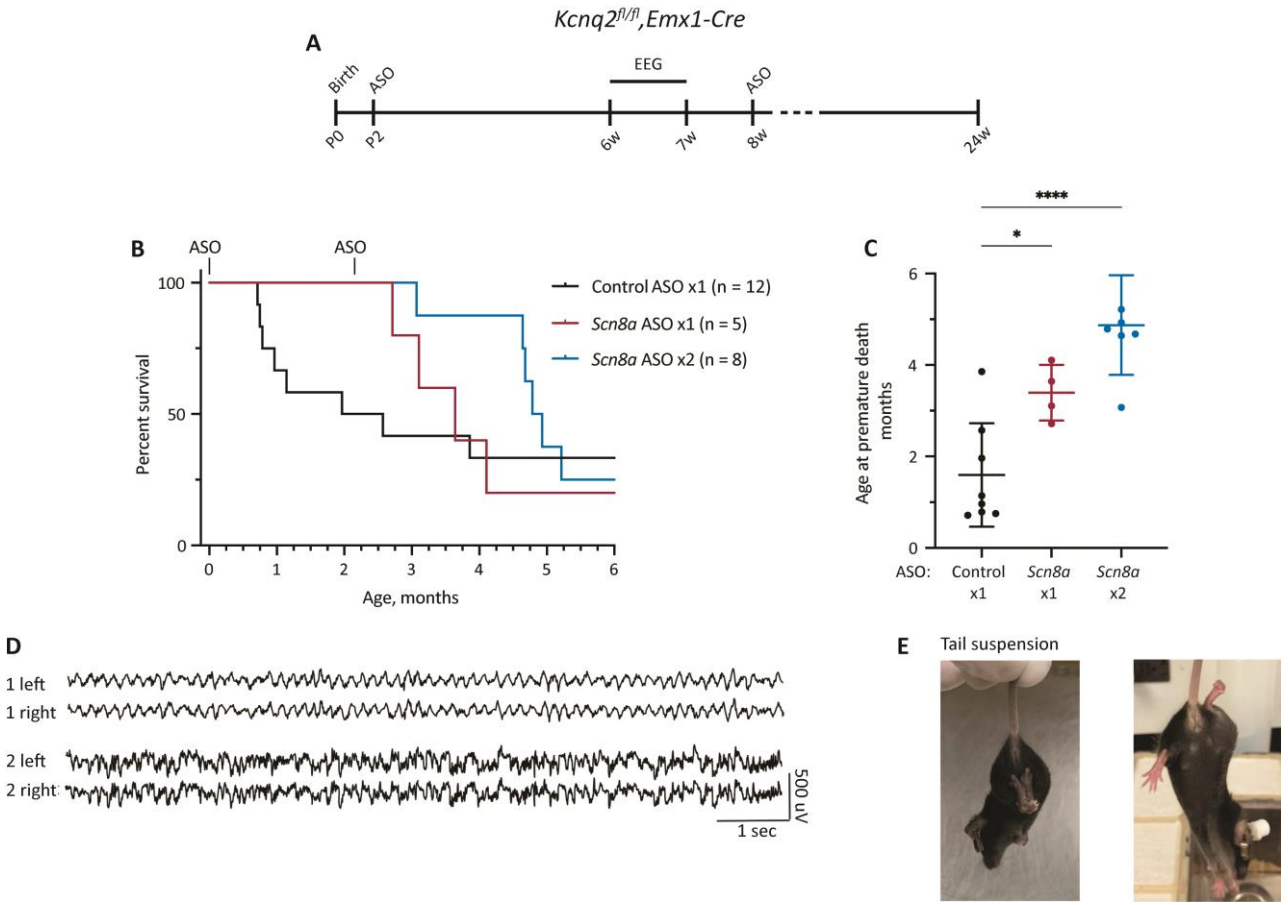

Figure 4-1. *Scn8a* ASO prolongs survival of *Kcnq2* mutant mice. (A) Timeline for treatment. (B, C) *Kcnq2*$^{fl/fl}$*,Emx1Cre* mice treated with Scn8a ASO survive longer than mice treated with control ASO. A second treatment prolonged the effect. Asterisks indicate significance of Bonferroni's multiple comparisons test: *, $p < 0.05$; ****, $p < 0.0001$. (D) Sample EEG recordings demonstrating normal EEG background in two mutant mice. (E) Abnormal hindlimb postures in *Kcnq2*$^{fl/fl}$*,Emx1Cre* mice after treatment with Scn8a ASO at P2.

The frequency of spontaneous seizures in untreated *Kcnq2*$^{fl/fl}$*,Emx1-Cre* mice was 40 seizures in 67 days of observation (Soh *et al.*, 2014; Aiba and Noebels, 2021). After treatment with *Scn8a* ASO, we did not observe any seizures or abnormal EEG activity in 16 days of observation ($p<0.0001$, χ^2 test) (Fig. 4-1D). However, the treated mice continued to exhibit hunched posture, scruffy appearance and hindlimb clasping (Fig. 4-1E). Reduction of *Scn8a* expression thus prevents seizures and delays premature death but does not correct the other neurological phenotypes in *Kcnq2* mutant mice. Postnatal growth of *Kcnq2*$^{fl/fl}$*,Emx1-Cre* mice did not differ from wildtype littermates.

Kcna1 mutant mice

KCNA1 encodes Kv1.1, an inward rectifier potassium channel concentrated at the AIS (D'Adamo *et al.*, 2020). Heterozygous loss-of-function mutations of *KCNA1* cause severe epilepsy and episodic ataxia type 1 that can be accompanied by seizures (D'Adamo *et al.*, 2020). Homozygous *Kcna1* null mice are a model of sudden unexpected death in epilepsy (SUDEP) (Smart *et al.*, 1998).

Kcna1$^{-/-}$ mice were treated with 45 ug *Scn8a* ASO or control ASO by ICV injection at P2 (Fig. 4-2A). Mice that received control ASO at P2 (n = 10) died between 2 and 6 weeks of age with 50% lethality by 1 month of age (Fig. 4-2B&C). A single dose of *Scn8a* ASO extended median lifespan to 3 months (n = 9) (Fig. 4-2B&C). To evaluate repeated treatments, additional doses of 100 ug ASO were administered at monthly intervals between 1 and 4 months of age (Fig. 4-2A). The repeated treatments delayed the earliest death to 13 weeks (n = 9), with less than 50% lethality at 6 months of age (Fig.

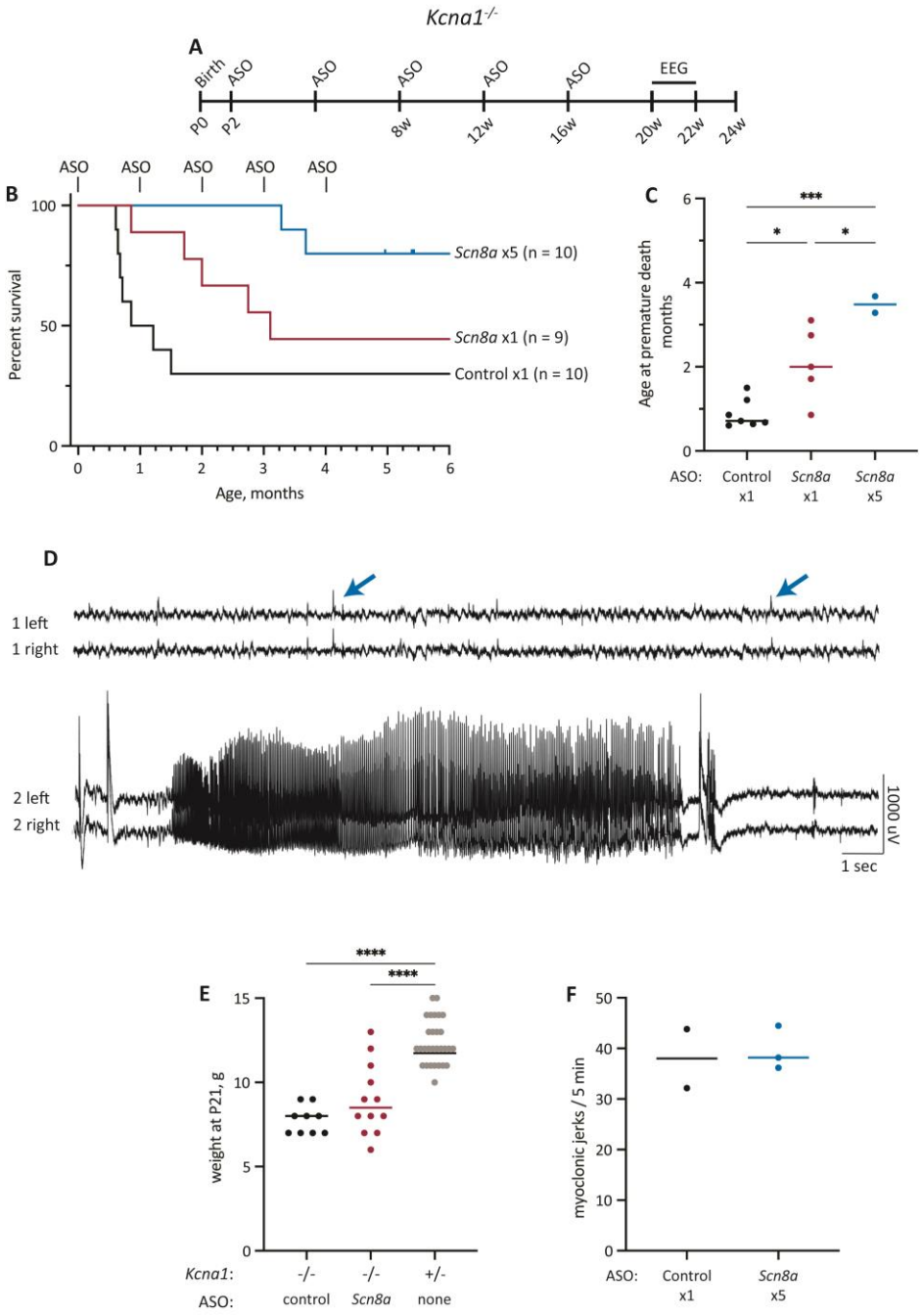

Figure 4-2. *Scn8a* ASO prolongs survival of *Kcna1* mutant mice. (A) Timeline for treatment. (B, C) *Kcna1*$^{-/-}$ mice treated with *Scn8a* ASO survive longer than mice treated with control ASO. Asterisks indicate significance of Bonferroni's multiple comparisons test: *, $p < 0.05$; ***, $p < 0.0005$. (D) EEG recordings showing abnormal interictal discharges (arrows) and electrographic seizure. (E) *Scn8a* ASO does not correct the growth deficit in *Kcna1*$^{-/-}$ mice. (F) *Scn8a* ASO does not prevent myoclonic jerks in *Kcna1*$^{-/-}$ mice.

4-2B&C). The penetrance of premature lethality was reduced from 70% (control ASO) to 20% (*Scn8a* ASO) (Chi-square test of proportions, χ^2=5.05, *df*=2, *p*=0.025).

Spontaneous seizures in untreated *Kcna1*$^{-/-}$ mice were reported to begin at 3 weeks of age (Smart *et al.*, 1998) and occur 5-20 times per day with diurnal variation in frequency (Smart *et al.*, 1998; Fenoglio-Simeone *et al.*, 2009). We implanted electrodes at 20 weeks of age in *Kcna1* null mice that had been treated with five doses of ASO starting at P2 (Fig. 4-2A). Electrographic and electro-clinical seizures were detected with an average frequency of 13 seizures per day (representative example, Fig. 4-2D).

Kcna1$^{-/-}$ mice also exhibit hunched posture, scruffy appearance, and impaired growth that was not corrected by the ASO (Fig. 4-2E). *Kcna1*$^{-/-}$ also mice exhibit myoclonic jerks that were not corrected by ASO treatment (Fig. 4-2F). Thus, reduction of *Scn8a* expression prolonged survival of *Kcna1*$^{-/-}$ mice but did not completely rescue the neurological abnormalities.

Lgi1 **mutant mice**

Loss-of-function mutations of *LGI1* are a rare cause of epilepsy (Lindy *et al.*, 2018; Yamagata *et al.*, 2018). Autoantibodies against *LGI1* also cause seizures (Yamagata *et al.*, 2018; Baudin *et al.*, 2021). *LGI1* encodes a secreted protein that interacts with ADAM22, ADAM23, and the Kv1 complex at the axon initial segment (Yamagata *et al.*, 2018). In the mouse, homozygous loss of *Lgi1* causes spontaneous seizures and death (Chabrol *et al.*, 2010).

We treated *Lgi1*$^{-/-}$ mice with 45 ug control or *Scn8a* ASO by ICV injection at P2. Mice treated with control ASO (n = 5) died with 100% penetrance between P18 and P21

(Fig. 4-3A). Mutant mice that received *Scn8a* ASO (n = 6) lived between 23 and 27 days, one week longer than control-treated mice (p = 0.0007, Mantel-Cox log-rank test, Fig. 4-3A). Due to the small size of this effect, we did not pursue repeated dosing in *Lgi1* mutant mice. We also observed that the *Lgi1*$^{-/-}$ mice are smaller than their unaffected littermates (Fig. 4-3B). This effect was not rescued by the *Scn8a* ASO (Fig. 4-3B).

DISCUSSION

Reduction of *Scn8a* expression had therapeutic benefits in two models of epilepsy caused by mutation of potassium channels localized at the AIS. *KCNQ2* is one of the most commonly mutated genes in childhood-onset epilepsy (Miceli *et al.*, 1993; Weckhuysen *et al.*, 2012). Reduced *Scn8a* extended the lifespan of *Kcnq2* mutant mice by 11 weeks and restored normal EEG activity but did not eliminate other neurological abnormalities. In the *Kcn1a* null mice, reduction of *Scn8a* expression significantly prolonged lifespan. The *Scn8a* ASO also prolonged the lifespan of *Lgi1* null mice, thought the effect was not long-lasting. The positive effect of reducing *Scn8a* is consistent with the therapeutic effectiveness of sodium channel blockers in some individuals with *KCNQ2* mutations (Miceli *et al.*, 1993) and in improving the symptoms of episodic ataxia in many individuals with null mutations of *KCNA1* (Lauxmann *et al.*, 2021). $Na_V1.6$ is a major source of persistent current in mammalian brain, and reduction of persistent current led to reduced seizures in an *in silico* model of Kv1 deficiency

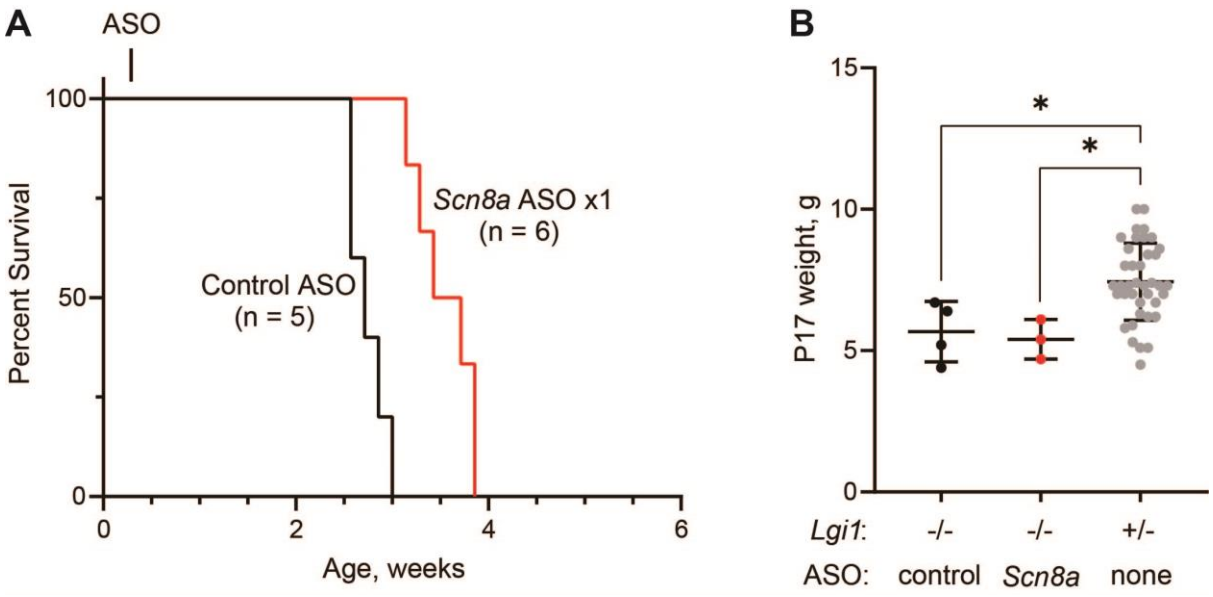

Figure 4-3. *Scn8a* ASO slightly prolongs survival of *Lgi1* mutant mice. (A) *Lgi1*$^{-/-}$ mice treated with *Scn8a* ASO survive longer than mice treated with control ASO. (B) *Scn8a* ASO does not correct the growth deficit in *Lgi1*$^{-/-}$ mice.

(Du *et al.*, 2020b). The effectiveness of the ASO in these two models demonstrates that specific reduction of *SCN8A* without changes in other sodium channels can be therapeutic for potassium channel deficiency.

The mechanism by which loss of *LGI1* leads to epilepsy is still unclear (Baudin et al., 2021), so we were surprised that reduced *Scn8a* expression improved survival in these mice. This effect may be mediated through the potassium channels, which are binding partners of *LGI1*, or may be due to the general inhibitory effect of reducing Nav1.6 activity. There is some evidence that sodium channel blockers are more effective than other drugs in individuals with *LGI1* autoencephalitis (Feyissa *et al.*, 2018; Uribe-San-Martin *et al.*, 2020). However, a P2 administration of the *Scn8a* ASO reduces *Scn8a* expression for approximately 6 weeks (Lenk *et al.*, 2020). The *Lgi1*$^{-/-}$ mice treated with *Scn8a* ASO died before *Scn8a* expression returned to wildtype levels. More drastic downregulation of *Scn8a* may be required to protect *Lgi1* mutants.

Our results add to a growing body of evidence demonstrating genetic interactions between genes encoding ion channels (Meisler *et al.*, 2010; Meisler *et al.*, 2021). The calcium channel genes *Cacna1a* and *Cacna1g* have been identified as modifiers of *Kcna1* epilepsy (Glasscock *et al.*, 2007) and Dravet syndrome (Calhoun *et al.*, 2017). Quantitative variation in the GABA receptor subunit *Gabra2* modifies the severity of *Scn8a* epilepsy and Dravet syndrome (Yu *et al.*, 2020; Meisler *et al.*, 2021; Yu *et al.*, 2022). The current work demonstrates that quantitative variation in *Scn8a* modifies the severity of *Kcna1* and *Kcnq2* epilepsy in mouse models. *Scn8a* is also a modifier of Dravet syndrome (Lenk *et al.*, 2020). *Scn2a* modifies the severity of *Kcna1* (Mishra *et al.*, 2017) and *Kcnq2* epilepsy (Kearney *et al.*, 2006). In a human pedigree, an allelic

variant of *SCN1A* was recently found to modify the severity of a null allele (Johnson *et al.*, 2022). Neuronal excitability is evidently influenced by overall ion channel content, and compensatory modulation of channel genes can restore the balance of excitation and inhibition that is disrupted in epilepsy.

The effects of *Scn8a* modulation shown here suggest that specific reduction of *Scn8a* might replace non-specific sodium channel blockers in treating epilepsies caused by *KCNQ2* and *KCNA1*. In contrast to heterozygous affected patients, the mouse models studied here were homozygous for the potassium channel deficits, and the *Kcnq2* deficiency was expressed only in forebrain excitatory neurons. The side effects associated with non-specific sodium channel blockers are likely to be reduced by specific reduction of *SCN8A*, for example with an Nav1.6-specific drug such as NBI-921352, which is currently in phase 1 clinical trial for treatment of patients with gain-of-function mutations of *Scn8a* (https://clinicaltrials.gov/ct2/show/NCT03467100). Genetic therapies such as viral delivery of shRNA or CRISPR/Cas9 knockout may also be applicable to the potassium channel disorders.

ACKNOWLEDGEMENTS

We are grateful to Dr. Anastasios Tzingounis for providing *Kcnq2*$^{fl/fl}$ mice and Dr. Edward Glasscock for providing *Kcna1*$^{+/-}$ mice. We thank Sanjna Chalasani and Aparna Sumanth for technical assistance with genotyping. This work was supported by NINDS Grant RO1 NS34509 from the National Institutes of Health and a grant from the Rackham School of Graduate Studies, University of Michigan.

Chapter V

Reduction of *Kcnt1* is Therapeutic in Mouse Models of *SCN8A* and *SCN1A* Epilepsy

ABSTRACT

Developmental and epileptic encephalopathies (DEEs) are severe seizure disorders with inadequate treatment options. Mutations of neuronal ion channel genes are common causes of DEE. We previously demonstrated that reduced expression of the sodium channel gene *Scn8a* is therapeutic in mouse models of potassium channel mutations. We tested whether reducing expression of the potassium channel *Kcnt1* with an antisense oligonucleotide (ASO) would be therapeutic in mouse sodium channel mutants. The *Kcnt1* ASO prolonged survival of *Scn8a* and *Scn1a* mutant mice. The non-specific KCNT1 channel blocker quinidine did not extend the survival of *Scn8a* mutant mice. Our results implicate KCNT1 as a target for therapy in *SCN8A* and *SCN1A* epilepsy.

INTRODUCTION

Developmental and epileptic encephalopathies (DEEs) are among the most severe and devastating epilepsies. A typical disease course begins with seizure onset before one year of life, followed by onset of developmental delay, movement disorders, intellectual disability, sleep disturbances, and feeding difficulties (Scheffer and Nabbout, 2019; Meisler *et al.*, 2021; Johannesen *et al.*, 2022). Seizures are often resistant to treatment with current antiepileptic drugs (Scheffer and Nabbout, 2019; Meisler *et al.*, 2021; Johannesen *et al.*, 2022).

Many DEE mutations occur in sodium and potassium channel genes (Lindy *et al.*, 2018; Symonds *et al.*, 2019). Based on their roles in the neuronal action potential, excessive sodium current or insufficient potassium current would be predicted to cause hyperexcitability and therefore epilepsy. Accordingly, missense mutations in the voltage-gated sodium channel gene *SCN8A* that result in excessive sodium current ('gain-of-function', or GOF, mutations) cause *SCN8A*-DEE (Veeramah *et al.*, 2012; Meisler *et al.*, 2021; Johannesen *et al.*, 2022). Expression of an *SCN8A* GOF mutation in excitatory neurons is sufficient to cause seizures and premature death, but expression only in inhibitory neurons is not (Bunton-Stasyshyn *et al.*, 2019).

However, not all genes follow this logic. Loss-of-function (LOF) mutations of the sodium channel gene *SCN1A* and GOF mutations of the potassium channel gene *KCNT1* cause epilepsy (Barcia *et al.*, 2012; Scheffer and Nabbout, 2019; Gribkoff and Winquist, 2023). In both cases, hyperexcitability results from preferential effects in

inhibitory neurons (Cheah *et al.*, 2012; Favero *et al.*, 2018; Shore *et al.*, 2020; Gertler *et al.*, 2022; Wu *et al.*, 2023).

KCNT1 is a sodium-activated potassium channel (also known as Slo2.2, $K_{Na}1.1$, or Slack) with widespread expression in the central nervous system (Rizzi *et al.*, 2016). In wildtype neurons, KCNT1 regulates the afterhyperpolarization amplitude and action potential threshold (Martinez-Espinosa *et al.*, 2015; Quraishi *et al.*, 2019; Shore *et al.*, 2020; Gertler *et al.*, 2022; Wu *et al.*, 2023). *KCNT1* GOF mutations enhance bursting behavior in excitatory neurons and reduce action potential firing in inhibitory neurons (Quraishi *et al.*, 2019; Shore *et al.*, 2020; Gertler *et al.*, 2022; Wu *et al.*, 2023).

In the mouse, homozygous knock-in of *KCNT1* GOF mutations causes spontaneous seizures, reduced seizure induction threshold, behavioral abnormalities, and premature lethality (Quraishi *et al.*, 2020; Shore *et al.*, 2020; Burbano *et al.*, 2022; Gertler *et al.*, 2022). Administration of an antisense oligonucleotide (ASO) that reduces *Kcnt1* expression improves these phenotypes (Burbano *et al.*, 2022). Homozygous loss of *Kcnt1* improves survival following electrically induced seizures (Quraishi *et al.*, 2020). Based on these results, we hypothesized that reduced expression of *KCNT1* could be protective against DEE.

We have previously shown that reducing expression of *Scn8a* prolongs survival of mice with epilepsy caused by loss of the potassium channel genes *Kcna1* and *Kcnq2* (Hill *et al.*, 2022). Here, we asked whether modulating potassium channel expression can improve the phenotype of sodium channel mutants. Administration of the *Kcnt1* ASO (Burbano *et al.*, 2022) on postnatal day 2 doubled the lifespan of an *Scn8a* mutant mouse and extended survival of *Scn1a* haploinsufficient mice. Our results suggest a

new avenue for therapeutic intervention in DEEs caused by mutations of *SCN1A* and *SCN8A*.

METHODS

Mice

The *Scn8a*^{cond} allele, which has Cre-dependent expression of the patient GOF mutation p.R1872W, was maintained on a C57BL/6J background (Bunton-Stasyshyn *et al.*, 2019). The R1872W mutation was activated in all cells by crossing to female mice carrying the *EIIa-Cre* transgene on a C57BL/6J background (JAX 003724). *Scn1a*$^{+/-}$ mice carry a deletion of exon 1 (Miller *et al.*, 2014). This model was maintained on the protective 129S6/SvEvTac strain background (Miller *et al.*, 2014). We carried out experiments on F1 (C57BL/6J X 129S6/SvEvTac) mice (Miller *et al.*, 2014). Both male and female mice were used for all experiments. All experiments were approved by the Committee on the Use and Care of Animals at the University of Michigan.

ASOs

ASOs were synthesized by Ionis Pharmaceuticals as described (Swayze *et al.*, 2007). Both the scrambled control and *Kcnt1* ASOs are 20-bp gap-mers with 5 2'-*O*-methoxyethyl modifications on the first and last 5 bases and phosphorothioate modifications on all 20 bases. The *Kcnt1* ASO (5' GCT TCA TGC CAC TTT CCA GA 3') is complementary to the 3' UTR of mouse *Kcnt1* and was previously described (Burbano *et al.*, 2022). The scrambled control ASO (5' CCT ATA GGA CTA TTC AGG

AA 3') is well-tolerated and is not complementary to any transcript encoded by the mouse genome (Swayze *et al.*, 2007).

Intracerebroventricular (ICV) injections

At postnatal day 2 (P2), mice were cryo-anesthetized for 3 minutes. ASO diluted in PBS (2 µL) was manually injected into the left ventricle as described (Lenk *et al.*, 2020). Animals were allowed to recover for 10 minutes at 37ºC before being returned to the home cage.

qRT-PCR

Brain and spinal cord from 3 week old mice treated with control or *Kcnt1* ASO were preserved in TRIzol (Invitrogen Cat. #15596026, Waltham, MA). RNA was extracted using the Direct-zol RNA Mini Prep kit from Zymo Research (Irvina, CA). cDNA was synthesized with the LunaScript kit from New England Biolabs (Ipwsich, MA). *Scn8a* (Mm00488110_m1), *Kcnt1* (Mm01330661_g1), and *Tbp* (Mm01277042_m1) transcripts were quantified using TaqMan gene expression assays (Applied Biosystems, Foster City, CA).

Quinidine administration

Quinidine (Sigma Aldrich, St. Louis MO) was diluted in phosphate-buffered saline (50 or 100 mg/kg) and administered by daily intraperitoneal injection beginning at P10.

RESULTS

Characterization of the *Kcnt1* ASO

We used an ASO to reduce expression of mouse *Kcnt1*. The 20 base-pair "gap-mer" ASO targets the 3' UTR of the mouse *Kcnt1* gene (Fig. 5-1A) and recruits RNaseH1 to degrade the transcript (Burbano *et al.*, 2022). We first administered the ASO to wild-type animals by ICV injection at P2. Three weeks later, we measured gene expression in brain and spinal cord by qRT-PCR (Fig. 5-1B). *Kcnt1* expression was reduced in a dose-dependent manner in both brain and spinal cord (two-way ANOVA, $p < 0.0001$). Reduction of *Kcnt1* transcript also reduces KCNT1 protein expression (Burbano *et al.*, 2022). Expression of *Scn8a* was unaffected (two-way ANOVA, $p = 0.5929$, Fig. 5-1C).

Kcnt1 ASO administration in a mouse model of *SCN8A* epilepsy

We previously generated a mouse with Cre-dependent expression of the patient p.R1872W mutation (Bunton-Stasyshyn *et al.*, 2019). Expression of this mutation in all cells by crossing with *EIIa-Cre* mice results in a single, lethal seizure at P14 (Bunton-Stasyshyn *et al.*, 2019). We treated *Scn8a*$^{cond/+}$*,EIIa-Cre* (W/+) animals with 15-45 µg *Kcnt1* ASO by ICV injection at P2. Control ASO-treated mice exhibited median survival of 16 days (n = 19) (Fig. 5-2A). Mice treated with 15 µg *Kcnt1* ASO lived three days longer (median survival = 19 days, n = 15, $p = 0.0493$, Mantel-Cox log-rank test). Treatment with 30 µg *Kcnt1* ASO extended median survival to 27 days (n = 20, $p < 0.0001$, Mantel- Cox log-rank test). Mice treated with 45 µg, the optimal dose, exhibited median survival of 36 days, more than double the lifespan of control ASO-treated mice (n =13, $p < 0.0001$, Mantel-Cox log-rank tests, Fig. 5-2A). Treatment with 60 or 75 µg *Kcnt1* ASO was tolerated, but no additional survival benefit was observed (Fig. 5-2B).

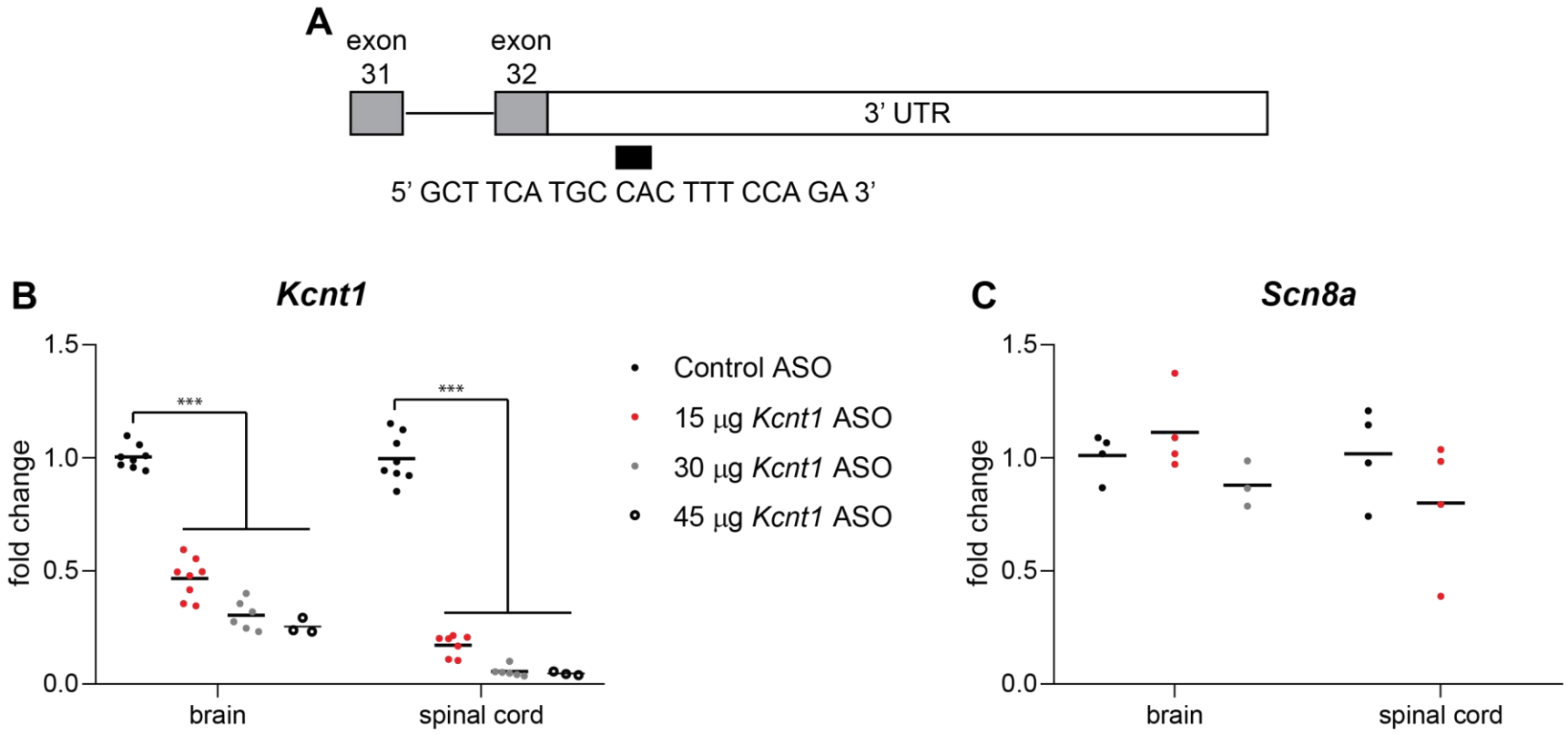

Figure 5-1. *Kcnt1* ASO reduces *Kcnt1* transcript without affecting *Scn8a* expression. (A) The *Kcnt1* ASO targets the proximal 3'UTR of the *Kcnt1* transcript. (B-C) Expression of *Kcnt1* (B) or *Scn8a* (C) in brain and spinal cord from P21 wildtype mice treated with *Kcnt1* ASO at P2, measured by qRT-PCR (*** indicates $p < 0.0001$, Sidak's multiple comparisons test).

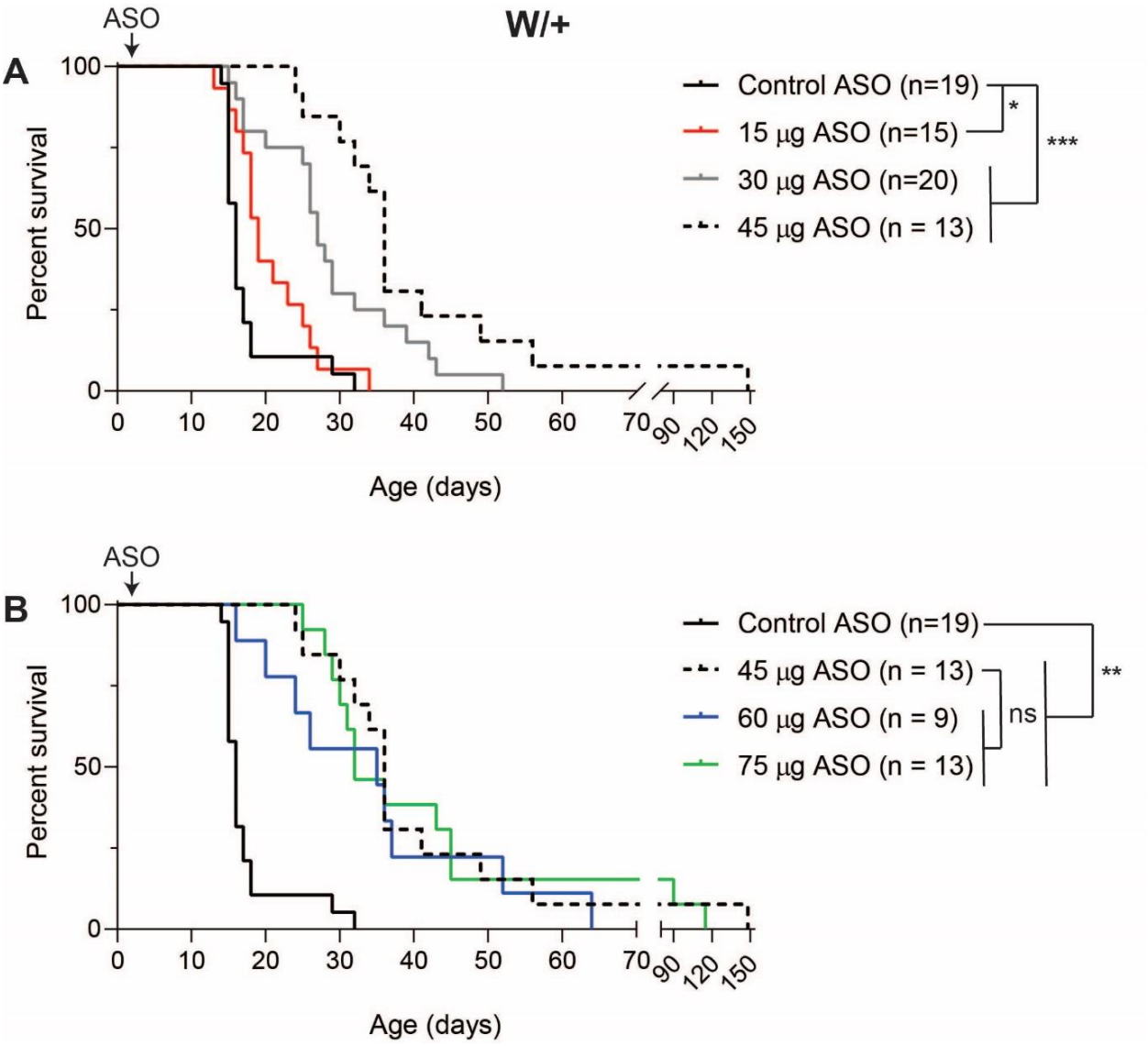

Figure 5-2. *Kcnt1* ASO prolongs survival of *Scn8a* mutant mice. Survival of *Scn8a*$^{cond/+}$,*EIIa-Cre* (W/+) mice treated 15-45 µg (A) or 45 -75 µg *Kcnt1* ASO at P2 compared to previously-published mice treated with control ASO (Lenk *et al.*, 2020). Asterisks indicate significance of Mantel-Cox log-rank tests: * = $p < 0.05$, ** = $p < 0.0005$, *** = $p < 0.0001$, ns = not significant.

Quinidine administration in a mouse model of *SCN8A* epilepsy

Quinidine is a nonspecific cation channel blocker used to treat cardiac arrhythmia. *In vitro*, quinidine blocks KCNT1 channel activity, suggesting that it could be a precision therapy for patients with gain-of-function *KCNT1* mutations (Mori *et al.*, 1998; Milligan *et al.*, 2014). *In vivo*, quinidine has demonstrated mixed efficacy in *KCNT1* epilepsy patients (Mikati *et al.*, 2015; Numis *et al.*, 2018; Fitzgerald *et al.*, 2019; Cole *et al.*, 2021).

To determine whether inhibition of KCNT1 channels by quinidine is therapeutic in *Scn8a* mutant mice, we administered 50 or 100 mg/kg quinidine to W/+ mice by daily intraperitoneal injection beginning at P10 (Fig. 5-3). Untreated mice exhibited median survival of 15 days (n = 47). Treatment with 50 or 100 mg/kg quinidine did not extend the lifespan of W/+ mice (median survival = 14 days; n = 7 & 9, respectively; Fig. 5-3).

***Kcnt1* ASO administration in a mouse model of *SCN1A* haploinsufficiency**

Because reducing *Kcnt1* expression was effective in *Scn8a* mutant mice, we also tested the *Kcnt1* ASO in *Scn1a*$^{+/-}$ mice. Consistent with previous studies (Miller *et al.*, 2014; Favero *et al.*, 2018), roughly 1/3 of untreated *Scn1a*$^{+/-}$ mice died between 3 and 4 weeks of age (n = 25), and during the remaining 6-month monitoring period, there were several sporadic deaths (Fig. 5-4). We administered 45 µg *Kcnt1* ASO to *Scn1a*$^{+/-}$ mice at P2. None of the treated mice died in the first 4 weeks, indicating that reduced *Kcnt1* expression during this critical period is sufficient to prevent death (n = 14, Fig. 5-4). There were four deaths during the 6-month monitoring period, all after 9 weeks of age (Fig. 5-4).

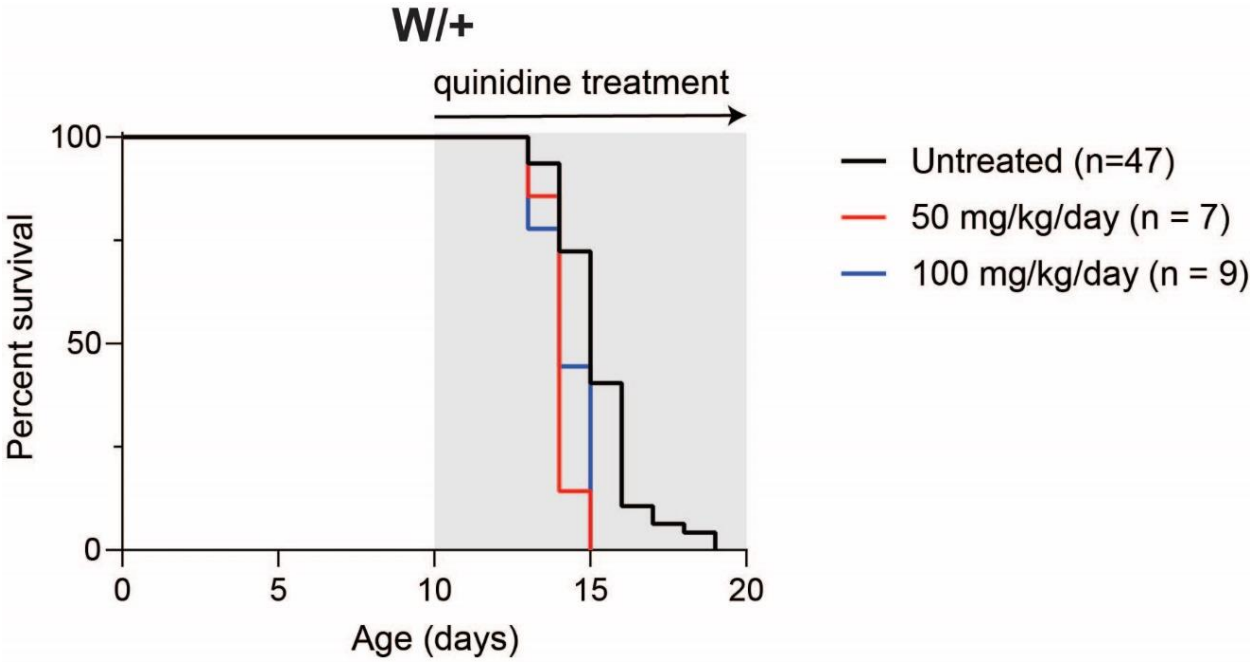

Figure 5-3. Quinidine does not prolong survival of *Scn8a* mutant mice. Survival of *Scn8a*$^{cond/+}$*,EIIa-Cre* (W/+) mice treated with 50 or 100 mg/kg quinidine daily compared to untreated mice. Grey shading indicates treatment period.

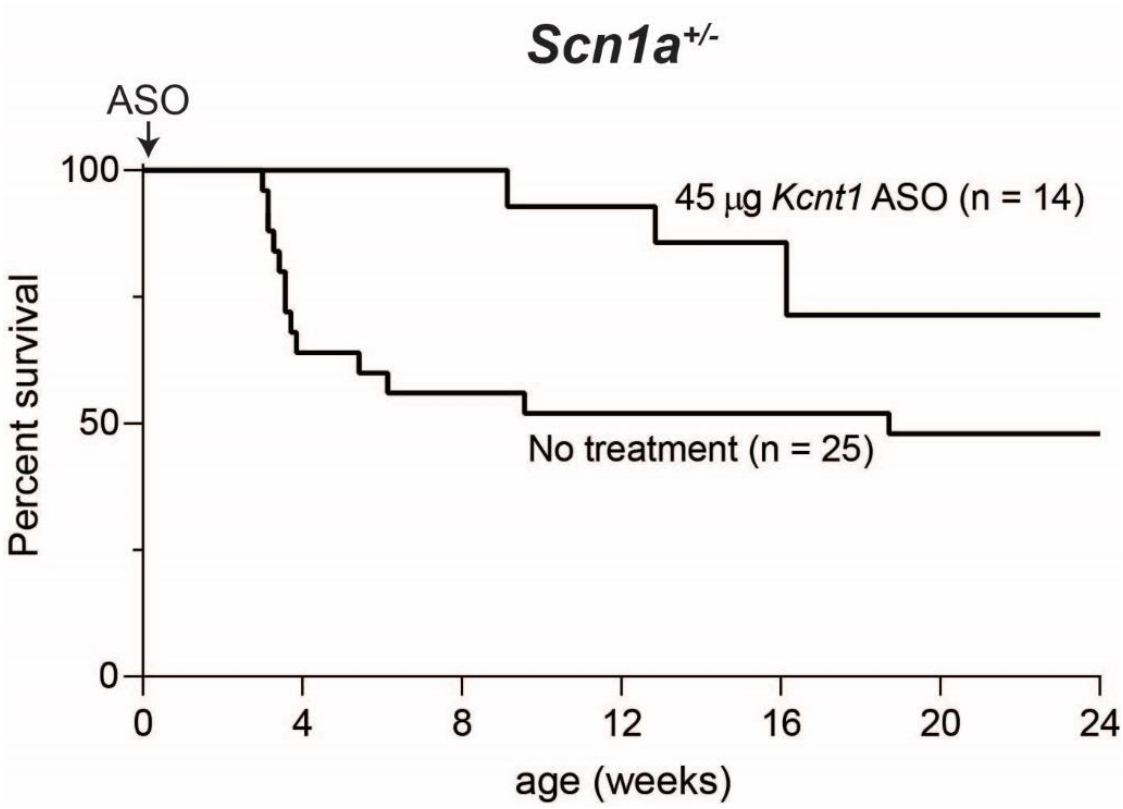

Figure 5-4. *Kcnt1* ASO prolongs survival of *Scn1a*$^{+/-}$ mice. Survival of *Scn1a*$^{+/-}$ mice treated with 45 μg *Kcnt1* ASO at P2 compared to untreated mice.

DISCUSSION

Developmental and epileptic encephalopathies are frequently caused by mutation of ion channel genes. Here, we showed that reduced *Kcnt1* expression is protective in mouse models of *Scn8a* and *Scn1a* epilepsy. Our findings suggest that patients with mutations of *SCN1A* and *SCN8A* could benefit from treatment with a *KCNT1* ASO or KCNT1-specific channel blocker.

A previous study of the same *Kcnt1* ASO demonstrated that reducing *Kcnt1* expression improved the survival, seizure, and behavioral phenotypes of mice homozygous for a patient *KCNT1* GOF mutation (Burbano *et al.*, 2022). Interestingly, the *Kcnt1* ASO was therapeutic at much lower doses in *Kcnt1* mutant mice than in *Scn8a* mutant mice (3.4 µg vs 15-45 µg) (Burbano *et al.*, 2022). More drastic *Kcnt1* reduction may be required to treat epilepsies caused by mutation of a different channel.

This *Kcnt1* ASO has not yet been administered to humans. Another ASO targeting *KCNT1* was developed as an n-of-1 therapy for two children with *KCNT1* GOF mutations (Hayden, 2022a). Although seizure frequency was reduced following ASO treatment, both children developed life-threatening hydrocephalus and the treatments had to be withdrawn (Hayden, 2022a). Rare cases of hydrocephalus have also been documented for ASOs to treat spinal muscular atrophy (Freigang *et al.*, 2021) and Huntington's disease (Stoker *et al.*, 2021).

We previously demonstrated that reducing *Scn8a* expression is therapeutic in *Scn1a*$^{+/-}$ mice (Lenk *et al.*, 2020) and in mice with epilepsy caused by loss of the potassium channel genes *Kcna1* and *Kcnq2* (Hill *et al.*, 2022). P2 administration of the *Scn8a* ASO completely rescued the *Scn1a* mutant mice (Lenk *et al.*, 2020). In the

current work, we showed that reduced *Kcnt1* expression protected *Scn1a*$^{+/-}$ mice during the critical period that occurs between 3-4 weeks of age, but not older mice. It is possible that the *Kcnt1* ASO has worn off by this time, or that reduced *Kcnt1* expression is only protective against lethality that occurs between 3-4 weeks. It is unclear why the *Scn8a* ASO was effective in the long term, since *Scn8a* expression returned to normal within 6 weeks (Lenk *et al.*, 2020). Other researchers have shown that viral overexpression of *Kcna1* is also protective against seizures (Snowball *et al.*, 2019; Qiu *et al.*, 2022). Taken together, these results suggest that modulating ion channel expression to compensate for epileptogenic mutations is a viable therapeutic strategy.

Of the possible ion channel genes that could be targeted to treat channelopathies, *KCNT1* is an attractive therapeutic target. Heterozygous loss-of-function mutations of *KCNT1* are tolerated and appear at predicted frequency in the general population (Lek *et al.*, 2016; Karczewski *et al.*, 2019). *Kcnt1*$^{-/-}$ mice are also healthy and fertile, with only minor abnormalities such as impaired reversal learning and slightly elevated pain sensitivity (Bausch *et al.*, 2015; Lu *et al.*, 2015; Martinez-Espinosa *et al.*, 2015; Quraishi *et al.*, 2020). Therapeutic reduction of *KCNT1* is therefore unlikely to cause unwanted side effects. In contrast, heterozygous loss of *Scn8a* is not tolerated in the healthy population (Lek *et al.*, 2016; Karczewski *et al.*, 2019) and homozygous loss is lethal in the mouse (Burgess *et al.*, 1995).

Quinidine has been proposed as a targeted therapy for patients with *KCNT1* epilepsy because high doses of quinidine can correct *KCNT1* GOF mutations *in vitro* (Milligan *et al.*, 2014; Numis *et al.*, 2018). However, the effects of quinidine are not specific to KCNT1 channels (Roden, 2014). Clinical application of quinidine in *KCNT1*

epilepsy has had mixed success (Mikati *et al.*, 2015; Numis *et al.*, 2018; Fitzgerald *et al.*, 2019; Cole *et al.*, 2021). Some individuals achieved seizure freedom with quinidine (Fitzgerald *et al.*, 2019), but most patients report no benefit or worsening seizures (Numis *et al.*, 2018; Cole *et al.*, 2020). It is possible that the high doses of quinidine required to block KCNT1 cannot be achieved *in vivo* without causing deleterious effects on other ion channels (Liu *et al.*, 2022b). Quinidine was not protective in our *Scn8a* mutant mice, but more specific KCNT1 channel blockers (Cole *et al.*, 2020; Griffin *et al.*, 2021) may be more effective in *KCNT1*, *SCN8A*, and SCN1A epilepsy.

CHAPTER VI

Single-Nucleus RNA-Sequencing Reveals Changes in Hippocampal Oligodendrocytes and Granule Cells in a Mouse Model of *Scn8a* Epilepsy

ABSTRACT

Mutations in voltage-gated sodium channel genes are a common cause of epilepsy, but little is known about the transcriptional changes that occur during the disease course. We studied gene expression changes in the hippocampus of *Scn8a*$^{N1768D/+}$ mice, which express a gain-of-function mutation of the voltage-gated sodium channel Nav1.6. We performed single-nucleus RNA-sequencing both before the onset of seizures and after 10 weeks of chronic, spontaneous seizures. Before seizure onset, gene expression changes were small, and we observed a small (1.3-fold) increase in the number of oligodendrocytes. After 10 weeks of chronic seizures, we observed an even greater increase (1.7-fold) in the number of hippocampal oligodendrocytes, and striking changes in granule cell gene expression. Our results suggest that oligodendrocytes and dentate gyrus granule cells are especially vulnerable cell types in the development of *SCN8A* epilepsy.

[1] The WT and pre-onset data described in this chapter are included in the submitted manuscript: Hill SF, Yu W, Ziobro J, Chalasani S, Reger F, Meisler MH. Long-term downregulation of *SCN8A* in mouse models of developmental and epileptic encephalopathy. *Submitted*, 2023.

INTRODUCTION

SCN8A encodes the voltage-gated sodium channel Nav1.6, which is responsible for the initiation of action potentials (Hu *et al.*, 2009; Meisler *et al.*, 2021). Gain-of-function mutations of *SCN8A* cause developmental and epileptic encephalopathy (DEE), a severe seizure disorder with few effective treatments (Meisler *et al.*, 2021; Johannesen *et al.*, 2022). Mice expressing the *SCN8A*-DEE mutation p.N1768D exhibit profound hippocampal hyperexcitability, resulting in spontaneous seizures that begin at 2-3 months of age and premature death 1-3 months later (Veeramah *et al.*, 2012; Wagnon *et al.*, 2015b; Lopez-Santiago *et al.*, 2017).

Previous studies have investigated transcriptional changes in mice with gain-of-function mutations of *Scn8a* (Sprissler *et al.*, 2017) or loss-of-function mutations of the related sodium channel gene *Scn1a* (Hawkins *et al.*, 2019; Valassina *et al.*, 2022). Before seizure onset, neither *Scn8a* nor *Scn1a* mutations caused transcriptional changes (Sprissler *et al.*, 2017; Hawkins *et al.*, 2019). However, bulk RNA-sequencing (RNAseq) approaches may have masked gene expression changes that occur in specific cell types.

After seizures, large gene expression changes were detectable in both *Scn8a* and *Scn1a* mutants (Sprissler *et al.*, 2017; Hawkins *et al.*, 2019; Valassina *et al.*, 2022). All three experiments detected widespread inflammation and astrogliosis in the epileptic mice (Sprissler *et al.*, 2017; Hawkins *et al.*, 2019; Valassina *et al.*, 2022). Because these effects were so large, bulk RNAseq could have masked changes that occur within other cell types.

We performed single-nucleus RNA-sequencing on hippocampus from *Scn8a*$^{N1768D/+}$ (D/+) mice before seizure onset and after 10 weeks of chronic seizures. We identified few transcriptional changes before the onset of seizures, even within specific cell types. After 10 weeks of chronic seizures, we identified widespread transcriptional changes. The dentate gyrus granule cells are by far the most vulnerable to gene expression change. We also observed a surprising increase in the number of oligodendrocytes both before seizure onset and after chronic seizures. However, interpretation of our results was complicated by a mismatch in age between chronic seizure and WT samples. Nevertheless, our findings suggest two uniquely vulnerable cell types, neither of which has been extensively studied in *SCN8A* epilepsy. (Results begin on p. 97)

METHODS

Mice

Scn8a$^{N1768D/+}$ (D/+) mice (Wagnon *et al.*, 2015b) were maintained on a C57BL/6J genetic background. Mice were housed and cared for in accordance with NIH guidelines in a 12/12-hour light/dark cycle with standard mouse chow and water available ad libitum. Beginning at 6 weeks of age, mice were directly monitored 8h / day (9 AM – 5 PM) for the development of seizures. For snRNA-seq experiments, only female mice were included. For validation studies, both male and female mice were included.

Sample preparation for single-nucleus RNA-sequencing

Single-nucleus RNA-sequencing (snRNAseq) sample collection was performed on fresh tissue over multiple batches: batch 1 (pre-onset 1 and control 1), batch 2 (pre-

onset 2 & 3 and control 2 & 3), batch 3 (chronic 1), batch 4 (chronic 2), and batch 5 (chronic 3). At postnatal day 50 (for control and pre-onset samples, n = 3 each) or 10 weeks after seizure onset (for chronic samples, n = 4), mice were euthanized and their brains were removed (Fig. 6-1). Bilateral hippocampi were immediately dissected and placed in a Dounce homogenizer with 1 mL lysis buffer: EZ Prep Lysis Buffer from Nuclei EZ Prep (Sigma #NUC101), 1mM DTT, 27U/mL Protector RNase inhibitor (Sigma #3335399001). Hippocampi were homogenized as follows: 25X with pestle A, 25X with pestle B, wait 2.5 minutes, 15X with pestle B, wait 2.5 minutes, 15X with pestle B. Samples were filtered through 30 um MACS strainers (Myltenyi, 130-098-458) and an additional 1 mL lysis buffer was added. Samples were centrifuged (500 rcf, 5 minutes, 4°C) and supernatant was discarded. Samples were resuspended in 750 uL wash buffer: 5mM $MgCl_2$, 10mM Tris buffer pH 8.0, 25 mM KCl, 1mM DTT, 27U/mL Protector RNase inhibitor, 1% bovine serum albumin. Samples were filtered through 30 um MACS strainers and centrifuged (500 rcf, 5 minutes, 4°C). Supernatant was discarded and pellets were resuspended in 1 mL wash buffer.

FACS

Nuclei were stained with propidium iodide at a final concentration of 0.4ug/mL. Sorting was performed at the University of Michigan Flow Cytometry Core on a MoFlo Astrios Cell Sorter (Beckman Coulter). Sorted nuclei were collected in pre-washed tubes containing 100 uL wash buffer.

Library preparation and sequencing

Library preparation and sequencing were performed by the University of

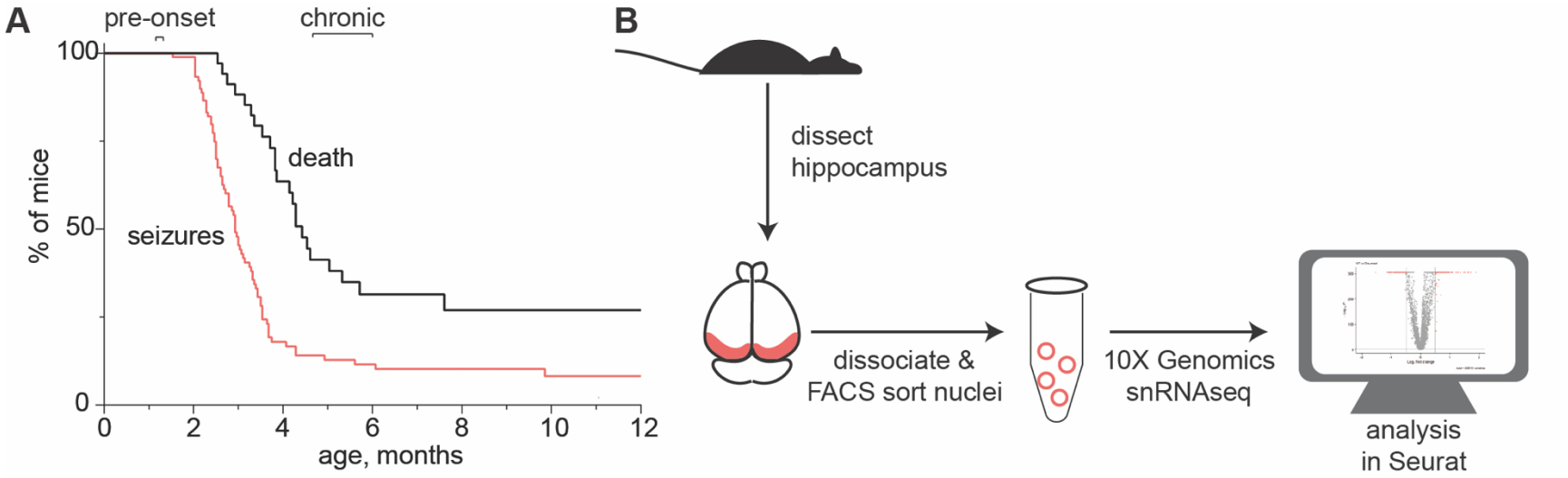

Figure 6-1. Design of single-nucleus RNA-sequencing experiment. (A) In Scn8aN1768D/+ mice, seizures begin around 2-3 months of age, followed by death between 3-6 months. WT and pre-onset samples were collected at P50, before seizure onset. Chronic seizure samples were collected 10 weeks after seizure onset (5-6 months of age). (B) Sample preparation was performed on fresh hippocampus. Nuclei were isolated and FACS sorted and 10X Genomics 3' single-nucleus RNA-sequencing was performed. Downstream analyses were performed in Seurat.

Michigan Advanced Genomics Core using the 10X Genomics single-nucleus 3' gene expression platform. Paired-end sequencing was performed on the NovaSeq6000. For each sample except chronic sample 2, 10,000 nuclei were targeted, and 60,000 reads were sequenced per nucleus. A FACS error prevented sorting of half of chronic sample 2, so only 5,000 nuclei were targeted (Table 6-1).

Data preprocessing and filtration

Data preprocessing was performed by the University of Michigan Advanced Genomics Core using the 10X Genomics Cell Ranger pipeline. At this stage, one chronic seizure sample was excluded due to a low fraction of reads in cells (56.4%; ideal is >70%), suggesting possible contamination. Downstream analyses on the remaining 9 samples were performed in R version 4.2.0 with Seurat version 4.2.0 (Hao *et al.*, 2021). Filtered counts matrices (filtered_feature_bc_matrix) were loaded into Seurat Objects and downsampled to match the lowest number of nuclei in a single sample (chronic sample 2, n = 2100 nuclei, Table 6-1). The 9 SeuratObjects were merged into one SeuratObject containing 18,869 nuclei and 32,285 genes. Genes with fewer than 10 total UMIs were removed from the dataset. Nuclei were excluded if they had fewer than 800 or more than 10,000 genes, if they had fewer than 1,000 or more than 60,000 UMIs, or if they had greater than 2% mitochondrial RNA content (Fig. 6-2A). Standard pre-processing was performed prior to doublet filtration (NormalizeData, FindVariableFeatures, ScaleData, RunPCA, and RunUMAP). Doublet filteration (doubletFinder_v3) was performed with DoubletFinder version 2.0.3 (McGinnis *et al.*, 2019) with the following parameters: pN = 0.25, pK = 0.09, nExp = 720, PCs = 1:10. This left 17,292 nuclei and 22,995 genes (Table 6-1; Fig. 6-2B).

Table 6-1. Single-nucleus RNA-sequencing sample statistics. WT, wildtype; QC, quality control; UMI, unique molecular identifier; SE, status epilepticus.

	WT			Pre-onset			Chronic		
	1	**2**	**3**	**1**	**2**	**3**	**1**	**2**	**3**
Time since most recent observed seizure							10 minutes	7 days	0 minutes (ongoing SE)
# nuclei before QC	7958	7764	7070	8579	7829	7008	8863	2069	4659
# nuclei after QC	1993	2017	1977	1951	1987	1984	1904	1852	1627
Avg. # UMIs/nucleus after QC	2320	2348	2302	2271	2313	2310	2217	2156	1894
Avg. # genes/nucleus after QC	1364	1380	1353	1335	1360	1358	1303	1268	1114
Average % mitochondrial read/nucleus after QC	0	0	0	0	0	0	0	0	0

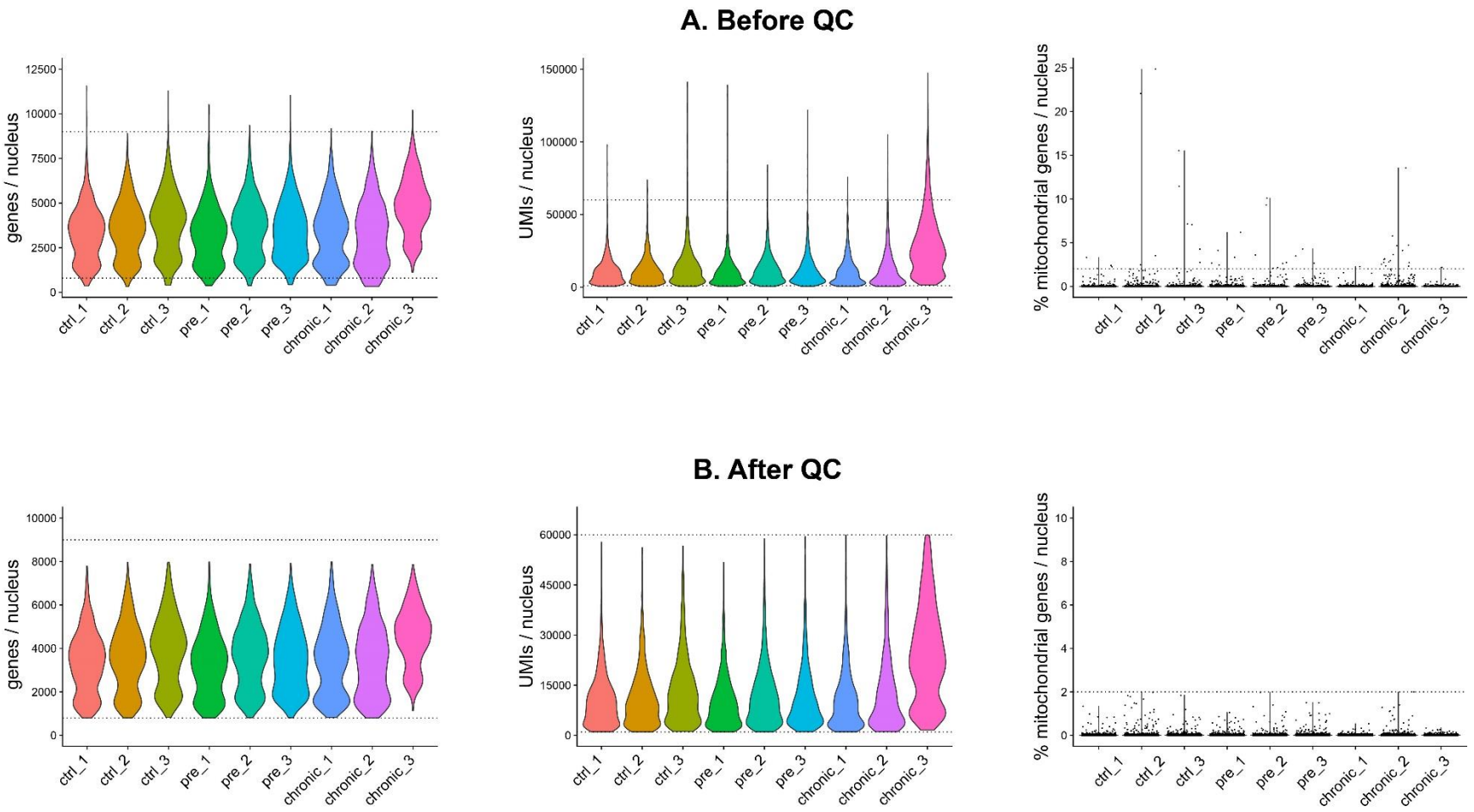

Figure 6-2. Single-nucleus RNA-sequencing dataset quality control metrics. QC, quality control. Number of genes and UMIs and percent mitochondrial genes detected per nucleus from raw (A) and post-quality control (B) data sets. Dotted lines indicate inclusion criteria.

Data integration

Data integration was performed using the recommended procedure for reciprocal PCA (Fig. 6-3A&B). Briefly, a list of SeuratObjects containing data from each sample was created with SplitObject. Normalization (NormalizeData) and variable feature identification (FindVariableFeatures, selection.method = 'vst', nFeatures = 2000) was performed on each dataset separately. Integration features were selected (SelectIntegrationFeatures) and used to scale each dataset (ScaleData) and run PCA (RunPCA). Integration anchors were identified (FindIntegrationAnchors, reduction = 'rpca') and used to integrate the datasets. The integrated data was then scaled (ScaleData), PCA was performed (RunPCA, npcs = 30), and UMAP was performed (RunUMAP, dims = 1:30).

Clustering and cell type assignment

The Shared Nearest Neighbors graph was constructed (FindNeighbors, reduction = 'pca', dims = 1:30). Twenty-three clusters were identified with the Louvain algorithm (FindClusters, resolution = 0.25, algorithm = 1, Fig. 6-3C). Each cluster was manually assigned to a cell type based on expression of the following marker genes (Cembrowski *et al.*, 2016): *Rbfox3* (neurons), *Slc17a7* (excitatory neurons), *Mag* (oligodendrocytes), *Prox1* (granule cells), *Ociad2* (pyramidal neurons), *Aqp4* (astrocytes), *Itgam* (immune cells), *Gad2* (inhibitory neurons), *Nr2f2* (endothelial cells), *Pdgfra* (oligodendrocyte precursor cells), *Ndnf* (Cajal-Retzius cells), *Map3k15* (CA2 pyramidal neurons), *Mpped1* (CA1 pyramidal neurons), and *Mndal* (CA3 pyramidal neurons) (Fig. 6-4 & Fig. 6-5). Cell type assignment was verified by computationally identifying marker genes for each assigned cell type (Fig. 6-6). Specificity of these computationally identified marker

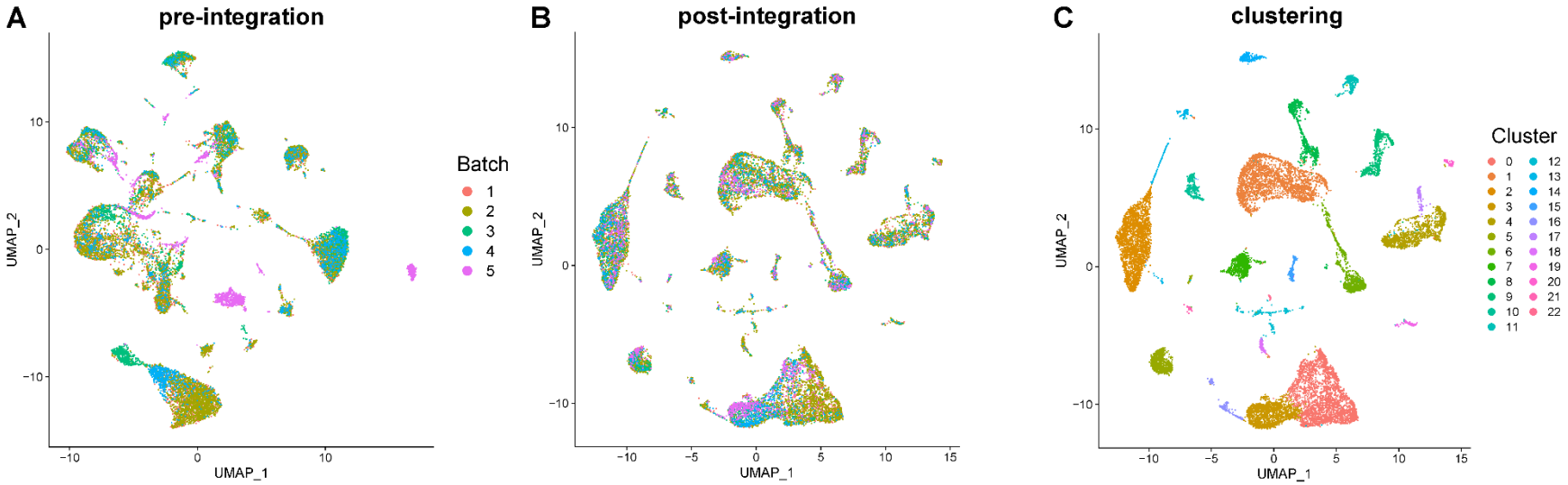

Figure 6-3. Data integration and clustering of snRNAseq dataset. (A-B) UMAP embeddings of snRNAseq dataset before (A) and after (B) data integration with reciprocal PCA. Colors indicate batches. (C) UMAP embedding of snRNAseq dataset. Colors indicate cluster assigned with the Louvain algorithm (resolution = 0.25). n = 17,292 nuclei per UMAP.

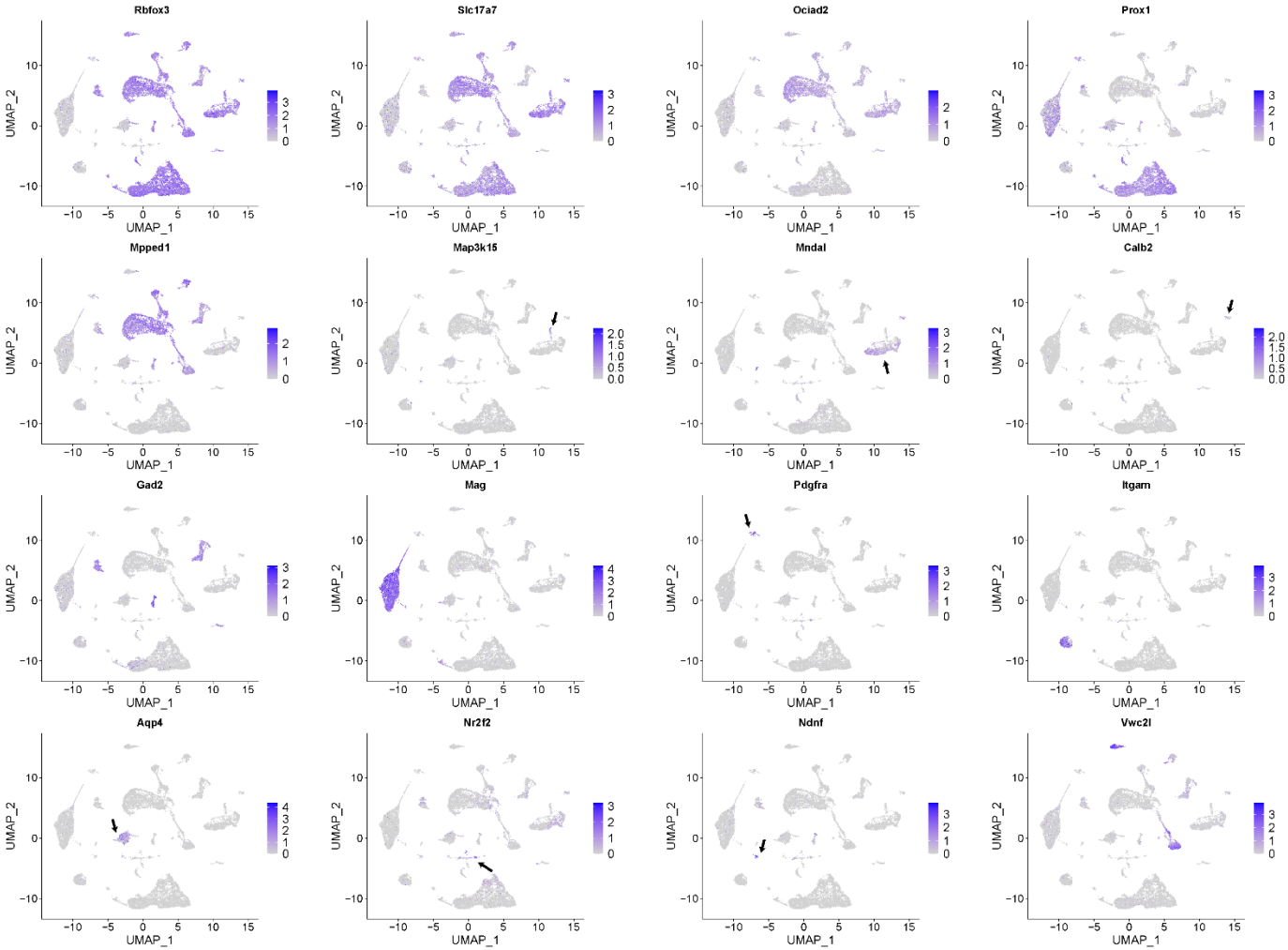

Figure 6-4. Expression of marker genes used to assign cell types. UMAP plots showing expression of marker genes: *Rbfox3* (neurons), *Slc17a7* (excitatory neurons), *Ociad2* (pyramidal neurons), *Prox1* (granule cells), *Mpped1* (CA1 pyramidal neurons), *Map3k15* (CA2 pyramidal neurons), *Mndal* (CA3 pyramidal neurons), *Calb2* (mossy cells), *Gad2* (inhibitory neurons), *Mag* (oligodendrocytes),), *Pdgfra* (oligodendrocyte precursor cells), *Itgam* (immune cells), *Aqp4* (astrocytes), *Nr2f2* (endothelial cells), *Ndnf* (Cajal-Retzius cells), and *Vwc2l* (subiculum neurons). Expression is shown in transcripts per 10,000.

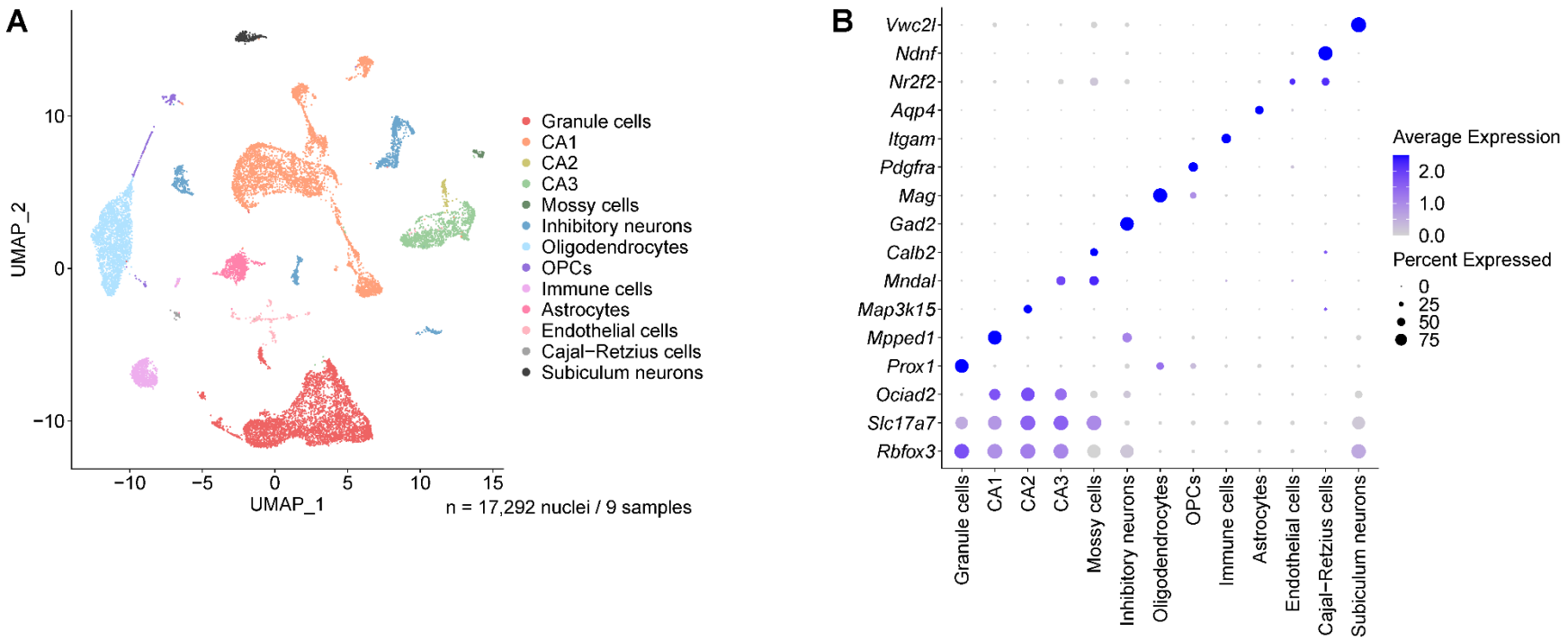

Figure 6-5. Cell type assignment of snRNAseq dataset. (A) UMAP embedding of snRNAseq dataset. Colors indicate manually assigned cell type. (B) Dotplot of canonical marker genes used to manually assign cell types. Expression is shown in transcripts per 10,000.

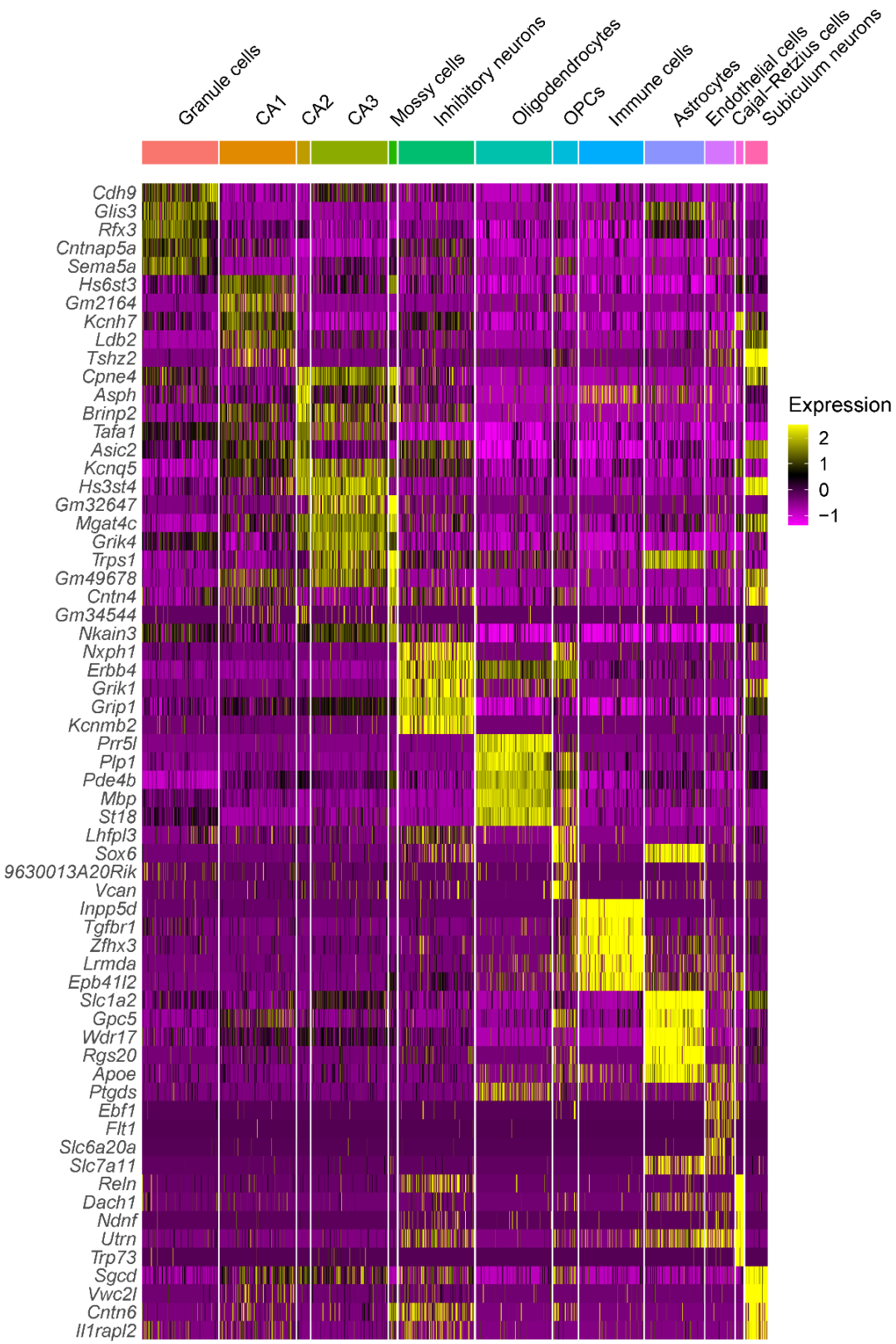

Figure 6-6. Unbiased detection of marker genes for manually assigned cell types. Heatmap of the top 5 unique computationally identified marker genes for each cell type (sorted by log2FC). Expression is shown in transcripts per 10,000.

genes was validated with the Allen Brain Map mouse 10X Genomics whole cortex and hippocampus database (https://celltypes.brain-map.org/rnaseq/mouse_ctx-hpf_10x). The number of nuclei in each cell type is shown in Table 6-2.

Differential gene expression analysis

The command wilcoxauc from PRESTO version 1.0.0 (McArdle *et al.*, 2018) was used to calculate changes in gene expression between WT and pre-onset or WT and chronic seizures. Genes were considered differentially expressed if the absolute value of the log2fold change (log2FC) was greater than 0.5 (fold change > 1.4) and the adjusted p-value was less than 0.05. EnhancedVolcano version 1.14.0 was used to construct volcano plots.

Gene set enrichment analysis

Gene set enrichment analysis was performed separately on up- and down-regulated genes. Gene Ontology Cellular Compartments and Biological Processes databases were accessed via http://geneontology.org/ (Ashburner *et al.*, 2000; Mi *et al.*, 2019; Gene Ontology, 2021).

Immunohistochemistry

Mice were transcardially perfused with PBS followed by 4% paraformaldehyde (PFA). The whole brain was extracted and drop-fixed in 4% PFA overnight at 4ºC. Brains were cryopreserved by incubating in 15% sucrose at 4ºC overnight, followed by incubation in 30% sucrose at 4ºC overnight. Brains were frozen into blocks of OCT Compound (Fisher Scientific #23730571) and cryosectioned at a thickness of 10 um (Leica CM1950). Sections were stored at -80ºC.

Table 6-2. Cell type composition of snRNAseq samples. Number of nuclei in each sample assigned to a given cell type. Percentages are shown in parentheses. OPC, oligodendrocyte precursor cells.

Cell type	WT			Pre-onset			Chronic		
	1	2	3	1	2	3	1	2	3
CA1	547 (27%)	565 (28%)	628 (32%)	487 (25%)	577 (29%)	421 (21%)	495 (23%)	425 (23%)	421 (26%)
Granule cells	477 (24%)	491 (24%)	468 (24%)	456 (23%)	502 (25%)	577 (29%)	466 (24%)	529 (29%)	575 (35%)
Oligodendrocytes	216 (11%)	235 (12%)	211 (11%)	295 (15%)	245 (12%)	285 (14%)	389 (20%)	356 (19%)	264 (16%)
CA3	211 (11%)	165 (8.2%)	151 (7.6%)	183 (7.6%)	132 (6.6%)	158 (6.7%)	129 (6.8%)	103 (5.6%)	60 (3.7%)
Inhibitory neurons	182 (9.1%)	208 (10%)	152 (7.7%)	208 (11%)	145 (7.3%)	141 (7.1%)	147 (7.7%)	105 (5.7%)	114 (7.0%)
Astrocytes	127 (6.4%)	79 (3.9%)	110 (5.6%)	89 (4.6%)	86 (4.3%)	116 (5.9%)	20 (1.1%)	107 (5.8%)	44 (2.7%)
Immune cells	60 (3.0%)	91 (4.5%)	93 (4.7%)	65 (3.3%)	126 (6.3%)	111 (5.6%)	147 (7.7%)	63 (3.4%)	89 (5.5%)
OPCs	46 (2.3%)	40 (2.0%)	43 (2.2%)	45 (2.3%)	37 (1.9%)	44 (2.2%)	34 (1.8%)	25 (1.4%)	8 (0.5%)
Subiculum neurons	38 (1.9%)	24 (1.2%)	39 (2.0%)	31 (1.6%)	55 (2.8%)	29 (1.5%)	21 (1.1%)	30 (1.6%)	29 (1.8%)
Endothelial cells	32 (1.6%)	77 (3.8%)	42 (2.1%)	41 (2.1%)	45 (2.3%)	50 (2.5%)	19 (1.0%)	66 (3.6%)	5 (0.3%)
CA2	25 (1.2%)	16 (0.8%)	13 (0.7%)	25 (1.3%)	18 (0.9%)	27 (1.4%)	15 (0.8%)	25 (1.4%)	6 (0.4%)
Cajal-Retzius cells	17 (0.9%)	11 (0.6%)	15 (0.8%)	8 (0.4%)	6 (0.3%)	10 (0.5%)	15 (0.8%)	13 (0.7%)	8 (0.5%)
Mossy cells	15 (0.8%)	15 (0.7%)	12 (0.6%)	18 (0.9%)	13 (0.7%)	15 (0.8%)	7 (0.4%)	5 (0.3%)	4 (0.3%)
TOTAL	**1993**	**2017**	**1977**	**1951**	**1987**	**1984**	**1904**	**1852**	**1627**

Sections were thawed at room temperature for 1 hour, then washed with PBS three times for 5 minutes each. Sections were permeabilized with 0.3% Triton X-100 (Roche Diagnostics cat. no. 11332481001) in PBS for 10 minutes at room temperature. Sections were blocked in blocking buffer (5% donkey serum (Sigma Aldrich cat. no. D9663), 1% bovine serum albumin (Fisher Scientific cat. no. BP1600), and 1% Triton X-100 in PBS) for 1 hour at room temperature. Primary antibody (Rabbit anti-OLIG2, Millipore AB9610 lot 3911642, 1:300) was diluted in blocking buffer and incubated overnight at 4ºC. Sections were washed with blocking buffer three times for 5 minutes each. Secondary antibody (Goat anti-rabbit AlexaFluor 594, Invitrogen A11012 lot 2506100, 1:500) was diluted in blocking buffer and incubated for 2 hours at room temperature. Sections were washed with blocking buffer three times for 5 minutes each. Sections were incubated with DAPI (1 µg/mL) in PBS for 5 minutes at room temperature. Sections were washed with PBS three times for 5 minutes each. Prolong Gold Antifade Mountant (ThermoFisher cat. no. P36930) was added. A coverslip was applied and fixed in place with clear nail polish.

For each section, whole bilateral hippocampi were imaged at 20X (Nikon Ti2 Widefield) at the University of Michigan Microscopy Core. Images were processed and quantified by an experimenter blinded to condition using Nikon Elements software. The DAPI and Olig2 channels were processed with Clarify.ai and rolling ball corrections (radius = 10 µm). Regions of interest were drawn around the hippocampus, excluding the dentate gyrus and pyramidal cell layers due to the high density of cells, which prevented quantification. Channels were thresholded and the numbers of DAPI+ and Olig2+ nuclei were automatically counted.

RESULTS

Generation of single-nucleus dataset

We performed single-nucleus RNA-sequencing (snRNAseq) to assess transcriptional changes in the *Scn8a*$^{N1768D/+}$ (D/+) hippocampus. We collected samples at two time points: before seizure onset, to identify gene expression changes directly caused by the D/+ mutation; and after 10 weeks of chronic seizures, to identify gene expression changes that occur as a result of seizures. We collected wildtype (WT) control and “pre-onset” D/+ samples at postnatal day 50 (P50), before seizure onset (n = 3 each) (Fig. 6-1). Beginning at 6 weeks of age, we directly monitored D/+ mice 8 hours per day to detect the onset of spontaneous seizures, which occurred between 2 and 3 months of age. After 10 weeks of chronic seizures, we collected “chronic seizure” samples (n = 3, Fig. 6-1). Because we studied spontaneous seizures, there was variation in the disease course, especially in the time since the most recent seizure (Table 6-1). It is also important to note that the chronic seizure samples were older than WT control samples (5 months vs. P50).

For each sample, we extracted hippocampus from fresh tissue, isolated nuclei, and performed FACS sorting to purify nuclei (Fig. 6-1). We then performed 10X Genomics 3’ gene expression single-nucleus RNA-sequencing targeting 10,000 nuclei per sample and 60,000 reads per nucleus. After quality control, our dataset includes 17,292 nuclei from 9 samples. We identified 23 clusters and manually assigned cell type based on expression of known marker genes. We observed all expected cell types in our sample (Fig. 6-5).

Expression of sodium channel genes in WT hippocampus

The four neuronal voltage-gated sodium channel genes (*Scn1a*, *Scn2a*, *Scn3a*, and *Scn8a*) exhibit distinct developmental and cell type expression patterns. We investigated expression of these four genes in P50 WT nuclei from our dataset (Fig. 6-7). Consistent with previous studies (Du *et al.*, 2020a; Liang *et al.*, 2021; Heighway *et al.*, 2022), we observed low expression of *Scn3a* in adult neurons compared to the other VGSC genes (average neuronal expression of *Scn1a*: 2.14 UMIs / 10,000; *Scn2a*: 3.44; *Scn3a*: 1.47; *Scn8a*: 3.89). We also approximately two-fold higher expression of *Scn1a* in inhibitory neurons (average expression in excitatory neurons: 1.99 UMIs / 10,0000; inhibitory neurons: 3.95), especially parvalbumin interneurons (average expression in *Pvalb* interneurons: 5.19 UMIs / 10,000; other interneurons: 3.64).

Although the sodium channels are thought to function primarily in neurons, we also detected expression in some glia. All four sodium channel genes are expressed in OPCs (average expression of *Scn1a*: 1.32 UMIs / 10,000; *Scn2a*: 1.89; *Scn3a*: 1.18; *Scn8a*: 2.59), where they may play a role in spiking behavior (Jiang *et al.*, 2013).

Chronic seizures, but not the *Scn8a* D/+ mutation alone, cause small changes in pseudo-bulk hippocampal gene expression

We asked whether overall hippocampal gene expression was affected by the *Scn8a* mutation by performing pseudo-bulk differential gene expression analysis. Before seizure onset, we identified no differentially expressed genes (DEGs) that met the significance criteria of greater than 1.4-fold change (log2 fold change > 0.5) with adjusted *p*-value < 0.05 (Fig. 6-8A). Changes in four genes were statistically significant, but less than 1.4-fold: the long non-coding RNAs *Gm47283* and *AY036118*, the uncharacterized gene *AC149090.1*, and *Ttr*, which encodes the cerebrospinal fluid

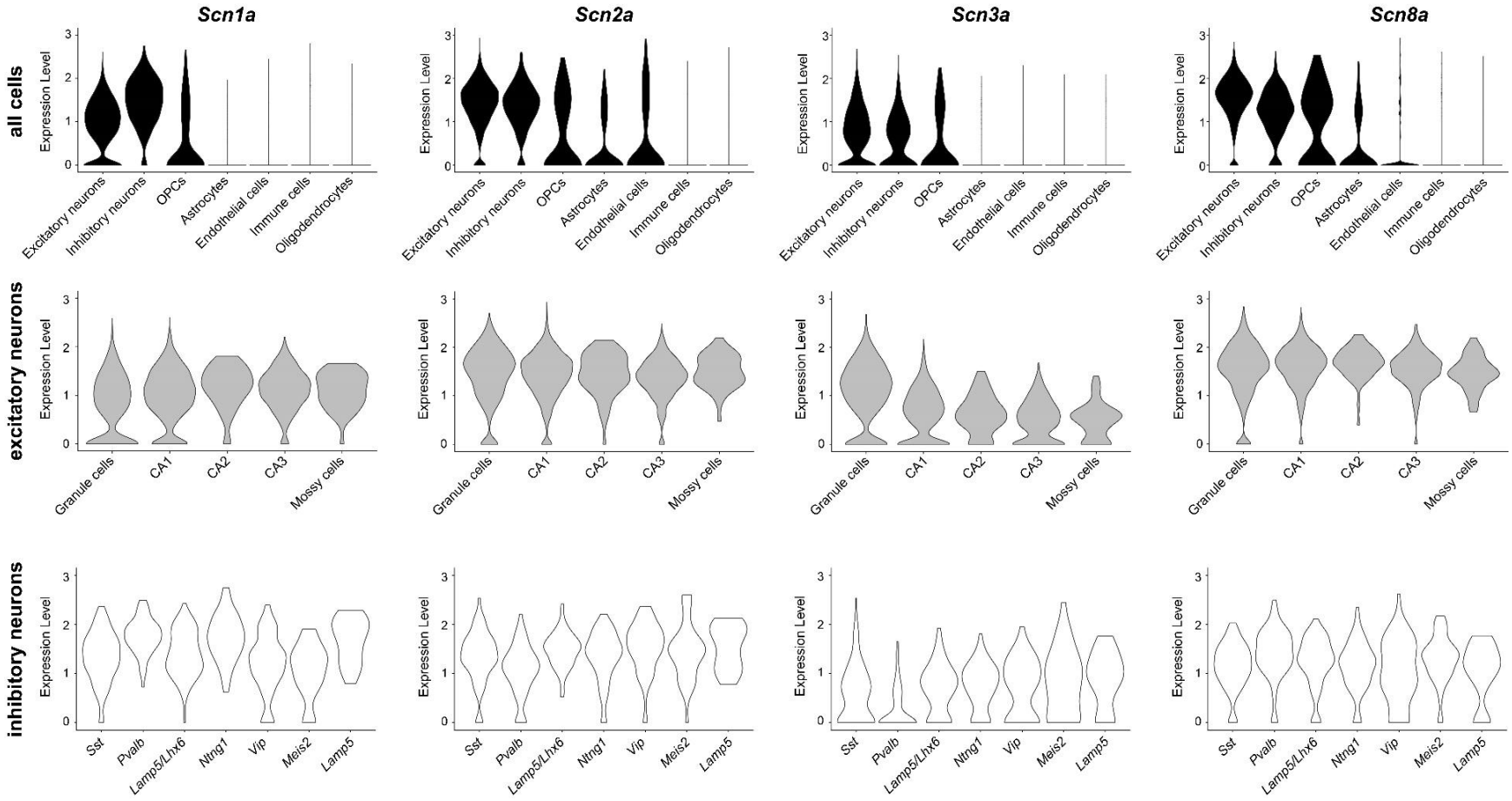

Figure 6-7. Expression of voltage-gated sodium channel genes across cell types. Expression of *Scn1a*, *Scn2a*, *Scn3a*, and *Scn8a* in WT nuclei of the indicated type. Expression is shown in transcripts per 10,000.

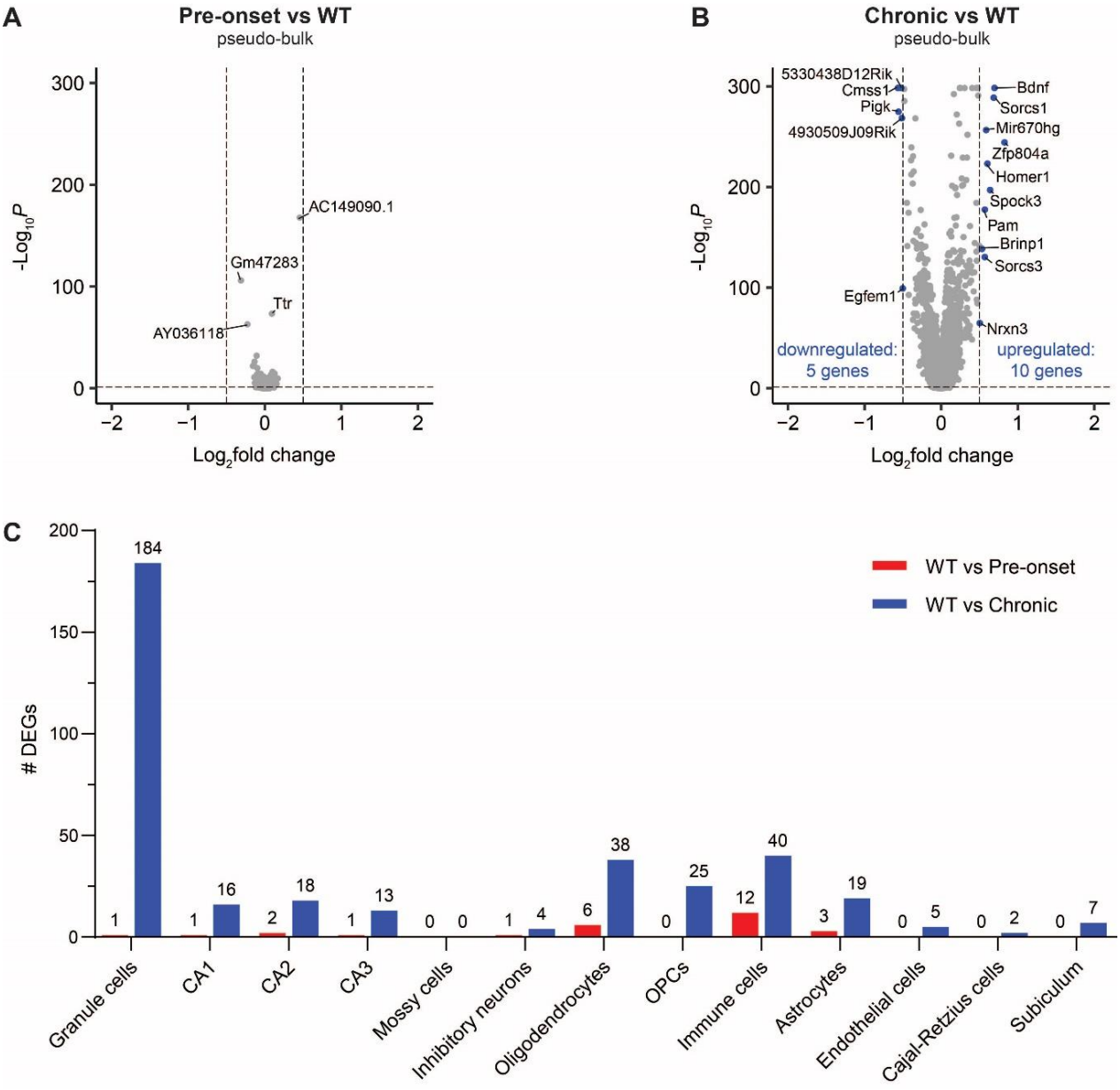

Figure 6-8. Chronic seizures alter hippocampal gene expression. (A-B) Pseudo-bulk differential gene expression analysis comparing WT and pre-onset (A) or chronic seizure samples (B). Dotted lines indicate significance cutoffs: |log2FC| > 0.5 and adjusted p-value < 0.05. (C) The number of differentially expressed genes (DEGs) between WT and pre-onset or WT and chronic seizures within a given cell type.

transport protein transthyretin. The *Scn8a* D/+ mutation is expressed well before P50 and causes neuronal hyperexcitability as early as P21 (Wagnon *et al.*, 2015b; Lopez-Santiago *et al.*, 2017; Bunton-Stasyshyn *et al.*, 2019), so I expected to identify larger gene expression changes by P50. However, previous bulk RNA-seq studies of *Scn8a* and *Scn1a* mutants also detected few changes before seizure onset (Sprissler *et al.*, 2017; Hawkins *et al.*, 2019).

Pseudo-bulk comparison of chronic seizure and wildtype samples revealed 15 DEGs (10 upregulated) with between 1.4 and 1.7 fold change (Fig. 6-8B, Appendix B1). Although the number of genes and the size of the effects are relatively small, several DEGs stood out. *Bdnf* encodes brain-derived neurotrophic factor, which is known to increase expression in response to elevated neuronal activity. Its receptor, *Ntrk2*, was also upregulated, although by less than 1.4-fold. *Bdnf* and four other DEGs (*Homer1*, *Sorcs1/3* and *Nrxn3*) have previously been linked to epilepsy (Table 6-3). The ten remaining DEGs were not previously associated with epilepsy (Table 6-3).

The snRNAseq technique allowed us to ask whether there were gene expression changes in specific cell types that were obscured in the bulk analysis. Before seizure onset, immune cells exhibited the most DEGs (n = 12), followed by oligodendrocytes (n = 6, Fig. 6-8C, Appendix A). After 10 weeks of chronic seizures, dentate gyrus granule cells (GCs) exhibited the most DEGs of any cell type (n = 184, Fig. 6-8C, Appendix B). Pre-onset GCs had only one significant DEG compared to WT GCs, the uncharacterized gene *AC149090.1* (Fig 6-8C). Thus, it appears that chronic seizures cause changes in GC gene expression, rather than the *Scn8a* mutation itself.

Table 6-3. Epilepsy involvement of differentially expressed genes in pseudo-bulk analysis. DEG, differentially expressed gene; FC, fold change in the pseudo-bulk WT vs chronic seizure comparison.

DEG	FC	Role in epilepsy	Citations
Bdnf	1.62	Upregulated in epilepsy Overexpression causes seizures	(Scharfman *et al.*, 2002; Iughetti *et al.*, 2018)
Sorcs1	1.61	Upregulated by kainate-induced seizures	(Hermey *et al.*, 2004)
Homer1	1.52	Upregulated by epileptic activity	(Li *et al.*, 2013; Shan *et al.*, 2018)
Sorcs3	1.48	Homozygous mutations cause DEE Upregulated by kainate-induced seizures	(Alfadhel *et al.*, 2018) (Hermey *et al.*, 2004)
Nrxn3	1.42	Microdeletions of the chromosomal region cause epilepsy	(Faheem *et al.*, 2015; Vlaskamp *et al.*, 2017)
Zfp804a	1.77	None	
Spock3	1.56	None	
Mir670hg	1.50	None	
Pam	1.48	None	
Brinp1	1.45	None	
Egfem1	0.71	None	
4930509J09Rik	0.70	None	
5330438D12Rik	0.70	None	
Pigk	0.68	None	
Cmss1	0.68	None	

We also examined the effect of the *Scn8a* D/+ mutation on compensatory changes in pseudo-bulk expression of other ion channel genes (Fig. 6-9). We observed no change in expression of any sodium, calcium, or potassium channel genes in the pre-onset or chronic seizure samples compared to WT. If there are compensatory changes in ion channel activity, they are not detectable at the RNA level in pseudo-bulk analysis.

Chronic seizures may increase oligodendrocyte number

The cell type composition of our snRNAseq samples suggested a progressive increase in the number of oligodendrocytes in both the pre-onset and chronic seizure samples compared to WT. In the WT samples, oligodendrocytes made up approximately 11% of nuclei (Table 6-2, Fig. 6-10). In pre-onset samples, oligodendrocytes were 14% of nuclei, a 1.3-fold increase. In the chronic seizure samples, oligodendrocytes made up 19% of nuclei, a 1.7-fold increase over WT.

We attempted to validate the increase in oligodendrocytes by staining for the oligodendrocyte lineage marker Olig2 in hippocampal sections. We collected a second cohort of pre-onset and chronic seizure D/+ mice and age-matched, wildtype controls (n = 3 each). In randomly selected sections, we did not detect a change in the number of oligodendrocytes in pre-onset or chronic seizure hippocampus (Fig. 6-11). However, we observed considerable variation in oligodendrocyte number from section to section, perhaps because sections were randomly selected and did not represent consistent regions of the hippocampus. Systematic analysis of oligodendrocyte content in the hippocampus would be required to confirm our snRNAseq findings.

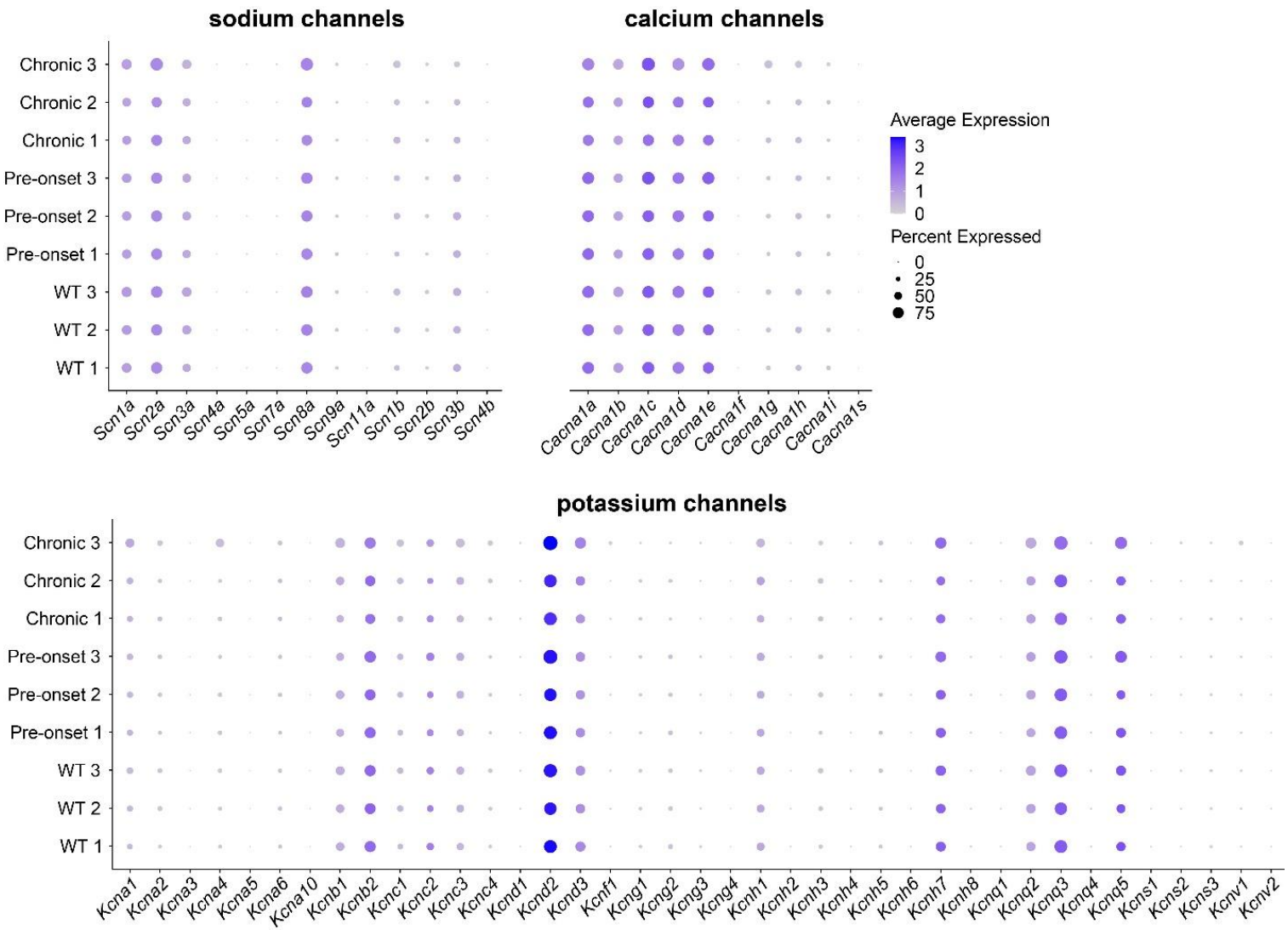

Figure 6-9. The *Scn8a* mutation does not cause compensatory changes in expression of sodium, calcium, or potassium channel genes. Pseudo-bulk expression of sodium, calcium, and potassium channel genes. Expression is shown in transcripts per 10,000.

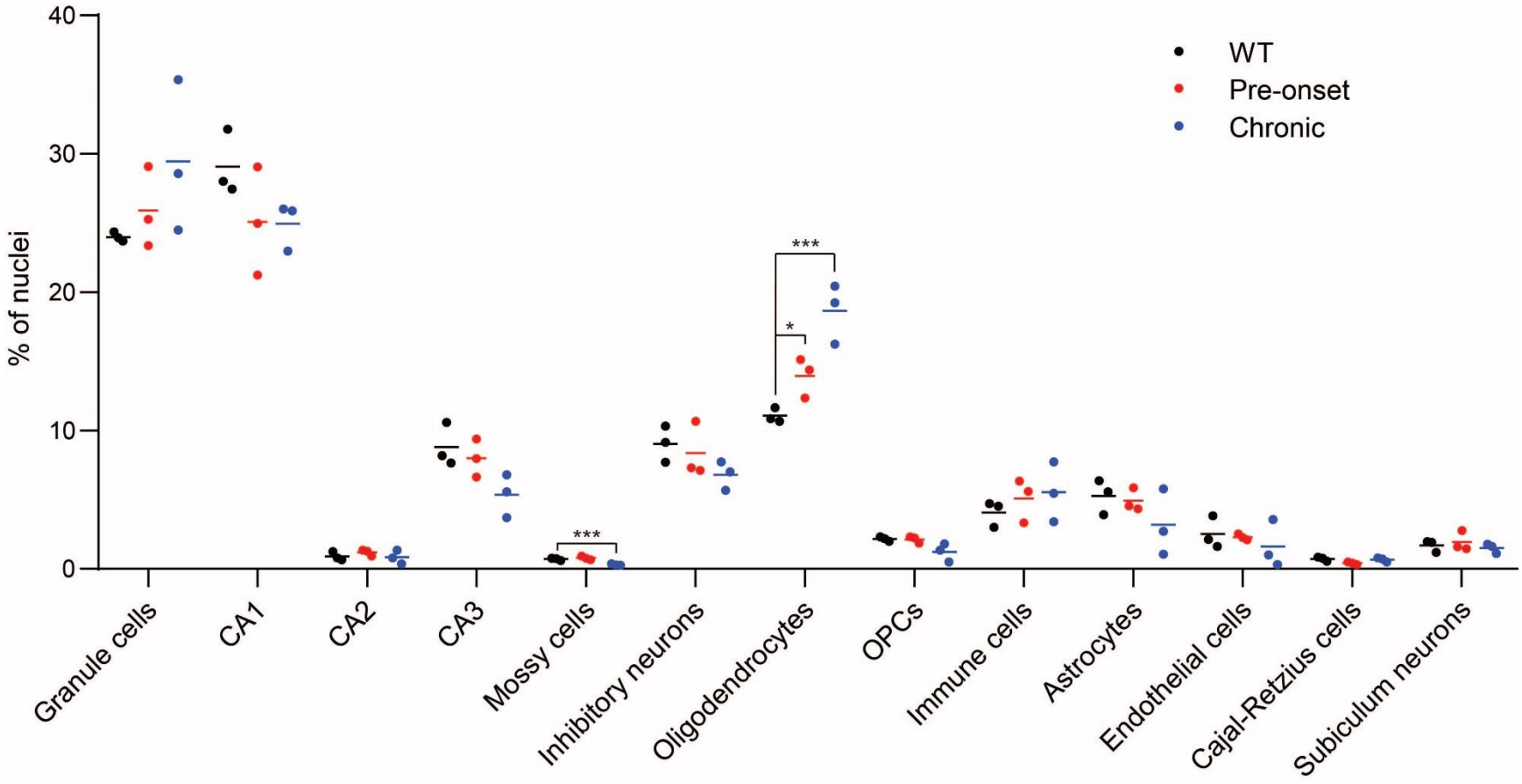

Figure 6-10. Cell type composition of snRNAseq samples. Asterisks indicate significance of Student's t-tests: *, $p < 0.05$; ***, $p < 0.005$.

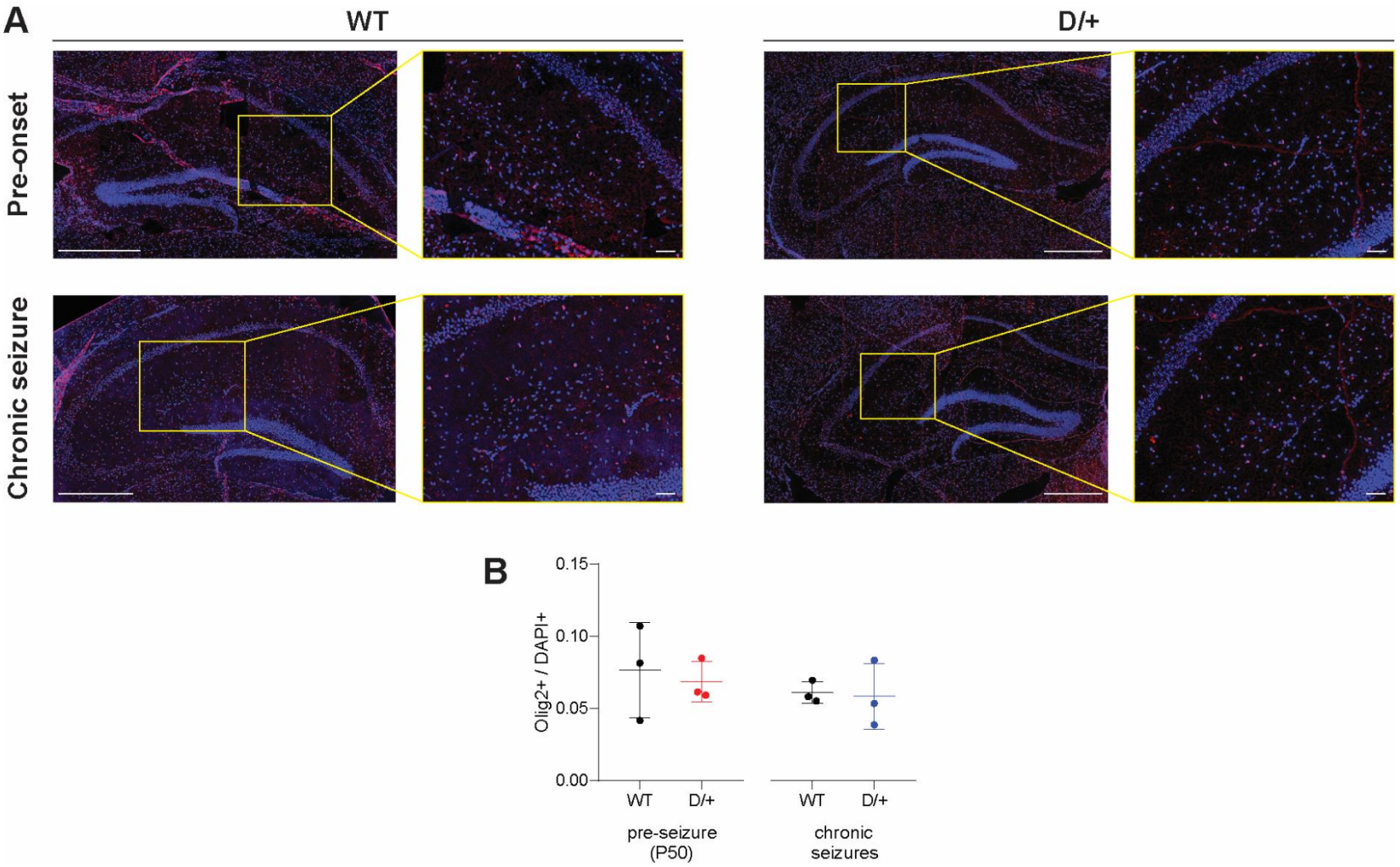

Figure 6-11. Estimated numbers of hippocampal oligodendrocytes. For each time point, 4-7 sections were randomly selected from 3 WT and 3 D/+ mice. (A) Immunostaining for the oligodendrocyte lineage marker Olig2 in hippocampus. Red, Olig2; Blue; DAPI. Large scale bars represent 500 µm; small scale bars, 100 µm. (B) Quantification of Olig2-positive nuclei. Each dot represents the average of at least 4 randomly chosen hippocampal sections.

We also observed a slight decrease in the mossy cell population in chronic seizure samples. The overall number of mossy cells was so small that this difference is unlikely to be meaningful (Table 6-2).

Chronic seizures alter oligodendrocyte gene expression

Because of the possible increase in the number of hippocampal oligodendrocytes, we were interested in gene expression changes in that population. Since mature oligodendrocytes do not express *Scn8a*, these changes must occur prior to differentiation of *Scn8a*-expressing OPCs, or be driven by non-cell autonomous effects from a different population of *Scn8a*-expresing cells.

We examined the genes that were differentially expressed between WT and pre-onset or chronic seizure oligodendrocytes (Fig. 6-12, Appendix A6). Before seizure onset, there were six DEGs compared to WT, all of which were upregulated by 1.5-fold: *Nrg3*, *Kcnip4*, *Nrxn3*, *Csmd1*, *Rbfox1*, and *Lrrtm4* (Fig. 6-12A, Appendix A6). All six genes are primarily expressed in neurons, with low expression in WT oligodendrocytes (Fig. 6-12D).

Chronic seizures caused many small changes in oligodendrocyte gene expression (Fig 6-12C, 11 downregulated genes and 27 upregulated genes, Appendix B7). Gene ontology analysis using the GOCC database identified enrichment of synaptic genes including *Syt1* (synaptotagmin) and *Nrxn1/3*. This was surprising, since mature oligodendrocytes do not transmit or receive direct synaptic input (Moura *et al.*, 2021).

The only DEG with greater than 2-fold change was *Neat1* (2.4-fold increase in chronic seizures), a long noncoding RNA involved in oligodendrocyte differentiation

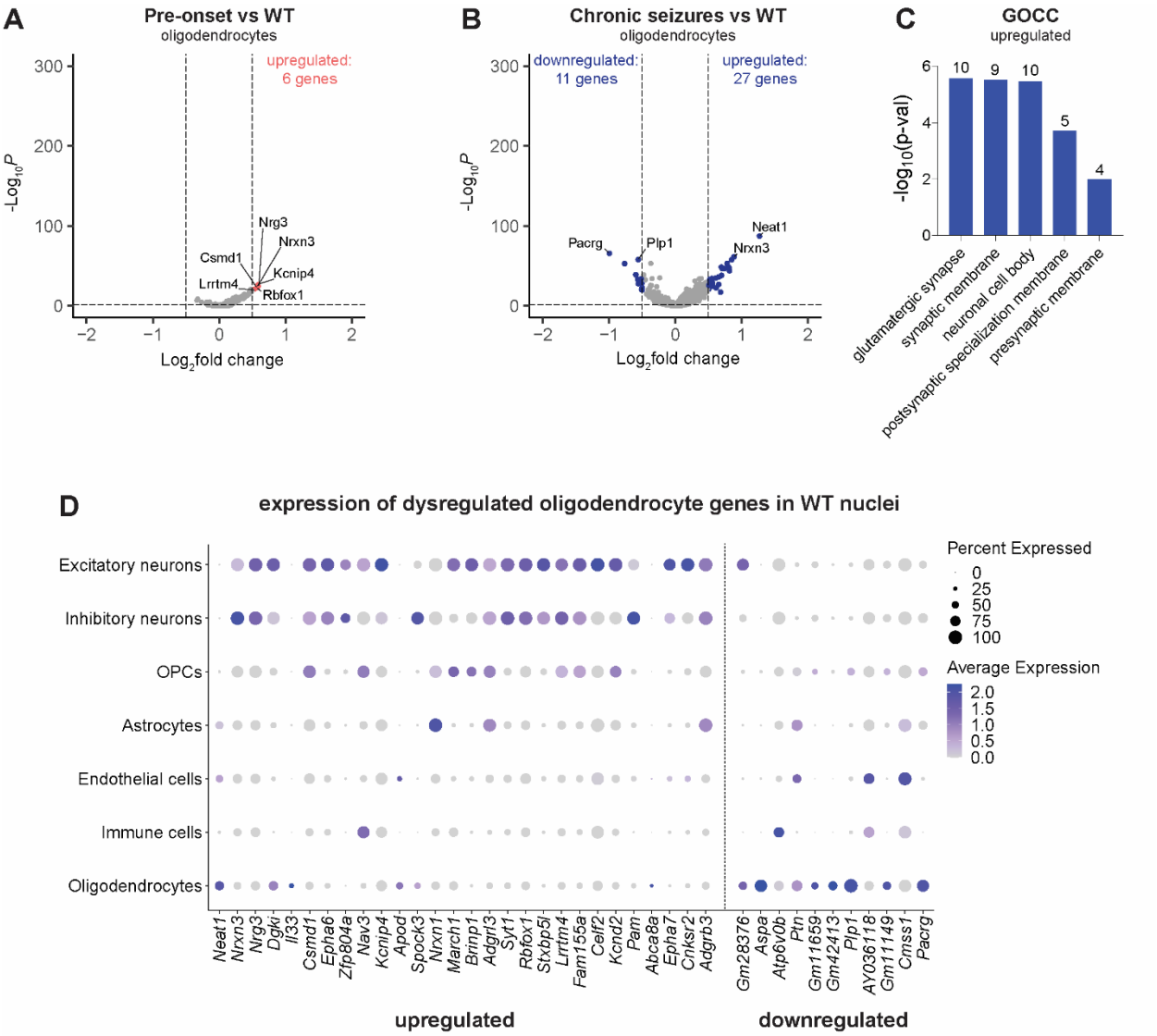

Figure 6-12. Chronic seizures cause small changes in oligodendrocyte gene expression. (A-B) Differential gene expression analysis comparing WT and pre-onset (A) or chronic seizure oligodendrocytes (B). Dotted lines indicate significance cutoffs: |log2FC| > 0.5 and adjusted *p*-value < 0.05. (C) Gene ontology analysis of upregulated genes using the Gene Ontology Cellular Compartments (GOCC) database. Numbers indicate the number of upregulated genes in each GOCC term. (D) Expression of dysregulated genes across cell types in wildtype (WT) nuclei. Expression is shown in transcripts per 10,000.

(Katsel *et al.*, 2019). *Neat1* is also upregulated in epilepsy and responsive to neuronal activity (Barry *et al.*, 2017). Fourteen other dysregulated genes also have a role in oligodendrocyte differentiation or epilepsy (Table 6-4).

The upregulated genes are not highly expressed in WT oligodendrocytes but have robust expression in WT neurons (Fig. 6-12D). Conversely, the downregulated genes are highly expressed in oligodendrocytes (Fig. 6-12D), and *Aspa* and *Plp1* are involved in myelination (Table 6-4).

The pattern of overexpression of neuronal genes and downregulation of oligodendrocyte genes may be explained in two ways. Expression of synaptic genes like the *Nrxn*s may be upregulated to allow oligodendrocytes to optimize myelination in response to changes in neuronal activity (Hughes and Appel, 2019). Altered expression of these genes could explain why *Scn8a* GOF hippocampi may contain elevated oligodendrocytes. It is also possible that excessive or too-rapid differentiation of OPCs into mature oligodendrocytes causes retention of synaptic genes, which are expressed in OPCs (Fig. 6-12D). Maladaptive myelination, in which excessive differentiation of oligodendrocytes exacerbates seizures, has been identified in another *Scn8a* mutant (Knowles *et al.*, 2022b).

Chronic seizures alter gene expression in dentate gyrus granule cells

Dentate gyrus granule cells (GCs) are excitatory neurons that receive input from the entorhinal cortex and relay these signals to pyramidal neurons in the CA3 region. GCs are the primary input neurons in the hippocampus. Due to their low firing rate and high threshold for excitation, GCs are classically thought of as “gates” or “filters” for incoming signals onto downstream pyramidal neurons (Lopez-Rojas and Kreutz, 2016).

Table 6-4. Differentially expressed genes in oligodendrocyte analysis with a role in oligodendrocyte differentiation or epilepsy. OL, oligodendrocyte; DEG, differentially expressed gene; FC, fold change in the oligodendrocyte WT vs chronic seizure comparison; LOF, loss of function; OPC, oligodendrocyte precursor cell.

DEG	FC	Role in OL differentiation	Role in epilepsy	Citations
Neat1	2.41	Knockout reduces the number of mature OLs	Increased expression in epilepsy	(Barry *et al.*, 2017; Katsel *et al.*, 2019)
Nrxn3	1.85		Microdeletions of the chromosomal region cause epilepsy	(Faheem *et al.*, 2015; Vlaskamp *et al.*, 2017)
Nrg3	1.80	Promotes survival of OPCs		(Carteron *et al.*, 2006)
Il33	1.75	Knockout reduces myelination and OL differentiation	Increased expression in epilepsy	(Sung *et al.*, 2019; Ethemoglu *et al.*, 2021)
Apod	1.61		Increased expression in epilepsy	(Ong *et al.*, 1997; Montpied *et al.*, 1999)
Rbfox1	1.47		LOF causes epilepsy in mouse and human	(Gehman *et al.*, 2011; Lal *et al.*, 2015)
Stxbp5l	1.47		Homozygous mutation causes epilepsy	(Kumar *et al.*, 2015)
Syt1	1.47		Heterozygous missense mutations cause epilepsy	(Melland *et al.*, 2022)
Celf2	1.45		Heterozygous LOF causes epilepsy	(Itai *et al.*, 2021)
Kcnd2	1.45		Heterozygous missense mutations cause epilepsy	(Zhang *et al.*, 2021)
Cnksr2	1.42		Hemizygous LOF causes epilepsy	(Higa *et al.*, 2021)
Aspa	0.71	Involved in myelination Homozygous LOF causes leukodystrophy	Double knockout of *Aspa* and *Atrn* causes seizures Homozygous LOF causes seizures	(Klugmann *et al.*, 2005; Gohma *et al.*, 2007)
Ptn	0.70	Promotes OL differentiation		(Kuboyama *et al.*, 2015)
Atp6v0b	0.70		Heterozygous missense mutations cause epilepsy	(Mattison *et al.*, 2023)
Plp1	0.68	Major component of myelin		(Khalaf *et al.*, 2022)

In our dataset, GCs exhibited the most DEGs compare to WT (n =184, 106 upregulated) and the highest fold changes (up to 3.2-fold) of any cell type in the chronic seizure samples (Fig. 6-8C, Fig. 6-13B, Appendix B2). All 15 genes that were dysregulated in the pseudo-bulk comparison were more strongly dysregulated in granule cells, suggesting that the global changes are driven by GC gene expression changes.

Gene ontology analysis with the GO Cellular Compartment dataset suggests that both up- and down-regulated genes are localized to synapses (Fig. 6-13C). The upregulated genes are enriched for GO Biological Processes terms related to chemical synaptic transmission (Fig. 6-13D). These changes occur at both the pre- and post-synaptic levels. Upregulated presynaptic genes include *Syn3* (synapsin-3), *Scg2*, *Nrg1* (neuregulin-1), *Grm8* (metabotropic glutamate receptor 8), *Lrrk2*, *Kcnj3*, *Nrg1* (neuregulin-1), and *Nrxn3* (neurexin-3). These changes suggest that hippocampal GCs may modulate their synaptic output in response to chronic seizures and elevated excitatory stimuli. GCs also exhibited upregulation of postsynaptic genes, including *Gria4* (glutamate receptor 4), *Lrrc4c*, *Epha7* (ephrin type-A receptor 7), *Sorcs3*, *Nectin3*, and *Adgrb1*.

The downregulated genes in GCs are enriched for GOBP terms related to neuronal development and cell morphology (Fig. 6-13D). Downregulated genes include the cell adhesion molecule genes *Dscam*, *Dscaml1*, *Kirrel3*, and *Cdh8*; and the axon guidance genes *Sema5a*, *Robo1*, *Slit1*, and *Dcc*. Chronic seizures might cause changes in GC synaptic wiring. It is also possible that downregulation of these genes, many of which are involved in neuronal development, is due to the age difference

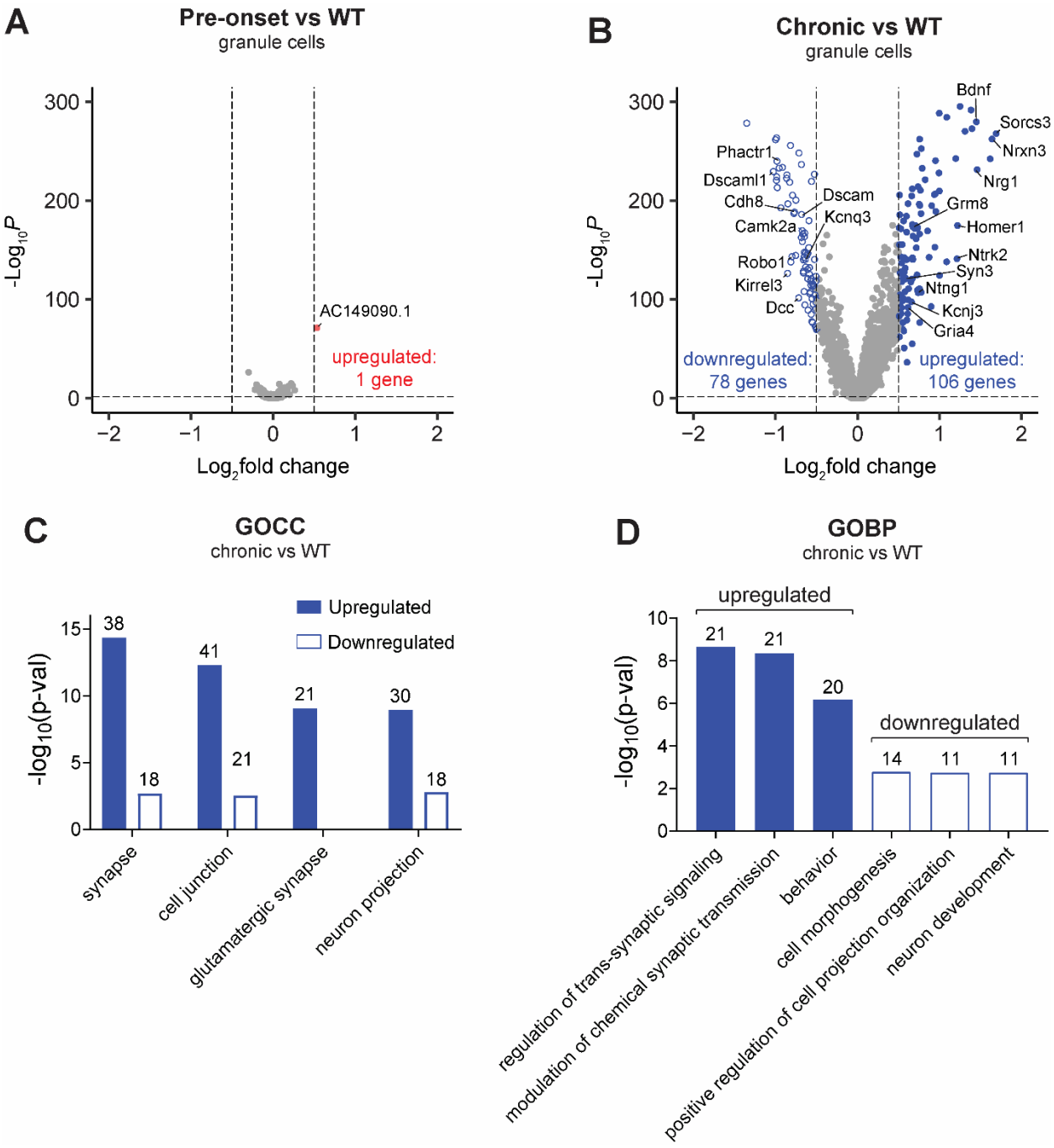

Figure 6-13. Chronic seizures alter gene expression in dentate gyrus granule cells. (A-B) Differential gene expression analysis comparing WT and pre-onset (A) or chronic seizure granule cells (B). Significance cutoffs were set at |log2FC| > 0.5 and adjusted *p*-value < 0.05. (C-D) Gene ontology analysis of up- or down-regulated genes using the Gene Ontology Cellular Compartments (GOCC) or Biological Processes (GOBP) databases. Numbers indicate the number of dysregulated genes in each GO term.

between our WT (P50) controls and the mice with chronic seizures (~5 months).

No evidence of aberrant neurogenesis caused by chronic seizures

Seizures cause aberrant granule cell neurogenesis in the subgranular zone of the adult mouse hippocampus (Parent *et al.*, 2006; Jessberger and Parent, 2015; Chen *et al.*, 2021a). To investigate whether the altered gene expression in granule cells was due to elevated neurogenesis, we examined expression of genes known to be involved in neurogenesis (Fig. 6-14) (von Bohlen Und Halbach, 2007). Among granule cells, we observed no change in expression of neural progenitor cell markers (*Gfap*, *Nestin*, and *Pax6*) or immature neuron markers (*Neurod1*, *Ncam1*, *Dcx*, *Dpysl3*, *Tubb3*, and *Calb2*). We also observed no change in the proportion of granule cells in our samples (Fig. 6-10). Aberrant adult neurogenesis does not appear to be the cause of altered granule cell gene expression, although neurogenesis may have occurred earlier in the interim between seizure onset (~3 months) and analysis (~5 months).

DISCUSSION

We performed single-nucleus RNA-sequencing to identify hippocampal gene expression changes caused by the *Scn8a* gain-of-function mutation p.N1768D. Before seizure onset, we identified few gene expression changes. The *Scn8a* mutation alone is evidently not sufficient to alter gene expression, although we identified a possible increase in the number of hippocampal oligodendrocytes in the pre-seizure samples. However, we were unable to confirm this effect by immunostaining. After 10 weeks of chronic seizures, the unconfirmed effect on oligodendrocyte number was magnified and accompanied by gene expression changes suggestive of synaptic function. Chronic seizures also caused many gene expression changes in dentate gyrus granule cells,

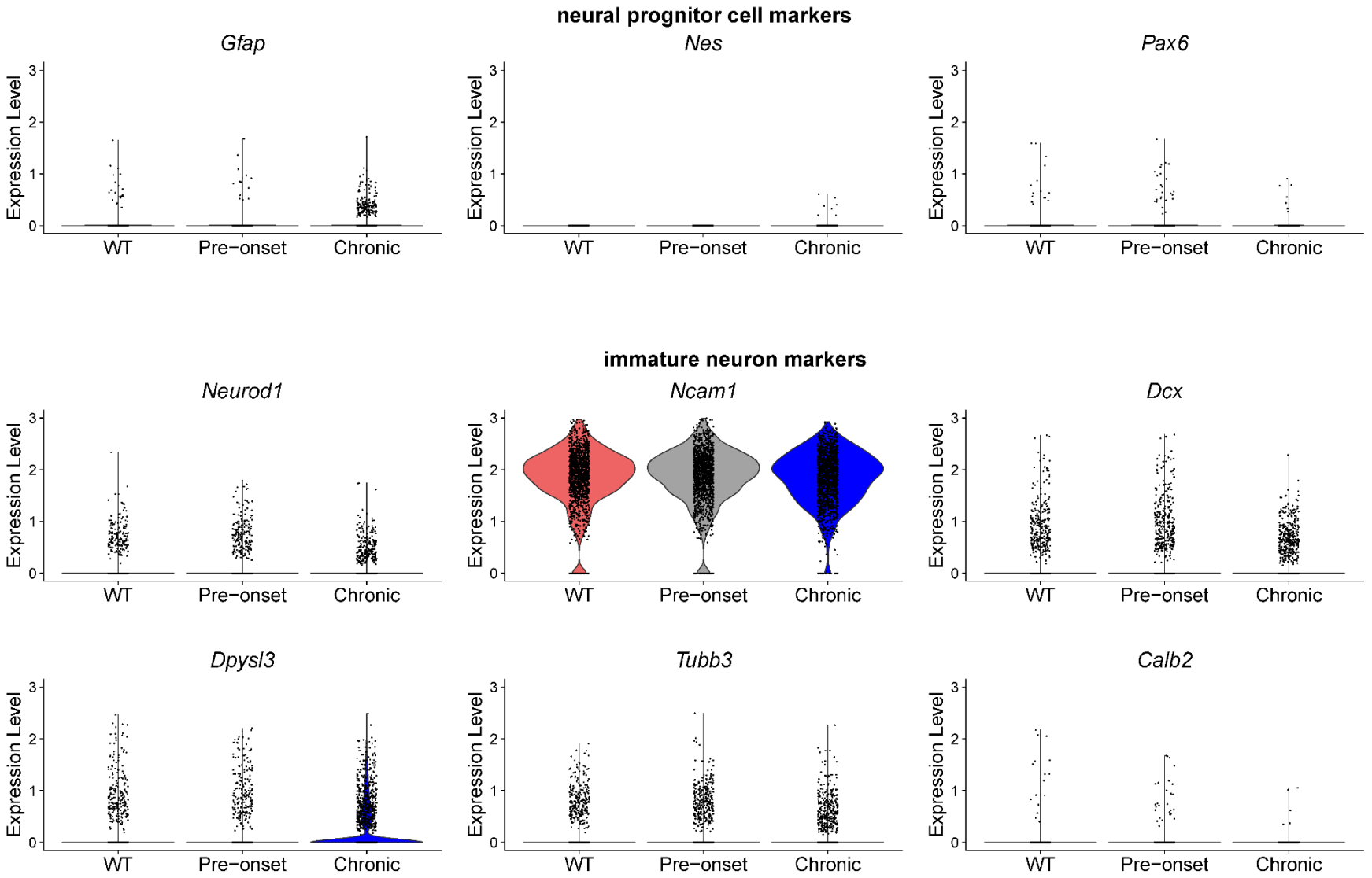

Figure 6-14. Chronic seizures do not cause aberrant adult neurogenesis in the D/+ model. Expression of adult neurogenesis genes in granule cells. Expression is shown in transcripts per 10,000.

which were not present before seizure onset. These gene expression changes suggest that granule cells regulate their excitability in response to excessive stimulation caused by chronic seizures. This is the first study to use single-nucleus RNA-sequencing to investigate transcriptional changes in a mouse model of genetic epilepsy. Our results suggest two uniquely vulnerable cell types, both of which are unexplored in *SCN8A* epilepsy: granule cells and oligodendrocytes.

Three previous studies have investigated transcriptional changes caused by mutation of the sodium channels *Scn1a* or *Scn8a* using bulk RNAseq (Sprissler *et al.*, 2017; Hawkins *et al.*, 2019; Valassina *et al.*, 2022). Before seizure onset, the earlier works did not detect large gene expression changes, suggesting hyperexcitability does not depend on transcriptional changes. Our findings agree with these reports. Even within specific neuronal and glial cell types, the *Scn8a* mutation causes only a few (≤12) small transcriptional changes before seizures begin.

We collected samples after 10 weeks of chronic seizures. Earlier bulk RNAseq studies collected samples much earlier in the disease course (24 hours after seizures in Sprissler *et al*) and observed large (~9-fold) gene expression changes, especially of immediate early genes and genes associated with astrogliosis (Sprissler *et al.*, 2017; Hawkins *et al.*, 2019; Valassina *et al.*, 2022). These findings agree with the wider epilepsy literature. Although bulk RNAseq in non-genetic epilepsy models has produced highly variable results (Dingledine *et al.*, 2017), one relatively consistent finding is activation of the inflammatory response and astrogliosis (Chen *et al.*, 2020; Cid *et al.*, 2021). We did not observe astrogliosis in the hippocampus from chronic seizure mice, perhaps due to the difference in sample collection point.

Among the cell types in our study, granule cells (GCs) had the greatest transcriptional change after chronic seizures. We hypothesize that the position of GCs as the first hippocampal neurons to receive cortical input makes them especially likely to exhibit transcriptional changes in response to seizures. The granule cells may reduce activity of their synapses as a homeostatic mechanism to prevent excitotoxicity. This adaptation would protect the downstream CA1 and CA3 pyramidal neurons, which exhibit fewer gene expression changes than the GCs (Fig. 6-8C).

Our study confirms long-held views in the sodium channel field about differences in sodium channel expression in different cell types. In our dataset, *Scn1a* is 2-fold more highly expressed in inhibitory neurons than excitatory neurons, and is expressed 1.5-fold higher in parvalbumin interneurons than other inhibitory neurons. *Scn2a* and *Scn8a* are highly expressed in all types of neurons, including interneurons. *Scn3a* has relatively low expression in all cell types, consistent with its less prominent role in adulthood. We also detected expression of the four sodium channel isoforms in oligodendrocyte precursor cells. The function of sodium channels in OPCs is not clear. Two reports suggest that expression of *Scn2a* is associated with action potential firing in a subset of OPCs (Jiang *et al.*, 2013; Gould and Kim, 2021).

We identified a possible increase in the number of hippocampal oligodendrocytes in pre-seizure and chronic seizure hippocampus, although we were not able to validate this effect with immunostaining. The increase in oligodendrocytes was small before disease onset (1.3-fold increase), but larger after 10 weeks of chronic seizures (1.7-fold increase). This effect would be surprising, since *Scn8a* is not expressed in oligodendrocytes (Fig. 6-7). One possible explanation is that excessive neuronal activity

causes increased OPC differentiation, resulting in an increased number of mature oligodendrocytes. This phenomenon was recently reported in white matter tracts associated with absence epilepsy in *Scn8a* loss-of-function mice (Knowles *et al.*, 2022b). In *Scn8a* haploinsufficient mice, the additional oligodendrocytes caused excessive myelination, exacerbating the absence seizure phenotype (Knowles *et al.*, 2022b).

White matter abnormalities have not been investigated in humans with *SCN8A* mutations, and hypermyelination is rarely reported in epilepsy. However, one emerging phenotype called mild malformation of cortical development with oligodendroglial hyperplasia in epilepsy (MOGHE) is characterized by increased density of oligodendrocytes and ectopic neurons in the white matter (Bonduelle *et al.*, 2021). Our results suggest that oligodendrocytes, a previously unstudied cell type in *SCN8A* epilepsy, may play a role in disease pathogenesis.

From this pilot study of transcriptional changes in D/+ hippocampal cell populations, the following observations warrant following:

1. Expression of the VGSCs, especially *Scn8a*, in OPCs: the role of the VGSCs in OPCs is not well characterized. More study is needed to understand their function.
2. Gene expression changes in chronic seizure granule cells: are they an artifact of sample collection time points or real changes due to seizures?
3. Increase in oligodendrocyte quantity: needs further confirmation

Chapter VII

Conclusions and Outstanding Questions

CONCLUSIONS

My dissertation began with the hypothesis that gain-of-function mutations of *Scn8a* could be counteracted by reducing expression of *Scn8a*. When I joined, the lab had recently discovered that the *Scn8a* ASO prolonged the survival of *Scn8a*-R1872W mutant mice. Since then, I have continued our study of the ASO. In Chapter 2, I investigated the kinetics of ASO effectiveness and showed that administering the ASO at postnatal day 2 (P2) reduces *Scn8a* expression for six weeks before its effects subside. I also demonstrated that the ASO does not cause substantial movement impairment in treated mice, consistent with previous observations of *Scn8a*$^{+/-}$ mice. I also found that treatment of another mouse mutant with *Scn1a* haploinsufficiency with a single dose of *Scn8a* ASO prevents premature death and seizures, even months after the ASO has worn off. This result inspired the experiments in Chapter 4, where I examined the effectiveness of the *Scn8a* ASO in other epileptic models. I showed that reducing *Scn8a* expression extends the lifespans of *Kcna1*, *Kcnq2*, and *Lgi1* mutant mice. This result is consistent with the view that Nav1.6 is a key determinant of the generation of action potentials in mice of various genotypes.

In Chapter 3, I made the important observation that the *Scn8a* ASO is effective even when administered to *Scn8a*-N1768D mice after the onset of seizures. This result

is important because successful therapeutic application requires that changes in the early stages of disease are reversible. Repeated doses of the *Scn8a* ASO prolonged median lifespan of the *Scn8a*-N1768D mice beyond one year after seizure onset, the longest these mice have ever been reported to live. Discontinuing treatment caused return to frequent seizures and death.

In Chapter 5, I tested the therapeutic potential of an ASO that reduces expression of *Kcnt1*, a potassium channel gene. I demonstrated that the *Kcnt1* ASO was effective in treating both *Scn8a* and *Scn1a* mutant mice, though not as effective as the *Scn8a* ASO. This result suggests that modulation of key ion channels like Nav1.6 and KCNT1 can be used to treat multiple types of epilepsy.

Finally, in Chapter 6, I performed single-nucleus RNA-sequencing to examine the molecular consequences of chronic seizure activity in the hippocampus of D/+ mice. Before seizure onset, I observed few gene expression changes in *Scn8a*-N1768D mutants compared with WT mice. After 10 weeks of seizures, I observed more than 150 differentially expressed genes in dentate gyrus granule cells, suggestive of altered synaptic transmission. I also observed a potential increase in the number of hippocampal oligodendrocytes. Although initial histological studies did not confirm an increase in hippocampal oligodendrocytes, a more extensive analysis with stereology and histology could be performed. The analysis of the chronic seizure sample is complicated by an age difference between the WT control (50 days) and chronic seizure samples (5 months), which may account for some of the observed changes. In the future, single-nucleus RNA-sequencing of age-matched WT hippocampus could be used to confirm my results.

OUTSTANDING QUESTIONS

Would the *Scn8a* ASO be effective in other types of epilepsy?

We showed that reducing *Scn8a* expression can extend the lifespan of *Scn1a*, *Kcna1*, *Kcnq2*, and *Lgi1* mouse mutants (Chapters 2 & 3). These findings raise the question of which other types of epilepsy could also be treated by reducing *SCN8A* expression.

The *Scn8a* ASO was differentially effective in the various mouse models we tested. A single dose of the *Scn8a* ASO at postnatal day 2 completely rescued the seizure and premature death phenotypes of *Scn1a* haploinsufficient mice. The lifespans of *Kcna1* and *Kcnq2* mutant mice were extended by the *Scn8a* ASO, but a single dose did not confer a permanent rescue. Mutation of *Lgi1*, the only non-ion channel gene we tested, demonstrated the smallest benefit from ASO treatment. *Lgi1*$^{-/-}$ mice survived only one week longer when treated with the *Scn8a* ASO. Greater reduction of *Scn8a* expression may be required for treatment of non-channelopathies.

Why does transient reduction of *Scn8a* cause long-term rescue of *Scn1a*$^{+/-}$ mice?

In Chapter 2, I treated *Scn1a*$^{+/-}$ mice with a single dose of the *Scn8a* ASO on postnatal day 2. Although the ASO reduces *Scn8a* expression for only six weeks, the mice were completely protected from seizures and death for at least six months. This effect is so far unique to *Scn1a*; the *Kcna1*, *Kcnq2*, and *Lgi1* mutant mice were rescued only for the short term.

Scn1a$^{+/-}$ mice undergo a critical period between 2 and 3 weeks of age in which the firing rate of cortical parvalbumin interneurons (PVINs) is reduced (Favero *et al.*, 2018). In the mice that survive to adulthood, PVIN firing is restored to normal, perhaps

due to compensatory changes in expression or localization of other sodium channel proteins (Kaneko *et al.*, 2022). It is unclear how reduced expression of *Scn8a* during this critical period could compensate for loss of *Scn1a*. One possibility is that reduced *Scn8a* primarily affects excitatory neurons, so the loss of PVIN input is balanced by reduced excitatory activity. However, *Scn8a* is expressed at nearly equal levels in excitatory and inhibitory neurons, so the explanation is likely more complex.

Similarly, it is unclear why reduced *Kcnt1* expression prolonged the lifespan of *Scn1a* and *Scn8a* mutant mice (Chapter 5). Electrophysiological characterization of interneurons, especially PVINs, and pyramidal neurons from mice treated with *Scn8a* and *Kcnt1* ASOs is needed to understand the mechanism of these effects.

How much reduction of *Scn8a* is required for the therapeutic benefit observed in mice treated with the ASO?

It is critical to establish exactly how much *SCN8A* reduction is required to prevent seizures so that deleterious effects from too much reduction can be avoided. In the mouse, 50% reduction with the *Scn8a* ASO was well-tolerated, even with >10 repeated doses (Chapter 3). However, *Scn8a*$^{+/-}$ mice with 50% of normal Nav1.6 activity have subtle anxiety-like behavior and absence seizures (McKinney *et al.*, 2008; Papale *et al.*, 2009). Some humans with *SCN8A* haploinsufficiency have movement disorders, generalized epilepsy, and intellectual disability (Trudeau *et al.*, 2006; Johannesen *et al.*, 2022). Although these side effects may be acceptable to patients with *SCN8A*-DEE, less severe reduction of *SCN8A* might cause fewer side effects.

Accurate assessment of *Scn8a* reduction is complicated by the time required for protein turnover. The half-life of Nav1.6 protein is less than 2 weeks (Makinson *et al.*,

2014). Administration of the *Scn8a* ASO at postnatal day 2 caused 50% reduction in *Scn8a* transcript at 3 weeks of age (Chapter 2). Nav1.6 protein was also reduced by approximately 50% at this time point (Chapter 2). At 5 weeks of age, *Scn8a* mRNA expression was 75% of WT. Approximately two weeks later, when seizures began, *Scn8a* transcript had returned to WT level. We did not assess Nav1.6 expression at these time points.

Wenxi Yu treated P2 *Scn8a*-R1872W mice with AAV-shRNA that reduces expression of *Scn8a* (personal communication). The treated mice survived for more than one year, while untreated mice lived only two weeks. One year after the AAV was administered, *Scn8a* transcript was reduced to approximately 75% of WT expression, and the mice were protected from seizures and death. There may be two alternative mechanisms for this 25% reduction in transcript: either the shRNA was widely expressed throughout the brain and all neurons exhibited a 25% reduction in *Scn8a* expression, or the shRNA was only expressed in 25% of neurons and those cells have almost no remaining *Scn8a* expression.

More study is needed to determine the minimum amount of *Scn8a* reduction required to prevent seizures. The ASO time course experiment described in Chapter 2 could be repeated with smaller doses of ASO to measure both Nav1.6 protein and *Scn8a* transcript. Due to the difficulty of quantitating antibody-based approaches, mass spectrometry could be used to assess Nav1.6 abundance (Li *et al.*, 2021).

We are currently exploring strategies to limit downregulation of *Scn8a* to 50%, which would prevent the most severe effects of *SCN8A* deficiency. An allele specific ASO treatment would target only the mutant allele and not reduce expression of WT

SCN8A. Current ASOs do not achieve allele-specificity with a single base pair change. Experiments with an allele-specific sgRNA that would direct Cas9-generated indel mutations into the mutant allele are ongoing in our lab (Wenxi Yu, unpublished). Preliminary data suggest that approximately 20% inactivation of the *Scn8a*-N1768D allele may be sufficient to protect the mice from premature death.

What is the function of *Scn8a* in oligodendrocyte precursor cells and its role in myelination?

In our single-nucleus RNA-sequencing study, we detected expression of *Scn8a* and other neuronal VGSCs in oligodendrocyte precursor cells. This is consistent with expression data available in public databases like the Allen Brain Map. Due to the presence of a “poison” exon in some *Scn8a* transcripts, it is unclear whether Nav1.6 protein is expressed in OPCs. As described in Chapter 1, *Scn8a* undergoes alternative splicing of exon 18. In cultured cells and knockout mice, the neuronal transcription factors RBFOX1 or RBFOX2 are required for expression of full-length Nav1.6 (Gehman *et al.*, 2012; O'Brien *et al.*, 2012a). Astrocytes and mature oligodendrocytes purified from mouse brain expressed only the truncated form of *Scn8a*; OPCs were not tested (O'Brien *et al.*, 2012a).

VGSC currents are detected in OPCs beginning at embryonic day 18 (Spitzer *et al.*, 2019). The strongest VGSC currents are detected during the first month after birth, coinciding with the development of myelination. Currents drop to a steady-state level during adulthood (Spitzer *et al.*, 2019). Upon differentiation, VGSC currents are lost from oligodendrocytes (Spitzer *et al.*, 2019). The largest peak sodium current densities

measured in OPCs are an order of magnitude lower than neurons (20 pA/pF) (Spitzer *et al.*, 2019).

The function of Nav1.6 has not been assessed in OPCs, but expression of Nav1.2 is well-established. Gould and Kim showed that Nav1.2 is necessary for OPC spiking behavior, which they observed in a transient population during differentiation into mature oligodendrocytes. Deletion of Nav1.2 in OPCs using *Pdgfra*-Cre resulted in loss of the spiking OPC population, a larger immature OPC population, and fewer mature oligodendrocytes (Gould and Kim, 2021). These results suggest that Nav1.2 current, and OPC spiking behavior in general, is required for differentiation of mature oligodendrocytes. It is possible that Nav1.6 plays a similar role in OPC differentiation, although it is apparently not required for spiking behavior. In this case, our finding that the *Scn8a*-N1768D mutation with excess firing caused increased hippocampal oligodendrocytes may be explained by increased OPC proliferation or differentiation.

The timing of Nav1.6 expression during neuronal development is suggestive of a causative interaction between Nav1.6 localization and myelination. Nav1.2 is expressed at the axon initial segment and along the distal axon early during neuronal development, before the onset of myelination (Boiko *et al.*, 2001). Coincident with the onset of myelination, Nav1.6 replaces Nav1.2 at the distal AIS and at the developing nodes of Ranvier (Boiko *et al.*, 2001). Most interestingly, unmyelinated axons of mature neurons are occupied by Nav1.2 (Boiko *et al.*, 2001; Liu *et al.*, 2022a). VGSC localization along unmyelinated axons is driven by a 36-amino acid sequence in intracellular loop 1 (Liu *et al.*, 2022a). Introduction of the Nav1.2 sequence is sufficient to cause Nav1.6 localization along unmyelinated axons (Liu *et al.*, 2022a). Conversely, the Nav1.6

sequence prevents localization of Nav1.2 along unmyelinated axons (Liu *et al.*, 2022a). This suggests that interaction with an unknown protein localizes or stabilizes Nav1.2, but not Nav1.6, on unmyelinated axons. I propose two explanations for these findings. First, myelination may cause Nav1.6 to localize at the nodes of Ranvier and exclude Nav1.2. Second, Nav1.6 localization at developing nodes of Ranvier may cause myelination of that axon.

Heterozygous loss of *Scn8a* has recently been associated with aberrant myelination (Knowles *et al.*, 2022b). Using *Scn8a*$^{+/-}$ mice as a model for absence seizures, Knowles *et al* identified increased OPCs and mature oligodendrocytes in white matter tracts associated with absence epilepsy. Deletion of *Ntrk2*, the BDNF receptor required for activity-dependent myelination, prevented aberrant myelination in *Scn8a*$^{+/-}$ mice and reduced the frequency of absence seizures (Knowles *et al.*, 2022b). It is not clear from these results whether the seizures or the *Scn8a* heterozygosity cause the aberrant myelination. Our snRNAseq study of the *Scn8a* gain-of-function mice suggests that both factors contribute (Chapter 6). Before the onset of seizures, we detected a slight (1.3-fold) increase of hippocampal oligodendrocytes. After 10 weeks of chronic seizures, we observed a larger (1.7-fold) increase of oligodendrocytes. However, these results were not confirmed by immunostaining. Interestingly, we also observed upregulation of *Bdnf* and *Ntrk2* in response to seizures in the *Scn8a*-N1768D mice (Chapter 6).

Based on these findings, closer study of potential white matter defects in mice and humans with *SCN8A* mutations is warranted. If *SCN8A* mutations cause white matter defects, they might be similar to mild malformation of cortical development with

oligodendroglial hyperplasia in epilepsy (MOGHE) (Bonduelle *et al.*, 2021). In that phenotype, increased oligodendrocytes and ectopic neurons in the white matter are observed (Bonduelle *et al.*, 2021). Future experiments could also delete *Scn8a* in OPCs or activate the *Scn8a*-R1872W mutation in OPCs using *Pdgfra*-Cre to determine the effect of *Scn8a* mutations on oligodendrogenesis and OPC function. It will also be interesting to investigate the spiking behavior of OPCs in *Scn8a* GOF and LOF mice.

Prospects for treatment of genetic epilepsies

Currently, there are three main approaches for the development of therapies to treat genetic epilepsies: small molecule drugs, ASOs, and gene therapies. The major advantage of the small molecule approach is that drugs can be selected to cross the blood-brain barrier, so dosing can be achieved through oral or intravenous administration. With current technology, neither ASOs nor viral vector-mediated gene therapies can cross the human blood-brain barrier and must be administered directly to the cerebrospinal fluid. In the future, lipid nanoparticles or new viral vectors may permit systemic administration of ASOs and gene therapies.

Sodium channel blockers are small molecule drugs that are effective in many types of epilepsy, including adult-onset seizures, traumatic brain injury, and focal cortical dysplasia (Kwan and Brodie, 2000; Szaflarski *et al.*, 2014; Chen *et al.*, 2021b; Smith, 2021). However, their nonspecific inhibition of VGSCs can cause toxicity at therapeutic doses. Side effects include ataxia, drowsiness, heart arrythmia, and birth defects (French *et al.*, 2021; Saenz-Farret *et al.*, 2022; Yang *et al.*, 2022a). Therapies that target only one sodium channel are expected to cause fewer side effects.

Reducing expression of *SCN8A* might avoid these side effects while retaining antiepileptic activity. The most urgent future direction of this work is to develop an ASO that reduces expression of the human *SCN8A* transcript. Due to the high cost of manufacturing and testing requirements, this work is best performed by a pharmaceutical company and not an academic lab. We are excited to be discussing collaboration with a company on this project.

Two new anti-seizure small molecule drugs with some preference for Nav1.6 are in clinical trials. NBI-921352 (formerly known as XEN901) is a small molecule sodium channel blocker with >500-fold higher potency for Nav1.6 than for the other neuronal VGSCs, when assessed in HEK293T cells (Johnson *et al.*, 2022). Acute administration to *Scn8a*$^{N1768D/+}$ mice reduced their susceptibility to electrically induced seizures (Johnson *et al.*, 2022). In a Phase 1 clinical trial, NBI-921352 was tolerated in healthy adults with rare, mild side effects including nausea and dizziness (Beatch *et al.*, 2020). A Phase 2 clinical trial, in which NBI-921352 will be evaluated as an add-on therapy in children with *SCN8A*, is currently underway.

Prax-562 is a second drug with some preference for Nav1.6. Standard sodium channel blockers inhibit several types of sodium current (peak current, persistent current, and resurgent current). Excessive persistent current is associated with seizures in *Scn8a* and *Scn2a* mutant animals (Stafstrom, 2007; Wengert and Patel, 2021), and Nav1.6 generates the most persistent current of the neuronal VGSCs (Raman *et al.*, 1997; Pan and Cummins, 2020). Specific inhibition of persistent current may reduce epileptic activity while preserving normal action potential firing. To this end, Prax-562 was developed as an inhibitor of persistent current (Kahlig *et al.*, 2022). Prax-562

increased latency to seizures in WT mice subjected to maximal electroshock model without impairing movement. In a Phase 1 clinical trial of healthy volunteers, Prax-562 was well-tolerated on its own. However, combination therapy with Prax-562 and the conventional sodium channel blocker oxcarbazepine caused significant side effects and the treatment was discontinued (Mahalingam *et al.*, 2023; Pfister *et al.*, 2023).

It will be interesting to determine which types of epilepsy can be treated with these small molecules and with ASOs, and to compare the effectiveness of the two approaches. Small molecule drugs generally exert their effects on proteins and rely on 3D structure to identify targets. Because the structure of functionally important regions is highly conserved between related proteins (for example, the pore domain of the VGSCs), small molecules often cause off-target effects. ASOs and gene therapies can achieve higher specificity by targeting gene-specific sequences. They can also be individually tailored to a patient's mutation (Kim *et al.*, 2019). Currently, these efforts are labor-intensive and cost hundreds of thousands to millions of dollars (Hayden, 2022b). In the future, algorithms to select optimal ASOs or sgRNAs could reduce the cost enough that hospitals could regularly offer patient-customized treatments for genetic epilepsies.

However, there are significant safety concerns associated with ASOs and gene therapy in humans. Recently, the only two people treated with an n-of-1 ASO that reduces expression of *Kcnt1* developed life-threatening hydrocephalus (Kaiser, 2022). Much more rarely, hydrocephalus was observed in larger clinical trials of ASOs to treat spinal muscular atrophy and Huntington's disease (Stoker *et al.*, 2021; Viscidi *et al.*, 2021). The cause of the hydrocephalus is unclear, as is the reason some ASOs are

apparently more toxic than others. If hydrocephalus is caused by the sequence or chemistry of the ASO, future ASOs could be designed to avoid this toxicity.

The safety of gene replacement therapy has been in question since 1999, when the injection of an adenovirus caused a massive immune response and led to the death of Jesse Gelsinger, a clinical trial participant (Raper *et al.*, 2003). A different trial using a retroviral vector caused five cases of leukemia due to insertional mutagenesis (Herzog, 2010). Since then, less immunogenic and non-insertional viruses have been developed and administered safely to humans (Uddin *et al.*, 2020; Kulkarni *et al.*, 2021). Two FDA-approved gene replacement therapies using these viruses target the nervous system: Luxturna, injected intraocularly to treat Leber congenital amaurosis, and Zolgensma, injected intrathecally to treat spinal muscular atrophy (Marrone *et al.*, 2022). These gene replacement approaches are limited to genes smaller than the carrying capacity of AAV vectors (~4.7 kb) (Marrone *et al.*, 2022). In addition, immune suppression is required for these treatments.

CRISPR/Cas9-based gene editing is a more controversial approach to gene therapy due to the potential for off-targeted editing. Theoretically, a single administration of CRISPR/Cas9-based gene editing would protect a person for the rest of their lives. A CRISPR-based therapy for Leber congenital amaurosis type 10 has entered clinical trials (Li *et al.*, 2023a). Leber congenital amaurosis type 10 is most often caused by an intronic missense mutation that creates a novel splice donor site (Maeder *et al.*, 2019). The CRISPR therapy uses Cas9 and two sgRNAs to cut out the affected intron, restoring the reading frame (Maeder *et al.*, 2019).

In addition to gene editing, Cas9 can be used to up- or down-regulate gene expression by fusion with transcriptional activators or repressors. CRISPRa-based upregulation of *Scn1a* rescued seizures and premature death in a mouse model of Dravet Syndrome, and upregulation of *Kcna1* reduced seizure frequency in a kainic acid-induced model of temporal lobe epilepsy (Snowball *et al.*, 2019; Colasante *et al.*, 2020a; Colasante *et al.*, 2020b). In the future, CRISPRi-based downregulation of *SCN8A* expression could be used to treat *SCN8A*-DEE.

Currently, ASOs and the next generation of small molecule drugs are in clinical trials for the treatment of genetic epilepsies. I expect that over the next decade, advances in viral vector design will make gene replacement more viable. It is unclear whether gene editing approaches for epilepsy will enter the clinic. The potential for a true cure is attractive, but the risk of causing further harm may deter patients and families. I believe that the precise targeting specificity of ASOs, combined with their relatively low risk, provide the best option for precision therapy in spite of the requirement for repeated administration.

Final remarks

My work in this dissertation provided proof-of-principle that reducing *SCN8A* expression could be therapeutic in a range of epilepsy disorders. I hope that the next few years will bring such therapies into clinical trials. In the meantime, work continues to understand the function of *SCN8A* and the consequences of mutations.

APPENDIX A

Significant Differentially Expressed Genes in Pre-Onset snRNAseq Dataset

Appendix A1. Granule cell comparison, pre-onset vs. WT.

Gene	-log10(*p*)	Log2FC	Fold change
AC149090.1	71	0.53	1.45

Appendix A2. CA1 comparison, pre-onset vs. WT

Gene	-log10(*p*)	Log2FC	Fold change
AC149090.1	81	0.53	1.45

Appendix A3. CA2 comparison, pre-onset vs. WT

Gene	-log10(*p*)	Log2FC	Fold change
AC149090.1	1.5	0.61	1.53
Gm47283	1.5	-0.51	0.70

Appendix A4. CA3 comparison, pre-onset vs. WT

Gene	-log10(*p*)	Log2FC	Fold change
AC149090.1	35	0.58	1.50

Appendix A5. Inhibitory neuron comparison, pre-onset vs. WT

Gene	-log10(*p*)	Log2FC	Fold change
AC149090.1	28	0.60	1.51

Appendix A6. Oligodendrocyte comparison, pre-onset vs. WT

Gene	-log10(*p*)	Log2FC	Fold change
Nrg3	25	0.59	1.50
Kcnip4	26	0.58	1.50
Nrxn3	24	0.58	1.49
Csmd1	24	0.57	1.49
Rbfox1	23	0.57	1.48
Lrrtm4	21	0.53	1.45

Appendix A7. Immune cell comparison, pre-onset vs. WT

Gene	-log10(*p*)	Log2FC	Fold change
Cadm2	7	0.69	1.61
Nlgn1	7	0.65	1.57
Csmd1	6	0.63	1.55
Syt1	6	0.61	1.53
Dlg2	6	0.59	1.51
Kcnip4	5	0.57	1.59
Grm5	5	0.55	1.46
Fgf14	4	0.54	1.46
Nrxn3	4	0.52	1.44
Nrg3	6	0.52	1.43
Dlgap1	6	0.51	1.43

Appendix A8. Astrocyte comparison, pre-onset vs. WT

Gene	-log10(*p*)	Log2FC	Fold change
Rbfox1	10	0.61	1.52
Dlg2	7	0.51	1.42
AY036118	9	-0.54	0.69

APPENDIX B

Significant Differentially Expressed Genes in Chronic Seizure snRNAseq Dataset

Appendix B1. Pseudo-bulk comparison, chronic seizures vs. WT

Gene	-log10(*p*)	Log2FC	Fold change
Zfp804a	244	0.83	1.77
Bdnf	∞	0.70	1.62
Sorcs1	289	0.69	1.61
Spock3	197	0.64	1.56
Homer1	233	0.60	1.52
Mir670hg	257	0.59	1.50
Pam	177	0.57	1.48
Sorcs3	130	0.57	1.48
Brinp1	138	0.53	1.45
Nrxn3	64.7	0.50	1.42
Egfem1	99.2	-0.50	0.71
4930509J09Rik	268	-0.51	0.70
5330438D12Rik	∞	-0.52	0.70
Cmss1	∞	-0.57	0.68
Pigk	275	-0.56	0.68

Appendix B2. Granule cell comparison, chronic seizures vs. WT sample 1

	WT 2			WT 3			Chronic 1			Chronic 2			Chronic 3			All chronic samples		
Gene	**-log (p)**	**logFC**	**FC**	**-log (p)**	**logFC**	**FC**	**-log (p)**	**logFC**	**FC**	**-log (p)**	**logFC**	**FC**	**-log (p)**	**logFC**	**FC**	**-log (p)**	**logFC**	**FC**
Sorcs3	0.2	-0.08	0.95	0.3	0.01	1.01	50	0.72	1.65	50	0.66	1.58	172	3.36	10.2	268	1.69	3.23
Nrxn3	0.0	0.04	1.03	0.3	0.15	1.11	122	2.03	4.08	27	0.71	1.63	152	2.35	5.09	262	1.64	3.11
Zfp804a	0.4	-0.10	0.93	1.4	-0.16	0.90	50	0.85	1.80	24	0.56	1.48	168	2.97	7.85	242	1.62	3.07
Nrg1	0.0	0.05	1.04	0.2	0.09	1.06	74	1.41	2.66	46	1.07	2.10	129	1.98	3.94	231	1.46	2.75
Bdnf	0.0	-0.02	0.99	0.0	-0.03	0.98	140	1.65	3.13	11	0.24	1.18	172	2.36	5.13	280	1.45	2.73
Unc5d	0.0	0.03	1.02	1.0	0.10	1.07	109	1.67	3.19	73	1.21	2.32	106	1.45	2.73	273	1.40	2.63
Mapk4	0.2	0.07	1.05	3.1	0.15	1.11	95	1.20	2.29	64	0.79	1.73	162	2.28	4.86	292	1.38	2.61
Pcdh7	0.2	0.06	1.04	2.0	0.15	1.11	81	1.21	2.32	82	1.18	2.27	124	1.69	3.22	270	1.31	2.48
Sorcs1	0.2	-0.04	0.97	0.0	-0.02	0.99	68	0.90	1.86	71	0.87	1.83	146	1.83	3.56	295	1.25	2.38
Homer1	0.2	0.04	1.03	0.2	0.02	1.01	137	1.86	3.64	3	-0.15	0.90	164	2.01	4.02	175	1.22	2.33
Ntrk2	0.5	-0.10	0.93	1.5	-0.13	0.92	50	0.61	1.52	2	-0.12	0.92	165	2.72	6.60	141	1.21	2.32
Spock3	0.2	-0.06	0.96	0.3	-0.06	0.96	56	0.81	1.75	31	0.58	1.50	164	1.97	3.91	243	1.20	2.29
Sema3e	0.1	-0.04	0.97	0.2	0.01	1.01	66	0.81	1.76	64	0.70	1.62	151	1.65	3.14	284	1.09	2.13
Pam	4.0	-0.20	0.87	5.4	-0.22	0.86	15	0.37	1.30	0	-0.02	0.98	166	2.30	4.93	138	1.09	2.12
Tll1	0.0	0.00	1.00	0.1	-0.01	0.99	6	0.11	1.08	1	0.01	1.00	174	2.63	6.18	124	1.00	2.00
Pappa	0.0	0.00	1.00	0.0	0.00	1.00	35	0.34	1.27	22	0.19	1.14	176	2.27	4.83	210	1.00	2.00
Adgrl3	0.1	-0.02	0.98	0.8	0.12	1.09	90	0.95	1.93	57	0.69	1.61	147	1.40	2.64	289	1.00	1.99
Frmd6	0.0	0.00	1.00	0.2	0.00	1.00	75	0.78	1.72	14	0.18	1.14	172	1.91	3.76	228	0.99	1.99
Cntn4	1.3	-0.14	0.91	0.0	-0.03	0.98	40	0.78	1.72	55	0.98	1.97	70	0.92	1.89	189	0.95	1.94
1700016P03Rik	0.1	-0.02	0.99	0.1	-0.02	0.99	136	1.41	2.66	0	-0.03	0.98	170	1.45	2.73	240	0.95	1.93
Dgkb	0.2	-0.07	0.95	0.2	-0.08	0.95	58	0.86	1.82	80	1.03	2.05	57	0.80	1.74	207	0.95	1.93
Arid5b	0.1	-0.04	0.98	0.3	-0.06	0.96	16	0.38	1.30	9	0.27	1.20	163	1.93	3.82	153	0.94	1.92
Brinp1	0.0	0.02	1.02	0.0	0.02	1.01	48	0.63	1.55	17	0.38	1.30	158	1.74	3.34	206	0.94	1.92
Snhg11	0.4	0.09	1.07	1.5	0.16	1.12	93	1.20	2.30	62	0.90	1.87	71	0.90	1.86	195	0.90	1.87
Slc2a13	0.1	-0.02	0.98	1.0	-0.08	0.94	6	0.23	1.17	0	-0.03	0.98	165	2.19	4.56	93	0.90	1.86
Rnf217	0.3	0.05	1.04	0.7	0.07	1.05	45	0.64	1.56	2	0.09	1.06	164	1.89	3.70	143	0.87	1.83

Fstl4	0.1	0.06	1.04	0.1	0.05	1.03	29	0.60	1.52	42	0.73	1.66	113	1.27	2.41	169	0.85	1.81
Nr4a2	0.0	0.00	1.00	0.5	0.02	1.01	158	1.93	3.81	1	0.02	1.01	121	0.68	1.60	221	0.82	1.77
Nr4a3	0.0	0.01	1.00	0.5	0.01	1.01	147	1.54	2.91	0	-0.01	0.99	154	0.94	1.92	233	0.79	1.73
Nr4a1	0.0	0.00	1.00	0.0	-0.01	1.00	164	1.58	2.99	1	-0.02	0.99	155	0.85	1.81	253	0.78	1.71
Osbpl6	0.0	0.03	1.02	0.0	0.00	1.00	9	0.27	1.20	2	0.11	1.08	161	1.82	3.54	107	0.78	1.71
Ankrd33b	0.1	-0.04	0.98	0.0	-0.01	1.00	38	0.54	1.46	20	0.36	1.28	139	1.30	2.47	187	0.77	1.71
Plk2	0.0	-0.01	0.99	0.1	-0.01	0.99	102	1.04	2.05	3	0.06	1.04	148	1.18	2.27	210	0.77	1.70
Xkr6	0.1	-0.04	0.97	0.0	0.03	1.02	25	0.48	1.39	64	0.78	1.72	97	0.96	1.94	195	0.76	1.69
Nptx2	0.0	-0.01	1.00	0.0	0.00	1.00	125	1.21	2.31	6	0.06	1.04	167	1.02	2.03	262	0.76	1.69
Jarid2	0.2	0.05	1.03	1.6	0.11	1.08	5	0.19	1.14	2	0.09	1.06	145	1.98	3.94	76	0.76	1.69
Tspan5	0.0	0.04	1.03	0.5	0.09	1.07	48	0.65	1.57	12	0.33	1.26	137	1.35	2.55	166	0.76	1.69
Mir670hg	0.5	-0.03	0.98	0.0	0.00	1.00	0	0.01	1.01	0	-0.03	0.98	170	2.06	4.17	111	0.76	1.69
Tanc1	0.0	0.00	1.00	0.0	-0.01	0.99	30	0.49	1.40	41	0.56	1.47	124	1.14	2.20	196	0.75	1.69
Cdh13	0.0	-0.03	0.98	0.1	-0.04	0.97	20	0.56	1.48	61	1.00	2.00	24	0.59	1.51	110	0.75	1.68
Ntng1	1.6	0.20	1.15	1.7	0.20	1.15	58	1.03	2.04	54	0.94	1.92	31	0.68	1.60	107	0.74	1.67
Stxbp5l	0.5	-0.06	0.96	0.4	-0.02	0.98	53	0.56	1.48	16	0.30	1.23	159	1.21	2.31	214	0.74	1.67
Ptprn	4.6	0.22	1.16	2.1	0.15	1.11	74	0.85	1.80	18	0.36	1.29	149	1.32	2.50	173	0.73	1.66
Brinp3	0.2	0.06	1.04	0.1	0.01	1.00	21	0.50	1.42	12	0.37	1.29	98	1.32	2.49	109	0.73	1.66
Pak7	0.4	0.09	1.06	1.1	0.14	1.10	25	0.46	1.38	9	0.26	1.20	141	1.57	2.98	125	0.73	1.65
Lhfp	0.4	0.02	1.01	0.2	0.01	1.01	102	0.90	1.86	27	0.24	1.18	144	1.05	2.07	247	0.72	1.65
Mpp7	0.1	0.01	1.01	2.1	0.08	1.06	68	0.70	1.63	9	0.13	1.09	116	1.36	2.56	152	0.72	1.64
Lmo7	0.6	0.11	1.08	0.5	0.09	1.06	42	0.60	1.52	15	0.36	1.28	144	1.32	2.49	161	0.71	1.64
Grm8	0.5	-0.07	0.95	0.2	-0.05	0.97	44	0.66	1.58	18	0.32	1.25	101	0.99	1.98	175	0.71	1.63
Nt5dc3	0.2	-0.05	0.97	0.1	0.02	1.01	89	1.00	2.00	3	0.12	1.09	117	0.97	1.95	172	0.70	1.63
Dclk1	0.1	-0.01	1.00	0.1	0.05	1.03	63	0.58	1.50	2	0.11	1.08	161	1.31	2.48	173	0.68	1.60
Rian	1.7	0.17	1.12	2.6	0.18	1.13	56	0.74	1.67	38	0.58	1.49	110	1.03	2.05	164	0.68	1.60
Nrn1	1.1	0.11	1.08	1.2	0.09	1.06	81	0.98	1.98	2	0.09	1.07	131	1.14	2.20	140	0.67	1.60
Fndc3a	0.3	0.06	1.04	1.3	0.09	1.07	47	0.61	1.52	44	0.56	1.48	105	0.96	1.95	174	0.67	1.59
Htr4	0.0	-0.02	0.98	0.4	-0.08	0.95	22	0.46	1.37	28	0.50	1.42	85	0.91	1.87	142	0.67	1.59
Efr3a	0.1	-0.03	0.98	0.4	0.06	1.04	68	0.79	1.73	46	0.59	1.51	66	0.67	1.59	176	0.67	1.59
Syne1	0.3	0.09	1.06	0.0	0.02	1.01	50	0.61	1.53	76	0.76	1.70	81	0.72	1.65	212	0.67	1.59

Maml3	0.2	-0.06	0.96	0.9	-0.10	0.93	2	0.13	1.10	17	0.40	1.32	114	1.20	2.29	121	0.67	1.59
Pde10a	7.1	-0.28	0.82	10.5	-0.31	0.81	7	-0.25	0.84	6	-0.22	0.86	149	1.68	3.21	55	0.67	1.59
Pcsk1	0.1	-0.01	0.99	0.0	0.00	1.00	72	0.73	1.65	0	-0.01	1.00	171	1.21	2.32	205	0.66	1.58
Kcnj3	0.2	0.07	1.05	0.0	0.02	1.01	8	0.25	1.19	3	0.14	1.10	147	1.54	2.92	98	0.66	1.58
Syn3	0.1	0.07	1.05	3.9	0.25	1.19	48	0.75	1.68	67	0.92	1.89	39	0.60	1.52	118	0.65	1.57
Lrrc4c	0.0	0.02	1.02	0.4	0.08	1.06	12	0.33	1.26	29	0.51	1.43	89	1.05	2.07	111	0.62	1.54
Chsy3	0.0	0.00	1.00	0.0	0.00	1.00	55	0.83	1.78	52	0.81	1.75	6	0.27	1.21	99	0.62	1.54
Rasgrp1	0.1	0.02	1.01	1.0	0.04	1.03	71	0.76	1.69	48	0.50	1.42	92	0.66	1.58	197	0.62	1.53
Gria4	0.1	-0.05	0.96	0.0	0.00	1.00	29	0.57	1.48	1	0.11	1.08	83	1.07	2.10	92	0.62	1.53
Zfp536	0.0	-0.03	0.98	0.0	0.00	1.00	3	0.16	1.12	2	0.13	1.09	139	1.40	2.63	85	0.61	1.53
Ppm1l	0.1	-0.05	0.97	0.1	-0.04	0.97	6	-0.24	0.85	1	-0.10	0.93	149	1.85	3.61	36	0.60	1.52
Epha7	0.1	0.08	1.05	1.0	0.16	1.12	17	0.43	1.35	0	0.01	1.01	145	1.51	2.84	79	0.60	1.52
Lrrk2	0.1	0.02	1.01	0.3	0.01	1.01	13	0.19	1.14	13	0.16	1.11	155	1.37	2.58	140	0.60	1.52
Tiparp	0.3	-0.04	0.97	0.1	-0.03	0.98	128	1.35	2.54	0	-0.04	0.97	85	0.52	1.43	168	0.60	1.52
Penk	0.0	0.00	1.00	0.0	0.00	1.00	56	0.56	1.47	6	0.06	1.04	141	1.12	2.17	184	0.60	1.51
Fam126b	0.0	-0.02	0.99	0.0	0.01	1.01	18	0.37	1.30	7	0.22	1.17	127	1.08	2.12	122	0.58	1.50
Ncam2	0.1	-0.01	0.99	1.0	-0.05	0.96	33	0.55	1.46	25	0.45	1.37	50	0.67	1.59	132	0.58	1.50
Cpeb3	0.4	0.08	1.06	0.7	0.09	1.06	20	0.39	1.31	11	0.28	1.22	117	1.16	2.24	108	0.58	1.49
Fras1	0.7	-0.08	0.94	2.5	-0.14	0.91	25	0.46	1.38	21	0.41	1.33	42	0.62	1.53	120	0.58	1.49
Enox1	0.8	-0.08	0.95	0.2	-0.02	0.99	12	0.24	1.18	8	0.18	1.13	154	1.10	2.15	142	0.57	1.48
Ndfip2	0.1	-0.04	0.97	0.1	0.01	1.00	78	0.92	1.89	1	0.07	1.05	79	0.72	1.64	127	0.57	1.48
Mlip	0.8	-0.11	0.93	1.9	-0.15	0.90	0	-0.03	0.98	6	-0.21	0.86	141	1.54	2.91	51	0.57	1.48
Kctd1	0.0	0.00	1.00	0.3	0.04	1.03	18	0.35	1.27	19	0.34	1.26	104	0.98	1.98	121	0.57	1.48
Usp29	0.3	-0.09	0.94	0.1	-0.04	0.97	1	0.11	1.08	1	0.09	1.06	109	1.25	2.38	68	0.56	1.48
Ptgs2	0.1	0.00	1.00	0.2	0.00	1.00	60	0.59	1.50	4	0.03	1.02	144	1.02	2.03	179	0.56	1.48
Gad1	0.0	0.00	1.00	0.2	0.01	1.01	12	0.25	1.19	1	0.03	1.02	144	1.31	2.47	101	0.56	1.47
Kcnip3	0.3	0.07	1.05	0.8	0.09	1.06	42	0.66	1.58	65	0.87	1.82	15	0.33	1.25	99	0.56	1.47
Unc5c	0.1	-0.05	0.97	1.5	-0.16	0.90	36	0.66	1.58	26	0.54	1.45	7	0.29	1.23	77	0.55	1.47
Olfm3	0.1	0.02	1.01	0.5	0.04	1.03	9	0.20	1.15	0	0.02	1.01	111	1.39	2.61	70	0.55	1.47
Large1	1.0	-0.07	0.95	0.2	0.00	1.00	56	0.55	1.47	2	0.14	1.10	120	0.84	1.80	155	0.54	1.46
Acvr1	1.0	0.13	1.09	0.3	0.07	1.05	48	0.64	1.56	34	0.51	1.42	59	0.68	1.60	118	0.54	1.46

Lncpint	0.1	0.04	1.03	0.4	0.05	1.04	8	0.23	1.17	15	0.29	1.22	146	1.10	2.15	120	0.54	1.45
Lhfpl3	0.0	-0.01	0.99	0.9	0.03	1.02	52	0.64	1.56	47	0.59	1.51	44	0.43	1.35	137	0.54	1.45
Adgrb1	4.5	0.20	1.15	1.4	0.11	1.08	75	0.82	1.77	27	0.44	1.36	74	0.69	1.61	128	0.54	1.45
Ppm1h	0.0	0.01	1.00	0.3	-0.05	0.96	3	0.14	1.10	5	0.22	1.16	127	1.11	2.17	92	0.54	1.45
Galntl6	0.4	-0.11	0.93	3.5	0.15	1.11	28	0.54	1.45	58	0.94	1.92	14	0.18	1.14	86	0.53	1.45
Sorbs2	0.0	0.03	1.02	0.6	0.08	1.05	51	0.53	1.44	38	0.42	1.34	87	0.72	1.65	171	0.53	1.44
Hsd17b12	0.0	-0.02	0.99	0.1	-0.01	0.99	7	0.13	1.09	1	-0.08	0.94	161	1.39	2.62	97	0.53	1.44
Scg2	0.4	0.03	1.02	0.8	0.02	1.02	55	0.61	1.53	3	0.07	1.05	132	0.92	1.90	143	0.53	1.44
Abhd2	0.5	0.07	1.05	0.7	0.05	1.03	43	0.59	1.51	15	0.28	1.21	100	0.80	1.74	127	0.52	1.43
Rock2	0.2	0.05	1.04	0.1	-0.03	0.98	25	0.44	1.36	1	0.10	1.07	116	0.98	1.97	104	0.52	1.43
Nectin3	0.0	0.00	1.00	0.5	0.02	1.02	38	0.37	1.29	24	0.22	1.17	145	0.92	1.89	186	0.52	1.43
Fosl2	0.0	0.00	1.00	0.2	-0.01	0.99	92	0.72	1.65	1	0.02	1.01	152	0.80	1.74	206	0.51	1.43
Malat1	21.1	-0.30	0.81	22.5	-0.30	0.81	89	0.67	1.59	3	-0.14	0.91	75	0.44	1.36	155	0.51	1.43
Sik2	0.3	0.06	1.04	0.6	0.05	1.04	7	0.20	1.15	0	-0.06	0.96	139	1.38	2.61	62	0.51	1.43
Rgs6	0.2	0.03	1.02	3.5	0.19	1.14	11	0.23	1.18	71	0.95	1.93	37	0.52	1.44	83	0.51	1.42
Sik3	0.8	-0.11	0.93	0.2	-0.04	0.97	0	0.03	1.02	6	0.22	1.17	119	1.01	2.02	90	0.51	1.42
Spred1	0.9	-0.09	0.94	1.1	-0.10	0.94	8	0.23	1.17	0	-0.05	0.97	129	1.08	2.11	95	0.51	1.42
Meg3	9.2	0.23	1.17	6.7	0.19	1.14	85	0.72	1.65	87	0.71	1.64	62	0.53	1.44	172	0.51	1.42
Sybu	0.7	0.11	1.08	0.7	0.08	1.06	23	-0.38	0.77	0	0.02	1.02	98	-0.91	0.53	99	-0.50	0.71
Sphkap	0.1	-0.05	0.96	1.1	-0.09	0.94	40	-0.55	0.68	13	-0.27	0.83	73	-0.82	0.57	97	-0.50	0.71
Fgfr2	0.1	-0.02	0.99	0.9	-0.06	0.96	18	-0.35	0.78	34	-0.50	0.71	76	-0.70	0.61	118	-0.50	0.71
Cpne4	0.5	-0.10	0.93	5.7	-0.25	0.84	64	-0.87	0.55	0	-0.03	0.98	86	-0.97	0.51	72	-0.50	0.71
Pgbd5	0.2	0.06	1.04	0.2	-0.03	0.98	15	-0.32	0.80	1	-0.06	0.96	110	-1.04	0.49	91	-0.51	0.70
Ror1	0.0	-0.02	0.99	0.1	-0.05	0.97	40	-0.53	0.69	34	-0.49	0.71	48	-0.56	0.68	123	-0.51	0.70
Nrg2	0.1	0.02	1.01	0.1	0.01	1.01	15	-0.31	0.81	2	0.12	1.08	135	-1.23	0.43	72	-0.51	0.70
Ssbp2	0.1	-0.03	0.98	0.0	0.00	1.00	41	-0.62	0.65	21	-0.41	0.75	42	-0.56	0.68	104	-0.52	0.70
Sema5a	0.6	-0.09	0.94	0.2	-0.04	0.97	53	-0.72	0.61	0	-0.03	0.98	97	-0.94	0.52	89	-0.52	0.70
Sorcs2	0.3	-0.07	0.95	0.5	-0.08	0.95	51	-0.63	0.65	28	-0.48	0.72	47	-0.62	0.65	113	-0.52	0.70
Tnrc6c	0.0	-0.01	0.99	0.7	-0.07	0.95	39	-0.43	0.74	8	-0.18	0.88	135	-0.99	0.50	140	-0.52	0.70
Zbtb20	0.0	-0.02	0.99	0.9	0.06	1.04	82	-0.62	0.65	36	-0.32	0.80	104	-0.60	0.66	227	-0.52	0.70
Gm15738	0.9	-0.11	0.93	9.8	-0.30	0.81	33	-0.55	0.69	53	-0.70	0.61	70	-0.74	0.60	114	-0.54	0.69

St6galnac5	0.0	0.03	1.02	0.1	0.00	1.00	43	-0.58	0.67	2	-0.05	0.96	73	-0.93	0.53	95	-0.54	0.69
Cmss1	6.9	-0.25	0.84	1.2	-0.09	0.94	32	-0.49	0.71	110	-1.12	0.46	31	-0.38	0.77	116	-0.55	0.69
Slc8a1	1.1	-0.16	0.89	0.5	-0.09	0.94	32	-0.65	0.64	40	-0.72	0.61	25	-0.53	0.69	76	-0.55	0.68
Aff2	2.0	-0.16	0.90	0.3	-0.06	0.96	49	-0.73	0.60	30	-0.54	0.69	47	-0.63	0.64	101	-0.55	0.68
Pde7b	0.1	-0.03	0.98	0.6	-0.09	0.94	63	-0.94	0.52	9	-0.30	0.81	27	-0.59	0.67	78	-0.56	0.68
Rbfox1	3.2	-0.10	0.93	2.0	-0.06	0.96	99	-0.62	0.65	25	-0.23	0.85	149	-0.97	0.51	219	-0.56	0.68
Nfia	0.0	-0.01	1.00	0.3	-0.04	0.97	60	-0.75	0.59	15	-0.30	0.81	55	-0.69	0.62	121	-0.56	0.68
Rtl4	0.0	-0.04	0.97	0.4	-0.09	0.94	38	-0.68	0.63	13	-0.41	0.75	47	-0.73	0.60	85	-0.56	0.68
Trpc5	0.9	-0.13	0.91	0.5	-0.09	0.94	47	-0.67	0.63	29	-0.53	0.69	61	-0.72	0.61	115	-0.57	0.68
Cblb	0.0	0.03	1.02	0.2	0.06	1.04	33	-0.56	0.68	24	-0.43	0.74	47	-0.63	0.65	119	-0.57	0.67
Zeb2	0.6	0.11	1.08	2.8	0.17	1.13	11	-0.30	0.81	8	-0.22	0.86	72	-0.87	0.55	107	-0.57	0.67
Shisa9	0.3	-0.04	0.98	3.9	-0.20	0.87	72	-0.82	0.57	1	-0.05	0.96	102	-1.08	0.47	106	-0.58	0.67
4921534H16Rik	0.0	-0.02	0.99	6.5	-0.24	0.85	22	-0.43	0.74	60	-0.73	0.60	80	-0.81	0.57	132	-0.58	0.67
Maml2	0.6	-0.06	0.96	3.2	-0.16	0.90	57	-0.68	0.62	18	-0.28	0.82	85	-0.98	0.51	125	-0.59	0.67
Ccbe1	1.0	0.13	1.09	1.6	0.13	1.10	52	-0.52	0.70	30	-0.42	0.75	67	-0.57	0.68	180	-0.59	0.66
Grb14	0.7	-0.11	0.93	1.8	-0.15	0.90	54	-0.67	0.63	38	-0.56	0.68	88	-0.80	0.58	152	-0.59	0.66
Kcnh7	1.9	-0.20	0.87	0.6	-0.10	0.93	34	-0.68	0.62	26	-0.58	0.67	57	-0.83	0.56	89	-0.60	0.66
Mctp1	4.8	-0.17	0.89	3.2	-0.14	0.91	75	-0.85	0.56	25	-0.37	0.78	101	-0.91	0.53	147	-0.60	0.66
P2ry14	0.2	0.07	1.05	1.4	-0.12	0.92	13	-0.34	0.79	33	-0.56	0.68	87	-0.91	0.53	121	-0.61	0.66
Carmil1	0.1	0.04	1.03	0.0	0.01	1.00	38	-0.59	0.66	18	-0.38	0.77	69	-0.79	0.58	130	-0.61	0.66
5330438D12Rik	0.0	0.00	1.00	2.0	-0.13	0.91	26	-0.46	0.73	54	-0.72	0.61	74	-0.76	0.59	144	-0.62	0.65
Lcorl	0.2	-0.06	0.96	0.6	-0.09	0.94	52	-0.69	0.62	39	-0.59	0.66	66	-0.75	0.59	147	-0.63	0.65
A830018L16Rik	0.1	0.03	1.02	0.0	0.00	1.00	30	-0.51	0.70	20	-0.38	0.77	83	-0.93	0.53	133	-0.63	0.65
Kcnq3	4.8	0.22	1.16	3.4	0.17	1.12	28	-0.48	0.72	4	-0.15	0.90	79	-0.85	0.55	140	-0.63	0.64
Cyp7b1	0.0	0.01	1.01	0.0	0.02	1.01	27	-0.54	0.69	0	-0.01	0.99	120	-1.27	0.41	94	-0.64	0.64
Dok6	0.0	0.04	1.03	0.5	0.09	1.06	40	-0.54	0.69	25	-0.39	0.76	91	-0.84	0.56	167	-0.64	0.64
F730043M19Rik	0.2	0.06	1.04	0.2	-0.04	0.97	63	-0.72	0.61	22	-0.39	0.76	83	-0.80	0.57	163	-0.65	0.64
Me3	0.1	0.05	1.04	0.0	0.00	1.00	61	-0.76	0.59	14	-0.33	0.80	73	-0.80	0.58	148	-0.65	0.64
Asic2	0.1	0.05	1.04	0.0	-0.01	0.99	43	-0.77	0.59	17	-0.39	0.76	46	-0.76	0.59	108	-0.65	0.64
Nr3c2	0.0	0.01	1.01	0.2	0.04	1.03	19	-0.39	0.76	25	-0.43	0.74	103	-1.03	0.49	142	-0.65	0.64
Tenm1	2.4	-0.16	0.89	1.6	-0.15	0.90	60	-0.92	0.53	64	-0.84	0.56	37	-0.57	0.68	127	-0.66	0.63

Slc44a5	0.6	-0.09	0.94	0.9	-0.12	0.92	44	-0.68	0.62	13	-0.33	0.79	110	-1.12	0.46	128	-0.66	0.63
Adamts17	0.1	0.05	1.04	3.4	0.22	1.16	40	-0.62	0.65	20	-0.43	0.74	50	-0.66	0.63	140	-0.66	0.63
Dapk1	0.0	0.02	1.01	0.1	-0.02	0.99	61	-0.71	0.61	13	-0.24	0.85	108	-1.02	0.49	166	-0.67	0.63
Eml6	0.0	0.01	1.01	0.4	0.04	1.03	35	-0.53	0.69	28	-0.45	0.73	100	-0.94	0.52	158	-0.67	0.63
Camk2a	0.5	0.09	1.06	0.9	-0.05	0.96	45	-0.38	0.77	17	-0.19	0.88	129	-1.32	0.40	170	-0.67	0.63
Dscam	0.0	0.03	1.02	0.9	0.09	1.06	74	-0.86	0.55	25	-0.35	0.78	78	-0.73	0.60	186	-0.68	0.62
Negr1	2.4	-0.10	0.93	2.1	-0.09	0.94	97	-0.93	0.53	51	-0.45	0.73	108	-0.86	0.55	237	-0.68	0.62
Ccdc85a	0.3	0.10	1.07	1.5	0.12	1.09	32	-0.46	0.73	9	-0.18	0.88	113	-1.12	0.46	163	-0.68	0.62
Tspan18	1.6	-0.15	0.90	1.7	-0.15	0.90	84	-0.82	0.57	82	-0.79	0.58	98	-0.83	0.56	248	-0.71	0.61
Dcc	1.0	-0.18	0.89	0.2	-0.02	0.98	48	-0.92	0.53	47	-0.90	0.53	25	-0.56	0.68	101	-0.72	0.61
Rfx3	0.0	0.00	1.00	1.9	0.14	1.10	61	-0.65	0.64	16	-0.24	0.85	130	-1.17	0.44	200	-0.75	0.59
Slit1	0.2	-0.02	0.98	2.0	-0.14	0.91	50	-0.75	0.59	12	-0.29	0.82	121	-1.33	0.40	144	-0.75	0.59
Cdh8	0.0	0.03	1.02	0.1	0.10	1.07	51	-0.76	0.59	41	-0.59	0.66	70	-0.82	0.57	188	-0.77	0.59
Pigk	0.0	-0.02	0.99	3.5	-0.18	0.88	54	-0.74	0.60	52	-0.70	0.61	97	-1.04	0.49	187	-0.77	0.58
Spon1	0.0	-0.02	0.98	0.0	0.00	1.00	66	-0.82	0.57	38	-0.60	0.66	100	-0.96	0.51	205	-0.79	0.58
Robo1	2.1	-0.23	0.86	2.3	-0.22	0.86	54	-0.93	0.53	51	-0.87	0.55	70	-1.03	0.49	143	-0.80	0.58
Chst9	0.2	0.11	1.08	0.1	0.04	1.03	39	-0.78	0.58	27	-0.62	0.65	53	-0.88	0.54	138	-0.81	0.57
Csmd3	1.0	-0.12	0.92	0.1	-0.05	0.97	96	-1.00	0.50	73	-0.71	0.61	105	-0.92	0.53	256	-0.82	0.57
Ralgapa2	0.1	-0.01	0.99	0.1	0.00	1.00	84	-1.02	0.49	56	-0.71	0.61	76	-0.79	0.58	219	-0.83	0.56
Slc4a4	0.1	-0.01	1.00	0.3	-0.06	0.96	72	-0.98	0.51	50	-0.69	0.62	82	-0.94	0.52	197	-0.85	0.56
Kirrel3	1.0	-0.05	0.97	0.2	-0.02	0.99	83	-1.05	0.48	0	0.06	1.04	115	-1.59	0.33	126	-0.85	0.55
Cdk14	0.8	0.11	1.08	0.8	0.10	1.07	81	-0.94	0.52	23	-0.34	0.79	106	-1.08	0.47	226	-0.86	0.55
Gm20754	1.0	-0.09	0.94	0.3	-0.04	0.97	89	-1.03	0.49	44	-0.55	0.69	112	-1.13	0.46	223	-0.86	0.55
Itpr1	0.3	-0.08	0.95	0.9	-0.09	0.94	92	-1.07	0.48	57	-0.77	0.58	100	-1.07	0.48	234	-0.91	0.53
Gm28376	0.0	0.02	1.01	3.3	-0.21	0.87	60	-0.92	0.53	67	-1.05	0.48	77	-1.00	0.50	193	-0.93	0.52
D430041D05Rik	0.4	-0.06	0.96	0.4	-0.05	0.96	74	-0.99	0.50	43	-0.67	0.63	122	-1.28	0.41	233	-0.95	0.52
1-Mar	0.1	0.00	1.00	0.0	0.00	1.00	0	0.00	1.00	0	0.00	1.00	0	0.00	1.00	213	-0.98	0.51
Phactr1	0.1	0.03	1.02	0.3	-0.07	0.95	80	-1.01	0.50	41	-0.58	0.67	130	-1.36	0.39	240	-0.98	0.51
Pip5k1b	0.5	-0.03	0.98	6.4	-0.21	0.86	101	-1.33	0.40	39	-0.53	0.69	110	-1.34	0.40	224	-0.98	0.51
Ahcyl2	0.7	-0.06	0.96	2.0	-0.13	0.91	87	-1.04	0.49	74	-0.78	0.58	121	-1.29	0.41	263	-0.99	0.51
Frmd4b	0.6	0.09	1.07	1.5	0.12	1.09	81	-1.04	0.49	10	-0.27	0.83	140	-1.40	0.38	220	-0.99	0.50

4930509J09Rik	0.6	-0.09	0.94	11.1	-0.33	0.79	88	-1.09	0.47	88	-1.07	0.48	114	-1.23	0.43	262	-1.00	0.50
Dscaml1	0.1	-0.01	1.00	2.9	-0.15	0.90	97	-1.23	0.43	30	-0.47	0.72	135	-1.51	0.35	229	-1.02	0.49
Egfem1	3.2	-0.15	0.90	3.5	-0.17	0.89	110	-1.68	0.31	63	-0.84	0.56	132	-1.84	0.28	278	-1.35	0.39

Appendix B3. Top 16 genes in granule cell comparison, chronic seizures vs. WT sample 1

	All chronic samples				Chronic 1			Chronic 2			Chronic 3	
Gene	**Log2FC**	**P**	**FC**		**Log2FC**	**P**		**Log2FC**	**P**		**Log2FC**	**p**
Sorcs3	1.68943	1.20E-268	3.225292		0.741994	3.10E-93		0.682103	4.78E-96		3.384006	0
Nrxn3	1.638966	4.41E-263	3.114426		1.968747	1.42E-175		0.646606	4.59E-39		2.284672	9.20E-233
Zfp804a	1.616154	5.93E-243	3.065568		0.935074	7.58E-92		0.647644	1.42E-51		3.059155	2.22E-268
Nrg1	1.458157	4.89E-232	2.747572		1.365337	7.87E-107		1.0258	1.23E-67		1.931151	3.78E-200
Bdnf	1.448313	1.97E-280	2.728888		1.66267	1.08E-236		0.25246	3.52E-22		2.374775	7.37E-299
Unc5d	1.395692	1.73E-273	2.631148		1.6337	2.16E-170		1.170342	6.29E-115		1.410124	5.25E-171
Mapk4	1.383354	1.91E-292	2.608742		1.123353	6.60E-138		0.718755	5.67E-89		2.205499	6.60E-266
Egfem1	-1.34868	5.17E-279	0.39265		-1.5771	5.06E-157		-0.73206	2.12E-81		-1.73086	4.13E-202
Pcdh7	1.309712	6.60E-271	2.47892		1.147384	1.34E-120		1.117163	5.56E-125		1.618412	3.82E-199
Sorcs1	1.249666	4.80E-296	2.377863		0.914907	2.25E-149		0.889141	2.98E-159		1.852648	0
Homer1	1.219006	1.80E-175	2.327863		1.845997	1.17E-215		-0.1709	7.38E-08		1.989579	4.68E-271
Ntrk2	1.212323	8.99E-142	2.317104		0.682238	4.42E-90		-0.04452	0.451545		2.798219	2.01E-265
Spock3	1.196732	2.52E-243	2.292198		0.851621	1.88E-90		0.620894	1.39E-55		2.006192	1.29E-260
Sema3e	1.087903	4.26E-285	2.125649		0.819948	9.81E-125		0.703726	1.13E-124		1.658507	1.53E-284
Pam	1.08585	1.02E-138	2.122626		0.514533	3.34E-45		0.116979	0.002541		2.440227	9.80E-267
Dscaml1	-1.02485	4.02E-230	0.49146		-1.17748	3.87E-139		-0.42111	3.83E-37		-1.4566	2.10E-210

Appendix B4. Top 16 genes in granule cell comparison, WT vs WT 1

	WT 1			**WT 2**			**WT 3**	
Gene	**Log2FC**	**P**		**Log2FC**	**P**		**Log2FC**	**P**
Sorcs3	0	1		-0.076411224	0.6522024		0.013468607	0.5307372
Nrxn3	0	1		0.03859549	1		0.148448626	0.4497202

Zfp804a	0	1		-0.102705273	0.3907116		-0.157237343	0.037444
Nrg1	0	1		0.051015519	0.9474448		0.085775402	0.6150891
Bdnf	0	1		-0.01679656	1		-0.027894166	0.9643636
Unc5d	0	1		0.025984054	1		0.098098034	0.1057279
Mapk4	0	1		0.069819502	0.6043319		0.154061778	0.0008706
Egfem1	0	1		-0.150027777	0.0006456		-0.167549368	0.000299
Pcdh7	0	1		0.055482481	0.5918369		0.146769287	0.0105568
Sorcs1	0	1		-0.042163798	0.6621995		-0.015695728	1
Homer1	0	1		0.039301971	0.6482791		0.016215797	0.6150891
Ntrk2	0	1		-0.102727893	0.3412163		-0.127229631	0.0293522
Spock3	0	1		-0.063839184	0.5716364		-0.056873404	0.4996888
Sema3e	0	1		-0.036684738	0.7387629		0.014573823	0.6875263
Pam	0	1		-0.201741745	9.66E-05		-0.217092402	4.42E-06
Dscaml1	0	1		-0.005758751	0.7538342		-0.146417001	0.0012763

Appendix B5. CA1 comparison, chronic seizures vs. WT

Gene	-log10(*p*)	Log2FC	Fold change
Mir670hg	136	0.87	1.82
Gpc5	46	0.71	1.64
Pigk	157	-0.65	0.64
Sorcs1	72	0.65	1.56
Ube3a	195	-0.64	0.64
Ppm1h	113	0.63	1.55
Zfp804a	44	0.59	1.50
Etl4	68	0.59	1.50
Gm13269	113	-0.54	0.69
Brinp1	54	0.53	1.44
Ntrk2	57	0.53	1.44
Maml3	74	0.51	1.42
Bdnf	95	0.51	1.42
Pam	60	0.50	1.42

4930419G24Rik	84	-0.50	0.71
5330438D12Rik	135	-0.50	0.71

Appendix B6. CA2 comparison, chronic seizures vs. WT

Gene	-log10(*p*)	Log2FC	Fold change
Mir670hg	2	0.55	1.47
Gm32250	5	-0.52	0.70
Gm11418	3	-0.53	0.69
Acp1	3	-0.54	0.69
P2ry14	3	-0.55	0.68
Atp6v0b	4	-0.56	0.68
Lysmd4	6	-0.56	0.68
Slc24a5	3	-0.57	0.68
Gm20275	5	-0.59	0.67
Pigk	5	-0.66	0.63
4921534H16Rik	4	-0.68	0.62
5330438D12Rik	5	-0.75	0.60
Gm20642	3	-0.75	0.59
Nrg3os	4	-0.78	0.58
Ube3a	7	-0.81	0.57
4930509J09Rik	6	-0.82	0.57
Gm12296	6	-0.86	0.55
Gm13269	7	-0.87	0.55

Appendix B7. CA3 comparison, chronic seizures vs. WT

Gene	-log10(*p*)	Log2FC	Fold change
Zfp804a	16	0.81	1.75
Gm48091	40	-0.54	0.69
Nrg3os	24	-0.55	0.68
Gm13269	40	-0.57	0.67

Gm32250	57	-0.58	0.67
Pigk	43	-0.58	0.67
Gm36975	36	-0.59	0.66
Gm20642	29	-0.61	0.65
4921534H16Rik	42	-0.63	0.65
Gm12296	44	-0.63	0.64
4930509J09Rik	43	-0.65	0.64
5330438D12Rik	56	-0.72	0.61
Ube3a	67	-0.76	0.59

Appendix B8. Inhibitory neuron comparison, chronic seizures vs. WT

Gene	-log10(*p*)	Log2FC	Fold change
Mir670hg	15	0.70	1.63
AY036118	44	-0.52	0.70
Nrg3os	26	-0.53	0.69
Ube3a	67	-0.67	0.63

Appendix B9. Oligodendrocyte comparison, chronic seizures vs. WT

Gene	-log10(*p*)	Log2FC	Fold change
Neat1	87	1.27	2.41
Nrxn3	61	0.88	1.85
Nrg3	58	0.85	1.80
Dgki	44	0.82	1.76
Il33	48	0.81	1.75
Csmd1	53	0.78	1.72
Epha6	47	0.74	1.67
Zfp804a	46	0.71	1.63
Nav3	38	0.70	1.62
Kcnip4	48	0.69	1.62
Apod	17	0.68	1.61

Spock3	27	0.65	1.57
Nrxn1	36	0.65	1.57
March1	22	0.61	1.53
Brinp1	35	0.61	1.52
Adgrl3	25	0.56	1.48
Syt1	29	0.56	1.47
Rbfox1	28	0.56	1.47
Stxbp5l	34	0.55	1.47
Fam155a	28	0.54	1.45
Celf2	28	0.54	1.45
Kcnd2	26	0.53	1.45
Pam	25	0.52	1.43
Abca8a	29	0.52	1.43
Epha7	33	0.52	1.43
Cnksr2	26	0.51	1.42
Adgrb3	21	0.50	1.41
Gm28376	20	-0.50	0.71
Aspa	23	-0.50	0.71
Atp6v0b	28	-0.51	0.70
Ptn	20	-0.51	0.70
Gm11659	34	-0.52	0.70
Gm42413	28	-0.56	0.68
Plp1	58	-0.56	0.68
AY036118	33	-0.57	0.68
Gm11149	39	-0.60	0.66
Cmss1	53	-0.76	0.59
Pacrg	66	-1.00	0.50

Appendix B10. Immune cell comparison, chronic seizures vs. WT

Gene	-log10(*p*)	Log2FC	Fold change
Zfp804a	20	0.82	1.77

Nrxn3	14	0.81	1.75
Lrmda	13	0.80	1.74
Arhgap24	14	0.75	1.68
Lrp1b	11	0.72	1.65
Nrg3	12	0.72	1.65
Csmd1	9	0.69	1.61
Stxbp5l	13	0.68	1.60
Brinp1	12	0.67	1.59
Hivep2	10	0.65	1.56
Magi2	8	0.63	1.55
Cadm2	7	0.63	1.54
Nlgn1	8	0.63	1.54
Fgf14	8	0.62	1.54
Pvt1	10	0.62	1.53
Adgrl3	9	0.61	1.53
Dlg2	8	0.60	1.52
Epha6	7	0.60	1.51
Cux1	7	0.58	1.49
Abr	7	0.57	1.49
Pcdh9	7	0.56	1.47
Ptprd	5	0.56	1.47
Kcnj3	12	0.55	1.47
Atrnl1	12	0.55	1.46
Epha7	9	0.54	1.45
Grm7	6	0.54	1.45
Ppfia2	9	0.53	1.45
Tenm2	6	0.53	1.44
Homer1	8	0.52	1.44
Kcnip4	6	0.52	1.44
Grik2	7	0.52	1.43
Enox1	13	0.50	1.42

Map4	5	0.50	1.42
Dclk1	9	0.50	1.42
Syt1	5	0.50	1.41
Maf	7	-0.60	0.66
Gm35188	12	-0.76	0.59
Cmss1	18	-0.78	0.58
Lysmd4	16	-0.79	0.58
AY036118	19	-0.83	0.56

Appendix B11. Astrocyte comparison, chronic seizures vs. WT

Gene	-log10(*p*)	Log2FC	Fold change
Gfap	6	0.66	1.58
Mt1	6	0.64	1.56
Mt2	8	0.62	1.54
Clu	6	0.62	1.53
Atp1b2	9	0.58	1.50
Ndrg2	7	0.57	1.48
C4b	13	0.56	1.48
Slc20a1	11	0.56	1.47
F3	6	0.53	1.45
Slc39a14	9	0.53	1.44
Gpam	6	0.51	1.43
Sik3	6	0.50	1.42
Gm48742	5	-0.51	0.70
Gm42418	7	-0.52	0.70
Ctnna2	6	-0.56	0.68
AY036118	16	-0.76	0.59
Gm20713	12	-0.77	0.59
Cmss1	16	-0.89	0.54
Wdr17	36	-1.43	0.37

Appendix B12. Endothelial cell comparison, chronic seizures vs. WT

Gene	-log10(*p*)	Log2FC	Fold change
Gm47283	2	0.65	1.57
Gm42418	3	-0.87	0.55
Cdk8	9	-1.00	0.50
AY036118	8	-1.21	0.43
Cmss1	10	-1.25	0.42

Appendix B13. Oligodendrocyte precursor cell comparison, chronic seizures vs. WT

Gene	-log10(*p*)	Log2FC	Fold change
Slc24a2	1	0.80	1.74
Lrmda	2	0.73	1.66
Inpp5d	3	0.72	1.65
Elmo1	2	0.72	1.64
Neat1	3	0.69	1.62
Epb41l2	2	0.64	1.55
Srgap2	2	0.62	1.54
Mef2c	3	0.61	1.53
Maml3	2	0.61	1.52
Rsrp1	3	0.60	1.51
Hexb	3	0.58	1.50
Slc8a1	2	0.57	1.48
Zfhx3	1	0.57	1.48
Serinc3	4	0.56	1.48
Csf3r	4	0.53	1.45
Dip2b	2	0.53	1.45
Foxp1	2	0.53	1.45
Ssh2	2	0.53	1.44
Lgmn	3	0.51	1.43

Pakap	2	0.51	1.42
Apbb1ip	3	0.50	1.42
Agmo	3	0.50	1.42
Cerk	4	0.50	1.41
AY036118	4	-0.71	0.61
Cmss1	6	-0.89	0.54

REFERENCES

Aiba, I, and Noebels, JL (2021). Kcnq2/Kv7.2 controls the threshold and bi-hemispheric symmetry of cortical spreading depolarization. Brain *144*, 2863-2878.

Akin, EJ, Sole, L, Dib-Hajj, SD, Waxman, SG, and Tamkun, MM (2015). Preferential targeting of Nav1.6 voltage-gated Na+ Channels to the axon initial segment during development. PLoS One *10*, e0124397.

Akin, EJ, Sole, L, Johnson, B, Beheiry, ME, Masson, JB, Krapf, D*, et al.* (2016). Single-Molecule Imaging of Nav1.6 on the Surface of Hippocampal Neurons Reveals Somatic Nanoclusters. Biophys J *111*, 1235-1247.

Alfadhel, M, Albahkali, S, Almuaysib, A, and Alrfaei, BM (2018). The SORCS3 gene is mutated in brothers with infantile spasms and intellectual disability. Discov Med *26*, 147-153.

Anderson, LL, Hawkins, NA, Thompson, CH, Kearney, JA, and George, AL, Jr. (2017). Unexpected Efficacy of a Novel Sodium Channel Modulator in Dravet Syndrome. Sci Rep *7*, 1682.

Anderson, LL, Thompson, CH, Hawkins, NA, Nath, RD, Petersohn, AA, Rajamani, S*, et al.* (2014). Antiepileptic activity of preferential inhibitors of persistent sodium current. Epilepsia *55*, 1274-1283.

Ashburner, M, Ball, CA, Blake, JA, Botstein, D, Butler, H, Cherry, JM*, et al.* (2000). Gene ontology: tool for the unification of biology. The Gene Ontology Consortium. Nat Genet *25*, 25-29.

Baker, EM, Thompson, CH, Hawkins, NA, Wagnon, JL, Wengert, ER, Patel, MK*, et al.* (2018). The novel sodium channel modulator GS-458967 (GS967) is an effective treatment in a mouse model of SCN8A encephalopathy. Epilepsia *59*, 1166-1176.

Barcia, G, Fleming, MR, Deligniere, A, Gazula, VR, Brown, MR, Langouet, M*, et al.* (2012). De novo gain-of-function KCNT1 channel mutations cause malignant migrating partial seizures of infancy. Nat Genet *44*, 1255-1259.

Barker, BS, Nigam, A, Ottolini, M, Gaykema, RP, Hargus, NJ, and Patel, MK (2017). Pro-excitatory alterations in sodium channel activity facilitate subiculum neuron hyperexcitability in temporal lobe epilepsy. Neurobiol Dis *108*, 183-194.

Barry, G, Briggs, JA, Hwang, DW, Nayler, SP, Fortuna, PR, Jonkhout, N*, et al.* (2017). The long non-coding RNA NEAT1 is responsive to neuronal activity and is associated with hyperexcitability states. Sci Rep *7*, 40127.

Baudin, P, Cousyn, L, and Navarro, V (2021). The LGI1 protein: molecular structure, physiological functions and disruption-related seizures. Cell Mol Life Sci *79*, 16.

Bausch, AE, Dieter, R, Nann, Y, Hausmann, M, Meyerdierks, N, Kaczmarek, LK*, et al.* (2015). The sodium-activated potassium channel Slack is required for optimal cognitive flexibility in mice. Learn Mem *22*, 323-335.

Bean, BP (2007). The action potential in mammalian central neurons. Nat Rev Neurosci *8*, 451-465.

Beatch, G, Namdari, R, Cadieux, J, Kato, H, and Aycardi, E (2020). A Phase 1 Study to Assess the Safety, Tolerability and Pharmacokinetics of Two Formulations of a Novel Nav1.6 Sodium Channnel Blocker (XEN901) in Healthy Adult Subjects. (4757). neurology *15*.

Becker, LA, Huang, B, Bieri, G, Ma, R, Knowles, DA, Jafar-Nejad, P*, et al.* (2017). Therapeutic reduction of ataxin-2 extends lifespan and reduces pathology in TDP-43 mice. Nature *544*, 367-371.

Ben-Shalom, R, Keeshen, CM, Berrios, KN, An, JY, Sanders, SJ, and Bender, KJ (2017). Opposing Effects on NaV1.2 Function Underlie Differences Between SCN2A Variants Observed in Individuals With Autism Spectrum Disorder or Infantile Seizures. Biol Psychiatry *82*, 224-232.

Bennett, CF (2019). Therapeutic Antisense Oligonucleotides Are Coming of Age. Annu Rev Med *70*, 307-321.

Bennett, CF, Krainer, AR, and Cleveland, DW (2019). Antisense Oligonucleotide Therapies for Neurodegenerative Diseases. Annu Rev Neurosci *42*, 385-406.

Berg, AT, Berkovic, SF, Brodie, MJ, Buchhalter, J, Cross, JH, van Emde Boas, W*, et al.* (2010). Revised terminology and concepts for organization of seizures and epilepsies: report of the ILAE Commission on Classification and Terminology, 2005-2009. Epilepsia *51*, 676-685.

Boerma, RS, Braun, KP, van den Broek, MP, van Berkestijn, FM, Swinkels, ME, Hagebeuk, EO*, et al.* (2016). Remarkable Phenytoin Sensitivity in 4 Children with SCN8A-related Epilepsy: A Molecular Neuropharmacological Approach. Neurotherapeutics *13*, 192-197.

Boiko, T, Rasband, MN, Levinson, SR, Caldwell, JH, Mandel, G, Trimmer, JS*, et al.* (2001). Compact myelin dictates the differential targeting of two sodium channel isoforms in the same axon. Neuron *30*, 91-104.

Boiko, T, Van Wart, A, Caldwell, JH, Levinson, SR, Trimmer, JS, and Matthews, G (2003). Functional specialization of the axon initial segment by isoform-specific sodium channel targeting. J Neurosci *23*, 2306-2313.

Bonduelle, T, Hartlieb, T, Baldassari, S, Sim, NS, Kim, SH, Kang, HC*, et al.* (2021). Frequent SLC35A2 brain mosaicism in mild malformation of cortical development with oligodendroglial hyperplasia in epilepsy (MOGHE). Acta Neuropathol Commun *9*, 3.

Bouza, AA, and Isom, LL (2018). Voltage-Gated Sodium Channel beta Subunits and Their Related Diseases. Handb Exp Pharmacol *246*, 423-450.

Brunklaus, A, Brunger, T, Feng, T, Fons, C, Lehikoinen, A, Panagiotakaki, E*, et al.* (2022). The gain of function SCN1A disorder spectrum: novel epilepsy phenotypes and therapeutic implications. Brain *145*, 3816-3831.

Bunton-Stasyshyn, RKA, Wagnon, JL, Wengert, ER, Barker, BS, Faulkner, A, Wagley, PK*, et al.* (2019). Prominent role of forebrain excitatory neurons in SCN8A encephalopathy. Brain *142*, 362-375.

Burbano, LE, Li, M, Jancovski, N, Jafar-Nejad, P, Richards, K, Sedo, A*, et al.* (2022). Antisense oligonucleotide therapy for KCNT1 encephalopathy. JCI Insight *7*.

Burgess, DL, Kohrman, DC, Galt, J, Plummer, NW, Jones, JM, Spear, B*, et al.* (1995). Mutation of a new sodium channel gene, Scn8a, in the mouse mutant 'motor endplate disease'. Nat Genet *10*, 461-465.

Calhoun, JD, Hawkins, NA, Zachwieja, NJ, and Kearney, JA (2017). Cacna1g is a genetic modifier of epilepsy in a mouse model of Dravet syndrome. Epilepsia *58*, e111-e115.

Calhoun, JD, and Isom, LL (2014). The role of non-pore-forming beta subunits in physiology and pathophysiology of voltage-gated sodium channels. Handb Exp Pharmacol *221*, 51-89.

Carteron, C, Ferrer-Montiel, A, and Cabedo, H (2006). Characterization of a neural-specific splicing form of the human neuregulin 3 gene involved in oligodendrocyte survival. J Cell Sci *119*, 898-909.

Cembrowski, MS, Wang, L, Sugino, K, Shields, BC, and Spruston, N (2016). Hipposeq: a comprehensive RNA-seq database of gene expression in hippocampal principal neurons. Elife *5*, e14997.

Chabrol, E, Navarro, V, Provenzano, G, Cohen, I, Dinocourt, C, Rivaud-Pechoux, S*, et al.* (2010). Electroclinical characterization of epileptic seizures in leucine-rich, glioma-inactivated 1-deficient mice. Brain *133*, 2749-2762.

Cheah, CS, Yu, FH, Westenbroek, RE, Kalume, FK, Oakley, JC, Potter, GB*, et al.* (2012). Specific deletion of NaV1.1 sodium channels in inhibitory interneurons causes

seizures and premature death in a mouse model of Dravet syndrome. Proc Natl Acad Sci U S A *109*, 14646-14651.

Chen, L, Huang, J, Zhao, P, Persson, AK, Dib-Hajj, FB, Cheng, X*, et al.* (2018). Conditional knockout of NaV1.6 in adult mice ameliorates neuropathic pain. Sci Rep *8*, 3845.

Chen, P, Chen, F, Wu, Y, and Zhou, B (2021a). New Insights Into the Role of Aberrant Hippocampal Neurogenesis in Epilepsy. Front Neurol *12*, 727065.

Chen, QL, Xia, L, Zhong, SP, Wang, Q, Ding, J, and Wang, X (2020). Bioinformatic analysis identifies key transcriptome signatures in temporal lobe epilepsy. CNS Neurosci Ther *26*, 1266-1277.

Chen, W, Jin, B, Aung, T, He, C, Chen, C, Wang, S*, et al.* (2021b). Response to antiseizure medications in epileptic patients with malformation of cortical development. Ther Adv Neurol Disord *14*, 17562864211050027.

Cid, E, Marquez-Galera, A, Valero, M, Gal, B, Medeiros, DC, Navarron, CM*, et al.* (2021). Sublayer- and cell-type-specific neurodegenerative transcriptional trajectories in hippocampal sclerosis. Cell Rep *35*, 109229.

Clatot, J, Hoshi, M, Wan, X, Liu, H, Jain, A, Shinlapawittayatorn, K*, et al.* (2017). Voltage-gated sodium channels assemble and gate as dimers. Nat Commun *8*, 2077.

Clatot, J, Parthasarathy, S, Cohen, S, McKee, JL, Massey, S, Somarowthu, A*, et al.* (2023). SCN1A gain-of-function mutation causing an early onset epileptic encephalopathy. Epilepsia *64*, 1318-1330.

Clatot, J, Zheng, Y, Girardeau, A, Liu, H, Laurita, KR, Marionneau, C*, et al.* (2018). Mutant voltage-gated Na(+) channels can exert a dominant negative effect through coupled gating. Am J Physiol Heart Circ Physiol *315*, H1250-H1257.

Colasante, G, Lignani, G, Brusco, S, Di Berardino, C, Carpenter, J, Giannelli, S*, et al.* (2020a). dCas9-Based Scn1a Gene Activation Restores Inhibitory Interneuron Excitability and Attenuates Seizures in Dravet Syndrome Mice. Mol Ther *28*, 235-253.

Colasante, G, Qiu, Y, Massimino, L, Di Berardino, C, Cornford, JH, Snowball, A*, et al.* (2020b). In vivo CRISPRa decreases seizures and rescues cognitive deficits in a rodent model of epilepsy. Brain *143*, 891-905.

Cole, BA, Clapcote, SJ, Muench, SP, and Lippiat, JD (2021). Targeting K(Na)1.1 channels in KCNT1-associated epilepsy. Trends Pharmacol Sci *42*, 700-713.

Cole, BA, Johnson, RM, Dejakaisaya, H, Pilati, N, Fishwick, CWG, Muench, SP*, et al.* (2020). Structure-Based Identification and Characterization of Inhibitors of the Epilepsy-Associated K(Na)1.1 (KCNT1) Potassium Channel. iScience *23*, 101100.

D'Adamo, MC, Liantonio, A, Rolland, JF, Pessia, M, and Imbrici, P (2020). Kv1.1 Channelopathies: Pathophysiological Mechanisms and Therapeutic Approaches. Int J Mol Sci *21*.

Dhifallah, S, Lancaster, E, Merrill, S, Leroudier, N, Mantegazza, M, and Cestele, S (2018). Gain of Function for the SCN1A/hNa(v)1.1-L1670W Mutation Responsible for Familial Hemiplegic Migraine. Front Mol Neurosci *11*, 232.

Dingledine, R, Coulter, DA, Fritsch, B, Gorter, JA, Lelutiu, N, McNamara, J*, et al.* (2017). Transcriptional profile of hippocampal dentate granule cells in four rat epilepsy models. Sci Data *4*, 170061.

Du, J, Simmons, S, Brunklaus, A, Adiconis, X, Hession, CC, Fu, Z*, et al.* (2020a). Differential excitatory vs inhibitory SCN expression at single cell level regulates brain sodium channel function in neurodevelopmental disorders. European Journal of Paediatric Neurology.

Du, J, Vegh, V, and Reutens, DC (2020b). Persistent sodium current blockers can suppress seizures caused by loss of low-threshold D-type potassium currents: Predictions from an in silico study of K(v)1 channel disorders. Epilepsia Open *5*, 86-96.

Duchen, LW (1970). Hereditary motor end-plate disease in the mouse: light and electron microscopic studies. J Neurol Neurosurg Psychiatry *33*, 238-250.

Epi25k (2019). Ultra-Rare Genetic Variation in the Epilepsies: A Whole-Exome Sequencing Study of 17,606 Individuals. Am J Hum Genet *105*, 267-282.

Epilepsy Genetics, I (2018). De novo variants in the alternative exon 5 of SCN8A cause epileptic encephalopathy. Genet Med *20*, 275-281.

Escayg, A, MacDonald, BT, Meisler, MH, Baulac, S, Huberfeld, G, An-Gourfinkel, I*, et al.* (2000). Mutations of SCN1A, encoding a neuronal sodium channel, in two families with GEFS+2. Nat Genet *24*, 343-345.

Ethemoglu, O, Calik, M, Koyuncu, I, Ethemoglu, KB, Gocmen, A, Guzelcicek, A*, et al.* (2021). Interleukin-33 and oxidative stress in epilepsy patients. Epilepsy Res *176*, 106738.

Fadila, S, Beucher, B, Dopeso-Reyes, IG, Mavashov, A, Brusel, M, Anderson, K*, et al.* (2023). Viral vector-mediated expression of NaV1.1, after seizure onset, reduces epilepsy in mice with Dravet syndrome. J Clin Invest.

Faheem, M, Naseer, MI, Chaudhary, AG, Kumosani, TA, Rasool, M, Algahtani, HA*, et al.* (2015). Array-comparative genomic hybridization analysis of a cohort of Saudi patients with epilepsy. CNS Neurol Disord Drug Targets *14*, 468-475.

Fan, C, Wolking, S, Lehmann-Horn, F, Hedrich, UB, Freilinger, T, Lerche, H*, et al.* (2016). Early-onset familial hemiplegic migraine due to a novel SCN1A mutation. Cephalalgia *36*, 1238-1247.

Fan, X, Huang, J, Jin, X, and Yan, N (2023). Cryo-EM structure of human voltage-gated sodium channel Na(v)1.6. Proc Natl Acad Sci U S A *120*, e2220578120.

Favero, M, Sotuyo, NP, Lopez, E, Kearney, JA, and Goldberg, EM (2018). A Transient Developmental Window of Fast-Spiking Interneuron Dysfunction in a Mouse Model of Dravet Syndrome. J Neurosci *38*, 7912-7927.

Fenoglio-Simeone, KA, Wilke, JC, Milligan, HL, Allen, CN, Rho, JM, and Maganti, RK (2009). Ketogenic diet treatment abolishes seizure periodicity and improves diurnal rhythmicity in epileptic Kcna1-null mice. Epilepsia *50*, 2027-2034.

Feyissa, AM, Lamb, C, Pittock, SJ, Gadoth, A, McKeon, A, Klein, CJ*, et al.* (2018). Antiepileptic drug therapy in autoimmune epilepsy associated with antibodies targeting the leucine-rich glioma-inactivated protein 1. Epilepsia Open *3*, 348-356.

Finkel, RS, Mercuri, E, Darras, BT, Connolly, AM, Kuntz, NL, Kirschner, J*, et al.* (2017). Nusinersen versus Sham Control in Infantile-Onset Spinal Muscular Atrophy. N Engl J Med *377*, 1723-1732.

Fitzgerald, MP, Fiannacca, M, Smith, DM, Gertler, TS, Gunning, B, Syrbe, S*, et al.* (2019). Treatment Responsiveness in KCNT1-Related Epilepsy. Neurotherapeutics.

Freigang, M, Steinacker, P, Wurster, CD, Schreiber-Katz, O, Osmanovic, A, Petri, S*, et al.* (2021). Increased chitotriosidase 1 concentration following nusinersen treatment in spinal muscular atrophy. Orphanet J Rare Dis *16*, 330.

French, JA, Perucca, E, Sander, JW, Bergfeldt, L, Baulac, M, Auerbach, DS*, et al.* (2021). FDA safety warning on the cardiac effects of lamotrigine: An advisory from the Ad Hoc ILAE/AES Task Force. Epilepsia Open *6*, 45-48.

Gardella, E, Becker, F, Moller, RS, Schubert, J, Lemke, JR, Larsen, LH*, et al.* (2016). Benign infantile seizures and paroxysmal dyskinesia caused by an SCN8A mutation. Ann Neurol *79*, 428-436.

Gardella, E, Marini, C, Trivisano, M, Fitzgerald, MP, Alber, M, Howell, KB*, et al.* (2018). The phenotype of SCN8A developmental and epileptic encephalopathy. Neurology *91*, e1112-e1124.

Gasser, A, Ho, TS, Cheng, X, Chang, KJ, Waxman, SG, Rasband, MN*, et al.* (2012). An ankyrinG-binding motif is necessary and sufficient for targeting Nav1.6 sodium channels to axon initial segments and nodes of Ranvier. J Neurosci *32*, 7232-7243.

Gehman, LT, Meera, P, Stoilov, P, Shiue, L, O'Brien, JE, Meisler, MH*, et al.* (2012). The splicing regulator Rbfox2 is required for both cerebellar development and mature motor function. Genes Dev *26*, 445-460.

Gehman, LT, Stoilov, P, Maguire, J, Damianov, A, Lin, CH, Shiue, L*, et al.* (2011). The splicing regulator Rbfox1 (A2BP1) controls neuronal excitation in the mammalian brain. Nat Genet *43*, 706-711.

Gene Ontology, C (2021). The Gene Ontology resource: enriching a GOld mine. Nucleic Acids Res *49*, D325-D334.

Gertler, TS, Cherian, S, DeKeyser, JM, Kearney, JA, and George, AL, Jr. (2022). K(Na)1.1 gain-of-function preferentially dampens excitability of murine parvalbumin-positive interneurons. Neurobiol Dis *168*, 105713.

Glasscock, E, Qian, J, Yoo, JW, and Noebels, JL (2007). Masking epilepsy by combining two epilepsy genes. Nat Neurosci *10*, 1554-1558.

Gohma, H, Kuramoto, T, Matalon, R, Surendran, S, Tyring, S, Kitada, K*, et al.* (2007). Absence-like and tonic seizures in aspartoacylase/attractin double-mutant mice. Exp Anim *56*, 161-165.

Gould, E, and Kim, JH (2021). SCN2A contributes to oligodendroglia excitability and development in the mammalian brain. Cell Rep *36*, 109653.

Green, MC, Beechey, CV, Davisson, MT, Evans, EP, Lane, PW, Lyon, MF*, et al.* (1981). Genetic Variants and Strian of the Laboratory Mouse (Gustav Fischer Verlag).

Gribkoff, VK, and Winquist, RJ (2023). Potassium channelopathies associated with epilepsy-related syndromes and directions for therapeutic intervention. Biochem Pharmacol *208*, 115413.

Griffin, A, Kahlig, KM, Hatch, RJ, Hughes, ZA, Chapman, ML, Antonio, B*, et al.* (2021). Discovery of the First Orally Available, Selective KNa1.1 Inhibitor: In Vitro and In Vivo Activity of an Oxadiazole Series. ACS Med Chem Lett *12*.

Guyenet, SJ, Furrer, SA, Damian, VM, Baughan, TD, La Spada, AR, and Garden, GA (2010). A simple composite phenotype scoring system for evaluating mouse models of cerebellar ataxia. J Vis Exp.

Han, Z, Chen, C, Christiansen, A, Ji, S, Lin, Q, Anumonwo, C*, et al.* (2020). Antisense oligonucleotides increase Scn1a expression and reduce seizures and SUDEP incidence in a mouse model of Dravet syndrome. Sci Transl Med *12*.

Hao, Y, Hao, S, Andersen-Nissen, E, Mauck, WM, 3rd, Zheng, S, Butler, A*, et al.* (2021). Integrated analysis of multimodal single-cell data. Cell *184*, 3573-3587 e3529.

Hawkins, NA, Calhoun, JD, Huffman, AM, and Kearney, JA (2019). Gene expression profiling in a mouse model of Dravet syndrome. Exp Neurol *311*, 247-256.

Hawkins, NA, Martin, MS, Frankel, WN, Kearney, JA, and Escayg, A (2011). Neuronal voltage-gated ion channels are genetic modifiers of generalized epilepsy with febrile seizures plus. Neurobiol Dis *41*, 655-660.

Hawkins, NA, Zachwieja, NJ, Miller, AR, Anderson, LL, and Kearney, JA (2016). Fine Mapping of a Dravet Syndrome Modifier Locus on Mouse Chromosome 5 and Candidate Gene Analysis by RNA-Seq. PLoS Genet *12*, e1006398.

Hayden, EC (2022a). Gene Treatment for Rare Epilepsy Causes Brain Side Effect in 2 Children. In New York Times.

Hayden, EC (2022b). They Created a Drug for Susannah. What About Millions of Other Patients? In New York Times.

Heighway, J, Sedo, A, Garg, A, Eldershaw, L, Perreau, V, Berecki, G*, et al.* (2022). Sodium channel expression and transcript variation in the developing brain of human, Rhesus monkey, and mouse. Neurobiol Dis *164*, 105622.

Hermey, G, Plath, N, Hubner, CA, Kuhl, D, Schaller, HC, and Hermans-Borgmeyer, I (2004). The three sorCS genes are differentially expressed and regulated by synaptic activity. J Neurochem *88*, 1470-1476.

Heron, SE, Crossland, KM, Andermann, E, Phillips, HA, Hall, AJ, Bleasel, A*, et al.* (2002). Sodium-channel defects in benign familial neonatal-infantile seizures. Lancet *360*, 851-852.

Herzog, RW (2010). Gene therapy for SCID-X1: round 2. Mol Ther *18*, 1891.

Higa, LA, Wardley, J, Wardley, C, Singh, S, Foster, T, and Shen, JJ (2021). CNKSR2-related neurodevelopmental and epilepsy disorder: a cohort of 13 new families and literature review indicating a predominance of loss of function pathogenic variants. BMC Med Genomics *14*, 186.

Hill, SF, Ziobro, JM, Jafar-Nejad, P, Rigo, F, and Meisler, MH (2022). Genetic interaction between Scn8a and potassium channel genes Kcna1 and Kcnq2. Epilepsia *63*, e125-e131.

Hu, W, Tian, C, Li, T, Yang, M, Hou, H, and Shu, Y (2009). Distinct contributions of Nav1.6 and Nav1.2 in action potential initiation and backpropagation. Nature Neuroscience *12*, 996 - 1005.

Huang, CY, and Rasband, MN (2018). Axon initial segments: structure, function, and disease. Ann N Y Acad Sci *1420*, 46-61.

Hughes, AN, and Appel, B (2019). Oligodendrocytes express synaptic proteins that modulate myelin sheath formation. Nat Commun *10*, 4125.

Isom, LL (2019). Is Targeting of Compensatory Ion Channel Gene Expression a Viable Therapeutic Strategy for Dravet Syndrome? Epilepsy Currents *19*.

Itai, T, Hamanaka, K, Sasaki, K, Wagner, M, Kotzaeridou, U, Brosse, I*, et al.* (2021). De novo variants in CELF2 that disrupt the nuclear localization signal cause developmental and epileptic encephalopathy. Hum Mutat *42*, 66-76.

Iughetti, L, Lucaccioni, L, Fugetto, F, Predieri, B, Berardi, A, and Ferrari, F (2018). Brain-derived neurotrophic factor and epilepsy: a systematic review. Neuropeptides *72*, 23-29.

Jenkins, SM, and Bennett, V (2001). Ankyrin-G coordinates assembly of the spectrin-based membrane skeleton, voltage-gated sodium channels, and L1 CAMs at Purkinje neuron initial segments. J Cell Biol *155*, 739-746.

Jessberger, S, and Parent, JM (2015). Epilepsy and Adult Neurogenesis. Cold Spring Harb Perspect Biol *7*.

Jiang, P, Chen, C, Liu, XB, Selvaraj, V, Liu, W, Feldman, DH*, et al.* (2013). Generation and characterization of spiking and nonspiking oligodendroglial progenitor cells from embryonic stem cells. Stem Cells *31*, 2620-2631.

Johannesen, KM, Gardella, E, Scheffer, I, Howell, K, Smith, DM, Helbig, I*, et al.* (2018). Early mortality in SCN8A-related epilepsies. Epilepsy Res *143*, 79-81.

Johannesen, KM, Liu, Y, Koko, M, Gjerulfsen, CE, Sonnenberg, L, Schubert, J*, et al.* (2022). Genotype-phenotype correlations in SCN8A-related disorders reveal prognostic and therapeutic implications. Brain *145*, 2991-3009.

Johnson, JP, Focken, T, Khakh, K, Tari, PK, Dube, C, Goodchild, SJ*, et al.* (2022). NBI-921352, a first-in-class, Na(V)1.6 selective, sodium channel inhibitor that prevents seizures in Scn8a gain-of-function mice, and wild-type mice and rats. Elife *11*.

Jorge, BS, Campbell, CM, Miller, AR, Rutter, ED, Gurnett, CA, Vanoye, CG*, et al.* (2011). Voltage-gated potassium channel KCNV2 (Kv8.2) contributes to epilepsy susceptibility. Proc Natl Acad Sci U S A *108*, 5443-5448.

Kahlig, KM, Scott, L, Hatch, RJ, Griffin, A, Martinez Botella, G, Hughes, ZA*, et al.* (2022). The novel persistent sodium current inhibitor PRAX-562 has potent anticonvulsant activity with improved protective index relative to standard of care sodium channel blockers. Epilepsia *63*, 697-708.

Kaiser, J (2022). Tailored genetic drug causes fatal brain swelling. In Science.

Kamiya, K, Kaneda, M, Sugawara, T, Mazaki, E, Okamura, N, Montal, M*, et al.* (2004). A nonsense mutation of the sodium channel gene SCN2A in a patient with intractable epilepsy and mental decline. J Neurosci *24*, 2690-2698.

Kaneko, K, Currin, CB, Goff, KM, Wengert, ER, Somarowthu, A, Vogels, TP*, et al.* (2022). Developmentally regulated impairment of parvalbumin interneuron synaptic transmission in an experimental model of Dravet syndrome. Cell Rep *38*, 110580.

Karczewski, KJ, Francioli, LC, Tiao, G, Cummings, BB, Alföldi, J, Wang, Q*, et al.* (2019). Variation across 141,456 human exomes and genomes reveals the spectrum of loss-offunction intolerance across human protein-coding genes bioRxiv.

Katsel, P, Roussos, P, Fam, P, Khan, S, Tan, W, Hirose, T*, et al.* (2019). The expression of long noncoding RNA NEAT1 is reduced in schizophrenia and modulates oligodendrocytes transcription. NPJ Schizophr *5*, 3.

Katz, E, Stoler, O, Scheller, A, Khrapunsky, Y, Goebbels, S, Kirchhoff, F*, et al.* (2018). Role of sodium channel subtype in action potential generation by neocortical pyramidal neurons. Proc Natl Acad Sci U S A *115*, E7184-E7192.

Kearney, JA, Buchner, DA, De Haan, G, Adamska, M, Levin, SI, Furay, AR*, et al.* (2002). Molecular and pathological effects of a modifier gene on deficiency of the sodium channel Scn8a (Na(v)1.6). Hum Mol Genet *11*, 2765-2775.

Kearney, JA, Yang, Y, Beyer, B, Bergren, SK, Claes, L, Dejonghe, P*, et al.* (2006). Severe epilepsy resulting from genetic interaction between Scn2a and Kcnq2. Hum Mol Genet *15*, 1043-1048.

Khalaf, G, Mattern, C, Begou, M, Boespflug-Tanguy, O, Massaad, C, and Massaad-Massade, L (2022). Mutation of Proteolipid Protein 1 Gene: From Severe Hypomyelinating Leukodystrophy to Inherited Spastic Paraplegia. Biomedicines *10*.

Khvorova, A, and Watts, JK (2017). The chemical evolution of oligonucleotide therapies of clinical utility. Nat Biotechnol *35*, 238-248.

Kim, HY, Lee, DK, Chung, BR, Kim, HV, and Kim, Y (2016). Intracerebroventricular Injection of Amyloid-beta Peptides in Normal Mice to Acutely Induce Alzheimer-like Cognitive Deficits. J Vis Exp.

Kim, J, Hu, C, Moufawad El Achkar, C, Black, LE, Douville, J, Larson, A*, et al.* (2019). Patient-Customized Oligonucleotide Therapy for a Rare Genetic Disease. N Engl J Med *381*, 1644-1652.

Kimura, K, Sugawara, T, Mazaki-Miyazaki, E, Hoshino, K, Nomura, Y, Tateno, A*, et al.* (2005). A missense mutation in SCN1A in brothers with severe myoclonic epilepsy in infancy (SMEI) inherited from a father with febrile seizures. Brain Dev *27*, 424-430.

Klugmann, M, Leichtlein, CB, Symes, CW, Serikawa, T, Young, D, and During, MJ (2005). Restoration of aspartoacylase activity in CNS neurons does not ameliorate motor deficits and demyelination in a model of Canavan disease. Mol Ther *11*, 745-753.

Knowles, JK, Helbig, I, Metcalf, CS, Lubbers, LS, Isom, LL, Demarest, S*, et al.* (2022a). Precision medicine for genetic epilepsy on the horizon: Recent advances, present challenges, and suggestions for continued progress. Epilepsia *63*, 2461-2475.

Knowles, JK, Xu, H, Soane, C, Batra, A, Saucedo, T, Frost, E*, et al.* (2022b). Maladaptive myelination promotes generalized epilepsy progression. Nat Neurosci *25*, 596-606.

Kohrman, DC, Smith, MR, Goldin, AL, Harris, J, and Meisler, MH (1996). A missense mutation in the sodium channel Scn8a is responsible for cerebellar ataxia in the mouse mutant jolting. J Neurosci *16*, 5993-5999.

Kuboyama, K, Fujikawa, A, Suzuki, R, and Noda, M (2015). Inactivation of Protein Tyrosine Phosphatase Receptor Type Z by Pleiotrophin Promotes Remyelination through Activation of Differentiation of Oligodendrocyte Precursor Cells. J Neurosci *35*, 12162-12171.

Kulkarni, JA, Witzigmann, D, Thomson, SB, Chen, S, Leavitt, BR, Cullis, PR*, et al.* (2021). The current landscape of nucleic acid therapeutics. Nat Nanotechnol *16*, 630-643.

Kumar, R, Corbett, MA, Smith, NJ, Jolly, LA, Tan, C, Keating, DJ*, et al.* (2015). Homozygous mutation of STXBP5L explains an autosomal recessive infantile-onset neurodegenerative disorder. Hum Mol Genet *24*, 2000-2010.

Kwan, P, and Brodie, MJ (2000). Early identification of refractory epilepsy. N Engl J Med *342*, 314-319.

Lal, D, Pernhorst, K, Klein, KM, Reif, P, Tozzi, R, Toliat, MR*, et al.* (2015). Extending the phenotypic spectrum of RBFOX1 deletions: Sporadic focal epilepsy. Epilepsia *56*, e129-133.

Laliberte, A, and Myers, KA (2023). Ataxia and Diplopia: A New SCN8A-Related Phenotype. Neurol Genet *9*, e200085.

Larsen, J, Carvill, GL, Gardella, E, Kluger, G, Schmiedel, G, Barisic, N*, et al.* (2015). The phenotypic spectrum of SCN8A encephalopathy. Neurology *84*, 480-489.

Lauxmann, S, Sonnenberg, L, Koch, NA, Bosselmann, C, Winter, N, Schwarz, N*, et al.* (2021). Therapeutic Potential of Sodium Channel Blockers as a Targeted Therapy Approach in KCNA1-Associated Episodic Ataxia and a Comprehensive Review of the Literature. Frontiers in Neurology *12*.

Lek, M, Karczewski, KJ, Minikel, EV, Samocha, KE, Banks, E, Fennell, T*, et al.* (2016). Analysis of protein-coding genetic variation in 60,706 humans. Nature *536*, 285-291.

Lemaillet, G, Walker, B, and Lambert, S (2003). Identification of a conserved ankyrin-binding motif in the family of sodium channel alpha subunits. J Biol Chem *278*, 27333-27339.

Lenk, GM, Jafar-Nejad, P, Hill, SF, Huffman, LD, Smolen, CE, Wagnon, JL*, et al.* (2020). Scn8a antisense oligonucleotide is protective in mouse models of SCN8A Encephalopathy and Dravet Syndrome. Ann Neurol.

Levin, SI, Khaliq, ZM, Aman, TK, Grieco, TM, Kearney, JA, Raman, IM*, et al.* (2006). Impaired motor function in mice with cell-specific knockout of sodium channel Scn8a (NaV1.6) in cerebellar purkinje neurons and granule cells. J Neurophysiol *96*, 785-793.

Levin, SI, and Meisler, MH (2004). Floxed allele for conditional inactivation of the voltage-gated sodium channel Scn8a (NaV1.6). Genesis *39*, 234-239.

Li, M, Jancovski, N, Jafar-Nejad, P, Burbano, LE, Rollo, B, Richards, K*, et al.* (2021). Antisense oligonucleotide therapy reduces seizures and extends life span in an SCN2A gain-of-function epilepsy model. J Clin Invest *131*.

Li, T, Yang, Y, Qi, H, Cui, W, Zhang, L, Fu, X*, et al.* (2023a). CRISPR/Cas9 therapeutics: progress and prospects. Signal Transduct Target Ther *8*, 36.

Li, Y, Popko, J, Krogh, KA, and Thayer, SA (2013). Epileptiform stimulus increases Homer 1a expression to modulate synapse number and activity in hippocampal cultures. J Neurophysiol *109*, 1494-1504.

Li, Y, Yuan, T, Huang, B, Zhou, F, Peng, C, Li, X*, et al.* (2023b). Structure of human Na(V)1.6 channel reveals Na(+) selectivity and pore blockade by 4,9-anhydro-tetrodotoxin. Nat Commun *14*, 1030.

Liang, L, Fazel Darbandi, S, Pochareddy, S, Gulden, FO, Gilson, MC, Sheppard, BK*, et al.* (2021). Developmental dynamics of voltage-gated sodium channel isoform expression in the human and mouse brain. Genome Med *13*, 135.

Liao, Y, Anttonen, AK, Liukkonen, E, Gaily, E, Maljevic, S, Schubert, S*, et al.* (2010). SCN2A mutation associated with neonatal epilepsy, late-onset episodic ataxia, myoclonus, and pain. Neurology *75*, 1454-1458.

Lim, KH, Han, Z, Jeon, HY, Kach, J, Jing, E, Weyn-Vanhentenryck, S*, et al.* (2020). Antisense oligonucleotide modulation of non-productive alternative splicing upregulates gene expression. Nat Commun *11*, 3501.

Lindy, AS, Stosser, MB, Butler, E, Downtain-Pickersgill, C, Shanmugham, A, Retterer, K*, et al.* (2018). Diagnostic outcomes for genetic testing of 70 genes in 8565 patients with epilepsy and neurodevelopmental disorders. Epilepsia *59*, 1062-1071.

Liu, H, Wang, HG, Pitt, GS, and Liu, ZJ (2022a). Direct Observation of Compartment-Specific Localization and Dynamics of Voltage-Gated Sodium Channels. J Neurosci *42*, 5482-5498.

Liu, R, Sun, L, Wang, Y, Wang, Q, and Wu, J (2022b). New use for an old drug: quinidine in KCNT1-related epilepsy therapy. Neurol Sci *44*, 1201-1206.

Liu, Y, Schubert, J, Sonnenberg, L, Helbig, KL, Hoei-Hansen, CE, Koko, M*, et al.* (2019). Neuronal mechanisms of mutations in SCN8A causing epilepsy or intellectual disability. Brain *142*, 376-390.

Lopez-Rojas, J, and Kreutz, MR (2016). Mature granule cells of the dentate gyrus--Passive bystanders or principal performers in hippocampal function? Neurosci Biobehav Rev *64*, 167-174.

Lopez-Santiago, LF, Yuan, Y, Wagnon, JL, Hull, JM, Frasier, CR, O'Malley, HA*, et al.* (2017). Neuronal hyperexcitability in a mouse model of SCN8A epileptic encephalopathy. Proc Natl Acad Sci U S A *114*, 2383-2388.

Lorincz, A, and Nusser, Z (2010). Molecular identity of dendritic voltage-gated sodium channels. Science *328*, 906-909.

Lossin, C, Shi, X, Rogawski, MA, and Hirose, S (2012). Compromised function in the Na(v)1.2 Dravet syndrome mutation R1312T. Neurobiol Dis *47*, 378-384.

Lu, R, Bausch, AE, Kallenborn-Gerhardt, W, Stoetzer, C, Debruin, N, Ruth, P*, et al.* (2015). Slack channels expressed in sensory neurons control neuropathic pain in mice. J Neurosci *35*, 1125-1135.

Maeder, ML, Stefanidakis, M, Wilson, CJ, Baral, R, Barrera, LA, Bounoutas, GS*, et al.* (2019). Development of a gene-editing approach to restore vision loss in Leber congenital amaurosis type 10. Nat Med *25*, 229-233.

Mahalingam, R, Oldham, MS, Puryear, C, Bansal, P, Sriram, B, Patel, D*, et al.* (2023). PRAX-562-102: A Phase 1 Trial Evaluating the Safety, Tolerability, Pharmacokinetics and Pharmacodynamics of PRAX-562 in Healthy Volunteers (P4-9.011). Neurology *17*.

Makinson, CD, Tanaka, BS, Lamar, T, Goldin, AL, and Escayg, A (2014). Role of the hippocampus in Nav1.6 (Scn8a) mediated seizure resistance. Neurobiol Dis *68*, 16-25.

Makinson, CD, Tanaka, BS, Sorokin, JM, Wong, JC, Christian, CA, Goldin, AL*, et al.* (2017). Regulation of Thalamic and Cortical Network Synchrony by Scn8a. Neuron *93*, 1165-1179 e1166.

Marrone, L, Marchi, PM, and Azzouz, M (2022). Circumventing the packaging limit of AAV-mediated gene replacement therapy for neurological disorders. Expert Opin Biol Ther *22*, 1163-1176.

Martin, MS, Tang, B, Papale, LA, Yu, FH, Catterall, WA, and Escayg, A (2007). The voltage-gated sodium channel Scn8a is a genetic modifier of severe myoclonic epilepsy of infancy. Hum Mol Genet *16*, 2892-2899.

Martinez-Espinosa, PL, Wu, J, Yang, C, Gonzalez-Perez, V, Zhou, H, Liang, H*, et al.* (2015). Knockout of Slo2.2 enhances itch, abolishes KNa current, and increases action potential firing frequency in DRG neurons. Elife *4*.

Mattison, KA, Tossing, G, Mulroe, F, Simmons, C, Butler, KM, Schreiber, A*, et al.* (2023). ATP6V0C variants impair V-ATPase function causing a neurodevelopmental disorder often associated with epilepsy. Brain *146*, 1357-1372.

Maurice, N, Tkatch, T, Meisler, M, Sprunger, LK, and Surmeier, DJ (2001). D1/D5 dopamine receptor activation differentially modulates rapidly inactivating and persistent sodium currents in prefrontal cortex pyramidal neurons. J Neurosci *21*, 2268-2277.

McArdle, S, Buscher, K, Ehinger, E, Pramod, A, Riley, N, and Ley, K (2018). PRESTO, a new tool for integrating large-scale -omics data and discovering disease-specific signatures. bioRxiv.

McCampbell, A, Cole, T, Wegener, AJ, Tomassy, GS, Setnicka, A, Farley, BJ*, et al.* (2018). Antisense oligonucleotides extend survival and reverse decrement in muscle response in ALS models. J Clin Invest *128*, 3558-3567.

McGinnis, CS, Murrow, LM, and Gartner, ZJ (2019). DoubletFinder: Doublet Detection in Single-Cell RNA Sequencing Data Using Artificial Nearest Neighbors. Cell Syst *8*, 329-337 e324.

McKay, RA, Miraglia, LJ, Cummins, LL, Owens, SR, Sasmor, H, and Dean, NM (1999). Characterization of a potent and specific class of antisense oligonucleotide inhibitor of human protein kinase C-alpha expression. J Biol Chem *274*, 1715-1722.

McKinney, BC, Chow, CY, Meisler, MH, and Murphy, GG (2008). Exaggerated emotional behavior in mice heterozygous null for the sodium channel Scn8a (Nav1.6). Genes Brain Behav *7*, 629-638.

Meisler, MH, Helman, G, Hammer, MF, Fureman, BE, Gaillard, WD, Goldin, AL*, et al.* (2016). SCN8A encephalopathy: Research progress and prospects. Epilepsia *57*, 1027-1035.

Meisler, MH, Hill, SF, and Yu, W (2021). Sodium channelopathies in neurodevelopmental disorders. Nat Rev Neurosci *22*, 152-166.

Meisler, MH, Kearney, J, Escayg, A, MacDonald, BT, and Sprunger, LK (2001). Sodium channels and neurological disease: insights from Scn8a mutations in the mouse. Neuroscientist *7*, 136-145.

Meisler, MH, and Kearney, JA (2005). Sodium channel mutations in epilepsy and other neurological disorders. J Clin Invest *115*, 2010-2017.

Meisler, MH, O'Brien, JE, and Sharkey, LM (2010). Sodium channel gene family: epilepsy mutations, gene interactions and modifier effects. J Physiol *588*, 1841-1848.

Melland, H, Bumbak, F, Kolesnik-Taylor, A, Ng-Cordell, E, John, A, Constantinou, P*, et al.* (2022). Expanding the genotype and phenotype spectrum of SYT1-associated neurodevelopmental disorder. Genet Med *24*, 880-893.

Mercer, JN, Chan, CS, Tkatch, T, Held, J, and Surmeier, DJ (2007). Nav1.6 sodium channels are critical to pacemaking and fast spiking in globus pallidus neurons. J Neurosci *27*, 13552-13566.

Mi, H, Muruganujan, A, Ebert, D, Huang, X, and Thomas, PD (2019). PANTHER version 14: more genomes, a new PANTHER GO-slim and improvements in enrichment analysis tools. Nucleic Acids Res *47*, D419-D426.

Miceli, F, Soldovieri, MV, Weckhuysen, S, Cooper, E, and Taglialatela, M (1993). KCNQ2-Related Disorders. In GeneReviews((R)), M.P. Adam, G.M. Mirzaa, R.A. Pagon, S.E. Wallace, L.J.H. Bean, K.W. Gripp, and A. Amemiya, eds. (Seattle (WA)).

Mikati, MA, Jiang, YH, Carboni, M, Shashi, V, Petrovski, S, Spillmann, R*, et al.* (2015). Quinidine in the treatment of KCNT1-positive epilepsies. Ann Neurol *78*, 995-999.

Miller, AR, Hawkins, NA, McCollom, CE, and Kearney, JA (2014). Mapping genetic modifiers of survival in a mouse model of Dravet syndrome. Genes Brain Behav *13*, 163-172.

Milligan, CJ, Li, M, Gazina, EV, Heron, SE, Nair, U, Trager, C*, et al.* (2014). KCNT1 gain of function in 2 epilepsy phenotypes is reversed by quinidine. Ann Neurol *75*, 581-590.

Mishra, V, Karumuri, BK, Gautier, NM, Liu, R, Hutson, TN, Vanhoof-Villalba, SL*, et al.* (2017). Scn2a deletion improves survival and brain-heart dynamics in the Kcna1-null mouse model of sudden unexpected death in epilepsy (SUDEP). Hum Mol Genet *26*, 2091-2103.

Monia, BP, Lesnik, EA, Gonzalez, C, Lima, WF, McGee, D, Guinosso, CJ*, et al.* (1993). Evaluation of 2'-modified oligonucleotides containing 2'-deoxy gaps as antisense inhibitors of gene expression. J Biol Chem *268*, 14514-14522.

Montpied, P, de Bock, F, Lerner-Natoli, M, Bockaert, J, and Rondouin, G (1999). Hippocampal alterations of apolipoprotein E and D mRNA levels in vivo and in vitro following kainate excitotoxicity. Epilepsy Res *35*, 135-146.

Mori, K, Kobayashi, S, Saito, T, Masuda, Y, and Nakaya, H (1998). Inhibitory effects of class I and IV antiarrhythmic drugs on the Na+-activated K+ channel current in guinea pig ventricular cells. Naunyn Schmiedebergs Arch Pharmacol *358*, 641-648.

Moura, DMS, Brennan, EJ, Brock, R, and Cocas, LA (2021). Neuron to Oligodendrocyte Precursor Cell Synapses: Protagonists in Oligodendrocyte Development and Myelination, and Targets for Therapeutics. Front Neurosci *15*, 779125.

Mulligan, MK, Abreo, T, Neuner, SM, Parks, C, Watkins, CE, Houseal, MT*, et al.* (2019). Identification of a Functional Non-coding Variant in the GABA A Receptor alpha2 Subunit of the C57BL/6J Mouse Reference Genome: Major Implications for Neuroscience Research. Front Genet *10*, 188.

Nassar, MA, Baker, MD, Levato, A, Ingram, R, Mallucci, G, McMahon, SB*, et al.* (2006). Nerve injury induces robust allodynia and ectopic discharges in Nav1.3 null mutant mice. Mol Pain *2*, 33.

Numis, AL, Nair, U, Datta, AN, Sands, TT, Oldham, MS, Patel, A*, et al.* (2018). Lack of response to quinidine in KCNT1-related neonatal epilepsy. Epilepsia *59*, 1889-1898.

O'Brien, JE, Drews, VL, Jones, JM, Dugas, JC, Barres, BA, and Meisler, MH (2012a). Rbfox proteins regulate alternative splicing of neuronal sodium channel SCN8A. Mol Cell Neurosci *49*, 120-126.

O'Brien, JE, Sharkey, LM, Vallianatos, CN, Han, C, Blossom, JC, Yu, T*, et al.* (2012b). Interaction of voltage-gated sodium channel Nav1.6 (SCN8A) with microtubule-associated protein Map1b. J Biol Chem *287*, 18459-18466.

Ogiwara, I, Ito, K, Sawaishi, Y, Osaka, H, Mazaki, E, Inoue, I*, et al.* (2009). De novo mutations of voltage-gated sodium channel alphaII gene SCN2A in intractable epilepsies. Neurology *73*, 1046-1053.

Ong, WY, He, Y, Suresh, S, and Patel, SC (1997). Differential expression of apolipoprotein D and apolipoprotein E in the kainic acid-lesioned rat hippocampus. Neuroscience *79*, 359-367.

Osorio, N, Cathala, L, Meisler, MH, Crest, M, Magistretti, J, and Delmas, P (2010). Persistent Nav1.6 current at axon initial segments tunes spike timing of cerebellar granule cells. J Physiol *588*, 651-670.

Ottolini, M, Barker, BS, Gaykema, RP, Meisler, MH, and Patel, MK (2017). Aberrant Sodium Channel Currents and Hyperexcitability of Medial Entorhinal Cortex Neurons in a Mouse Model of SCN8A Encephalopathy. J Neurosci *37*, 7643-7655.

Pan, Y, and Cummins, TR (2020). Distinct functional alterations in SCN8A epilepsy mutant channels. J Physiol *598*, 381-401.

Papale, LA, Beyer, B, Jones, JM, Sharkey, LM, Tufik, S, Epstein, M*, et al.* (2009). Heterozygous mutations of the voltage-gated sodium channel SCN8A are associated with spike-wave discharges and absence epilepsy in mice. Hum Mol Genet *18*, 1633-1641.

Parent, JM, Elliott, RC, Pleasure, SJ, Barbaro, NM, and Lowenstein, DH (2006). Aberrant seizure-induced neurogenesis in experimental temporal lobe epilepsy. Ann Neurol *59*, 81-91.

Pfister, B, Mahalingam, R, Oldham, MS, Patel, D, Jacotin, H, Hard, M*, et al.* (2023). PRAX-562-101: A Phase 1 Trial Evaluating the Safety, Tolerability, Pharmacokinetics and Food Effect of PRAX-562 in Healthy Volunteers (P8-9.011). Neurology *17*.

Plummer, NW, Galt, J, Jones, JM, Burgess, DL, Sprunger, LK, Kohrman, DC*, et al.* (1998). Exon organization, coding sequence, physical mapping, and polymorphic intragenic markers for the human neuronal sodium channel gene SCN8A. Genomics *54*, 287-296.

Plummer, NW, McBurney, MW, and Meisler, MH (1997). Alternative splicing of the sodium channel SCN8A predicts a truncated two-domain protein in fetal brain and non-neuronal cells. J Biol Chem *272*, 24008-24015.

Plummer, NW, and Meisler, MH (1999). Evolution and diversity of mammalian sodium channel genes. Genomics *57*, 323-331.

Pong, AW, Ross, J, Tyrlikova, I, Giermek, AJ, Kohli, MP, Khan, YA*, et al.* (2022). Epilepsy: expert opinion on emerging drugs in phase 2/3 clinical trials. Expert Opin Emerg Drugs *27*, 75-90.

Qiu, Y, O'Neill, N, Maffei, B, Zourray, C, Almacellas-Barbanoj, A, Carpenter, JC*, et al.* (2022). On-demand cell-autonomous gene therapy for brain circuit disorders. Science *378*, 523-532.

Quraishi, IH, Mercier, MR, McClure, H, Couture, RL, Schwartz, ML, Lukowski, R*, et al.* (2020). Impaired motor skill learning and altered seizure susceptibility in mice with loss or gain of function of the Kcnt1 gene encoding Slack (KNa1.1) Na(+)-activated K(+) channels. Sci Rep *10*, 3213.

Quraishi, IH, Stern, S, Mangan, KP, Zhang, Y, Ali, SR, Mercier, MR*, et al.* (2019). An Epilepsy-Associated KCNT1 Mutation Enhances Excitability of Human iPSC-Derived Neurons by Increasing Slack KNa Currents. J Neurosci *39*, 7438-7449.

Raman, IM, Sprunger, LK, Meisler, MH, and Bean, BP (1997). Altered subthreshold sodium currents and disrupted firing patterns in Purkinje neurons of Scn8a mutant mice. Neuron *19*, 881-891.

Raper, SE, Chirmule, N, Lee, FS, Wivel, NA, Bagg, A, Gao, GP*, et al.* (2003). Fatal systemic inflammatory response syndrome in a ornithine transcarbamylase deficient patient following adenoviral gene transfer. Mol Genet Metab *80*, 148-158.

Rizzi, S, Knaus, HG, and Schwarzer, C (2016). Differential distribution of the sodium-activated potassium channels slick and slack in mouse brain. J Comp Neurol *524*, 2093-2116.

Roden, DM (2014). Pharmacology and Toxicology of Nav1.5-Class 1 anti-arrhythmic drugs. Card Electrophysiol Clin *6*, 695-704.

Roovers, J, De Jonghe, P, and Weckhuysen, S (2018). The therapeutic potential of RNA regulation in neurological disorders. Expert Opin Ther Targets *22*, 1017-1028.

Royeck, M, Horstmann, MT, Remy, S, Reitze, M, Yaari, Y, and Beck, H (2008). Role of axonal NaV1.6 sodium channels in action potential initiation of CA1 pyramidal neurons. J Neurophysiol *100*, 2361-2380.

Rush, AM, Dib-Hajj, SD, and Waxman, SG (2005). Electrophysiological properties of two axonal sodium channels, Nav1.2 and Nav1.6, expressed in mouse spinal sensory neurones. J Physiol *564*, 803-815.

Saenz-Farret, M, Tijssen, MAJ, Eliashiv, D, Fisher, RS, Sethi, K, and Fasano, A (2022). Antiseizure Drugs and Movement Disorders. CNS Drugs *36*, 859-876.

Sanders, SJ, Campbell, AJ, Cottrell, JR, Moller, RS, Wagner, FF, Auldridge, AL*, et al.* (2018). Progress in Understanding and Treating SCN2A-Mediated Disorders. Trends Neurosci *41*, 442-456.

Scharfman, HE, Goodman, JH, Sollas, AL, and Croll, SD (2002). Spontaneous limbic seizures after intrahippocampal infusion of brain-derived neurotrophic factor. Exp Neurol *174*, 201-214.

Scheffer, IE, Berkovic, S, Capovilla, G, Connolly, MB, French, J, Guilhoto, L*, et al.* (2017). ILAE classification of the epilepsies: Position paper of the ILAE Commission for Classification and Terminology. Epilepsia *58*, 512-521.

Scheffer, IE, and Nabbout, R (2019). SCN1A-related phenotypes: Epilepsy and beyond. Epilepsia *60 Suppl 3*, S17-S24.

Schmittgen, TD, and Livak, KJ (2008). Analyzing real-time PCR data by the comparative C(T) method. Nat Protoc *3*, 1101-1108.

Schwarz, N, Bast, T, Gaily, E, Golla, G, Gorman, KM, Griffiths, LR*, et al.* (2019). Clinical and genetic spectrum of SCN2A-associated episodic ataxia. Eur J Paediatr Neurol *23*, 438-447.

Shan, W, Nagai, T, Tanaka, M, Itoh, N, Furukawa-Hibi, Y, Nabeshima, T*, et al.* (2018). Neuronal PAS domain protein 4 (Npas4) controls neuronal homeostasis in pentylenetetrazole-induced epilepsy through the induction of Homer1a. J Neurochem *145*, 19-33.

Shao, N, Zhang, H, Wang, X, Zhang, W, Yu, M, and Meng, H (2018). Familial Hemiplegic Migraine Type 3 (FHM3) With an SCN1A Mutation in a Chinese Family: A Case Report. Front Neurol *9*, 976.

Shen, W, De Hoyos, CL, Migawa, MT, Vickers, TA, Sun, H, Low, A*, et al.* (2019). Chemical modification of PS-ASO therapeutics reduces cellular protein-binding and improves the therapeutic index. Nat Biotechnol *37*, 640-650.

Shore, AN, Colombo, S, Tobin, WF, Petri, S, Cullen, ER, Dominguez, S*, et al.* (2020). Reduced GABAergic Neuron Excitability, Altered Synaptic Connectivity, and Seizures in a KCNT1 Gain-of-Function Mouse Model of Childhood Epilepsy. Cell Rep *33*, 108303.

Smart, SL, Lopantsev, V, Zhang, CL, Robbins, CA, Wang, H, Chiu, SY*, et al.* (1998). Deletion of the KV1.1 Potassium Channel Causes Epilepsy in Mice. Neuron *20*, 809-819.

Smith, MR, Smith, RD, Plummer, NW, Meisler, MH, and Goldin, AL (1998). Functional analysis of the mouse Scn8a sodium channel. J Neurosci *18*, 6093-6102.

Smith, PEM (2021). Initial Management of Seizure in Adults. N Engl J Med *385*, 251-263.

Smith, RS, Kenny, CJ, Ganesh, V, Jang, A, Borges-Monroy, R, Partlow, JN*, et al.* (2018). Sodium Channel SCN3A (Na(V)1.3) Regulation of Human Cerebral Cortical Folding and Oral Motor Development. Neuron *99*, 905-913 e907.

Snowball, A, Chabrol, E, Wykes, RC, Shekh-Ahmad, T, Cornford, JH, Lieb, A*, et al.* (2019). Epilepsy Gene Therapy Using an Engineered Potassium Channel. J Neurosci *39*, 3159-3169.

Soh, H, Pant, R, LoTurco, JJ, and Tzingounis, AV (2014). Conditional deletions of epilepsy-associated KCNQ2 and KCNQ3 channels from cerebral cortex cause differential effects on neuronal excitability. J Neurosci *34*, 5311-5321.

Sole, L, Wagnon, JL, Akin, EJ, Meisler, MH, and Tamkun, MM (2019). The MAP1B Binding Domain of Nav1.6 Is Required for Stable Expression at the Axon Initial Segment. J Neurosci *39*, 4238-4251.

Southwell, AL, Kordasiewicz, HB, Langbehn, D, Skotte, NH, Parsons, MP, Villanueva, EB*, et al.* (2018). Huntingtin suppression restores cognitive function in a mouse model of Huntington's disease. Sci Transl Med *10*.

Spitzer, SO, Sitnikov, S, Kamen, Y, Evans, KA, Kronenberg-Versteeg, D, Dietmann, S*, et al.* (2019). Oligodendrocyte Progenitor Cells Become Regionally Diverse and Heterogeneous with Age. Neuron *101*, 459-471 e455.

Sprissler, RS, Wagnon, JL, Bunton-Stasyshyn, RK, Meisler, MH, and Hammer, MF (2017). Altered gene expression profile in a mouse model of SCN8A encephalopathy. Exp Neurol *288*, 134-141.

Sprunger, LK, Escayg, A, Tallaksen-Greene, S, Albin, RL, and Meisler, MH (1999). Dystonia associated with mutation of the neuronal sodium channel Scn8a and identification of the modifier locus Scnm1 on mouse chromosome 3. Hum Mol Genet *8*, 471-479.

Stafstrom, CE (2007). Persistent sodium current and its role in epilepsy. Epilepsy Curr *7*, 15-22.

Stoker, TB, Andresen, KER, and Barker, RA (2021). Hydrocephalus Complicating Intrathecal Antisense Oligonucleotide Therapy for Huntington's Disease. Mov Disord *36*, 263-264.

Sung, HY, Chen, WY, Huang, HT, Wang, CY, Chang, SB, and Tzeng, SF (2019). Down-regulation of interleukin-33 expression in oligodendrocyte precursor cells impairs oligodendrocyte lineage progression. J Neurochem *150*, 691-708.

Swayze, EE, Siwkowski, AM, Wancewicz, EV, Migawa, MT, Wyrzykiewicz, TK, Hung, G*, et al.* (2007). Antisense oligonucleotides containing locked nucleic acid improve potency but cause significant hepatotoxicity in animals. Nucleic Acids Res *35*, 687-700.

Symonds, JD, Zuberi, SM, Stewart, K, McLellan, A, O'Regan, M, MacLeod, S*, et al.* (2019). Incidence and phenotypes of childhood-onset genetic epilepsies: a prospective population-based national cohort. Brain *142*, 2303-2318.

Szaflarski, JP, Nazzal, Y, and Dreer, LE (2014). Post-traumatic epilepsy: current and emerging treatment options. Neuropsychiatr Dis Treat *10*, 1469-1477.

Tian, C, Wang, K, Ke, W, Guo, H, and Shu, Y (2014). Molecular identity of axonal sodium channels in human cortical pyramidal cells. Front Cell Neurosci *8*, 297.

Tidball, AM, Lopez-Santiago, LF, Yuan, Y, Glenn, TW, Margolis, JL, Clayton Walker, J*, et al.* (2020). Variant-specific changes in persistent or resurgent sodium current in SCN8A-related epilepsy patient-derived neurons. Brain *143*, 3025-3040.

Trudeau, MM, Dalton, JC, Day, JW, Ranum, LP, and Meisler, MH (2006). Heterozygosity for a protein truncation mutation of sodium channel SCN8A in a patient with cerebellar atrophy, ataxia, and mental retardation. J Med Genet *43*, 527-530.

Uddin, F, Rudin, CM, and Sen, T (2020). CRISPR Gene Therapy: Applications, Limitations, and Implications for the Future. Front Oncol *10*, 1387.

Uribe-San-Martin, R, Ciampi, E, Santibanez, R, Irani, SR, Marquez, A, Cruz, JP*, et al.* (2020). LGI1-antibody associated epilepsy successfully treated in the outpatient setting. J Neuroimmunol *345*, 577268.

Valassina, N, Brusco, S, Salamone, A, Serra, L, Luoni, M, Giannelli, S*, et al.* (2022). Scn1a gene reactivation after symptom onset rescues pathological phenotypes in a mouse model of Dravet syndrome. Nat Commun *13*, 161.

Van Wart, A, and Matthews, G (2006). Impaired firing and cell-specific compensation in neurons lacking Na(v)1.6 sodium channels. J Neurosci *26*, 7172-7180.

Van Wart, A, Trimmer, JS, and Matthews, G (2007). Polarized distribution of ion channels within microdomains of the axon initial segment. J Comp Neurol *500*, 339-352.

Veeramah, KR, O'Brien, JE, Meisler, MH, Cheng, XY, Dib-Hajj, SD, Waxman, SG*, et al.* (2012). De Novo Pathogenic SCN8A Mutation Identified by Whole-Genome Sequencing of a Family Quartet Affected by Infantile Epileptic Encephalopathy and SUDEP. Am J Hum Genet *90*, 502-510.

Viscidi, E, Wang, N, Juneja, M, Bhan, I, Prada, C, James, D*, et al.* (2021). The incidence of hydrocephalus among patients with and without spinal muscular atrophy (SMA): Results from a US electronic health records study. Orphanet J Rare Dis *16*, 207.

Vlaskamp, DRM, Callenbach, PMC, Rump, P, Giannini, LAA, Dijkhuizen, T, Brouwer, OF*, et al.* (2017). Copy number variation in a hospital-based cohort of children with epilepsy. Epilepsia Open *2*, 244-254.

von Bohlen Und Halbach, O (2007). Immunohistological markers for staging neurogenesis in adult hippocampus. Cell Tissue Res *329*, 409-420.

Wagnon, JL, Barker, BS, Hounshell, JA, Haaxma, CA, Shealy, A, Moss, T*, et al.* (2015a). Pathogenic mechanism of recurrent mutations of SCN8A in epileptic encephalopathy. Ann Clin Transl Neurol *3*, 114-123.

Wagnon, JL, Barker, BS, Ottolini, M, Park, Y, Volkheimer, A, Valdez, P*, et al.* (2017). Loss-of-function variants of SCN8A in intellectual disability without seizures. Neurol Genet *3*, e170.

Wagnon, JL, Korn, MJ, Parent, R, Tarpey, TA, Jones, JM, Hammer, MF*, et al.* (2015b). Convulsive seizures and SUDEP in a mouse model of SCN8A epileptic encephalopathy. Hum Mol Genet *24*, 506-515.

Wagnon, JL, and Meisler, MH (2015). Recurrent and Non-Recurrent Mutations of SCN8A in Epileptic Encephalopathy. Front Neurol *6*, 104.

Wagnon, JL, Mencacci, NE, Barker, BS, Wengert, ER, Bhatia, KP, Balint, B*, et al.* (2018). Partial loss-of-function of sodium channel SCN8A in familial isolated myoclonus. Hum Mutat *39*, 965-969.

Weckhuysen, S, Mandelstam, S, Suls, A, Audenaert, D, Deconinck, T, Claes, LR*, et al.* (2012). KCNQ2 encephalopathy: emerging phenotype of a neonatal epileptic encephalopathy. Ann Neurol *71*, 15-25.

Wengert, ER, Miralles, RM, Wedgwood, KCA, Wagley, PK, Strohm, SM, Panchal, PS*, et al.* (2021). Somatostatin-Positive Interneurons Contribute to Seizures in SCN8A Epileptic Encephalopathy. J Neurosci *41*, 9257-9273.

Wengert, ER, and Patel, MK (2021). The Role of the Persistent Sodium Current in Epilepsy. Epilepsy Curr *21*, 40-47.

Wengert, ER, Saga, AU, Panchal, PS, Barker, BS, and Patel, MK (2019a). Prax330 reduces persistent and resurgent sodium channel currents and neuronal hyperexcitability of subiculum neurons in a mouse model of SCN8A epileptic encephalopathy. Neuropharmacology *158*, 107699.

Wengert, ER, Tronhjem, CE, Wagnon, JL, Johannesen, KM, Petit, H, Krey, I*, et al.* (2019b). Biallelic inherited SCN8A variants, a rare cause of SCN8A-related developmental and epileptic encephalopathy. Epilepsia *60*, 2277-2285.

Westenbroek, RE, Merrick, DK, and Catterall, WA (1989). Differential subcellular localization of the RI and RII Na+ channel subtypes in central neurons. Neuron *3*, 695-704.

Whitaker, WR, Faull, RL, Waldvogel, HJ, Plumpton, CJ, Emson, PC, and Clare, JJ (2001). Comparative distribution of voltage-gated sodium channel proteins in human brain. Brain Res Mol Brain Res *88*, 37-53.

Wolff, M, Brunklaus, A, and Zuberi, SM (2019). Phenotypic spectrum and genetics of SCN2A-related disorders, treatment options, and outcomes in epilepsy and beyond. Epilepsia *60 Suppl 3*, S59-S67.

Wolff, M, Johannesen, KM, Hedrich, UBS, Masnada, S, Rubboli, G, Gardella, E*, et al.* (2017). Genetic and phenotypic heterogeneity suggest therapeutic implications in SCN2A-related disorders. Brain *140*, 1316-1336.

Wong, JC, Grieco, SF, Dutt, K, Chen, L, Thelin, JT, Inglis, GAS*, et al.* (2021). Autistic-like behavior, spontaneous seizures, and increased neuronal excitability in a Scn8a mouse model. Neuropsychopharmacology *46*, 2011-2020.

Wong, JC, Makinson, CD, Lamar, T, Cheng, Q, Wingard, JC, Terwilliger, EF*, et al.* (2018). Selective targeting of Scn8a prevents seizure development in a mouse model of mesial temporal lobe epilepsy. Sci Rep *8*, 126.

Woodruff-Pak, DS, Green, JT, Levin, SI, and Meisler, MH (2006). Inactivation of Sodium Channel *Scn8a* (Nav1.6) in Purkinje Neurons Impairs Learning in Morris Water Maze and Delay but Not Trace Eyeblink Classical Conditioning. Behavioral Neuroscience *120*, 229-240.

Wu, J, Quraishi, IH, Zhang, Y, Bromwich, M, and Kaczmarek, LK (2023). Disease-causing Slack potassium channel mutations produce opposite effects on excitability of excitatory and inhibitory neurons. bioRxiv.

Wu, YW, Sullivan, J, McDaniel, SS, Meisler, MH, Walsh, EM, Li, SX*, et al.* (2015). Incidence of Dravet Syndrome in a US Population. Pediatrics *136*, e1310-1315.

Xu, L, Ding, X, Wang, T, Mou, S, Sun, H, and Hou, T (2019). Voltage-gated sodium channels: structures, functions, and molecular modeling. Drug Discov Today *24*, 1389-1397.

Yamagata, A, Miyazaki, Y, Yokoi, N, Shigematsu, H, Sato, Y, Goto-Ito, S*, et al.* (2018). Structural basis of epilepsy-related ligand-receptor complex LGI1-ADAM22. Nat Commun *9*, 1546.

Yamagata, T, Ogiwara, I, Tatsukawa, T, Suzuki, T, Otsuka, Y, Imaeda, N*, et al.* (2023). Scn1a-GFP transgenic mouse revealed Nav1.1 expression in neocortical pyramidal tract projection neurons. Elife *12*.

Yamagata, T, Raveau, M, Kobayashi, K, Miyamoto, H, Tatsukawa, T, Ogiwara, I*, et al.* (2020). CRISPR/dCas9-based Scn1a gene activation in inhibitory neurons ameliorates epileptic and behavioral phenotypes of Dravet syndrome model mice. Neurobiol Dis *141*, 104954.

Yang, C, Yang, Y, Peng, Y, Zhang, L, and Yu, D (2022a). Efficacy and safety of lacosamide in pediatric patients with epilepsy: A systematic review and meta-analysis. Epilepsy Behav *134*, 108781.

Yang, X, Yin, H, Wang, X, Sun, Y, Bian, X, Zhang, G*, et al.* (2022b). Social Deficits and Cerebellar Degeneration in Purkinje Cell Scn8a Knockout Mice. Front Mol Neurosci *15*, 822129.

Yu, FH, Mantegazza, M, Westenbroek, RE, Robbins, CA, Kalume, F, Burton, KA*, et al.* (2006). Reduced sodium current in GABAergic interneurons in a mouse model of severe myoclonic epilepsy in infancy. Nat Neurosci *9*, 1142-1149.

Yu, W, Hill, SF, Xenakis, JG, Pardo-Manuel de Villena, F, Wagnon, JL, and Meisler, M (2020). *Gabra2* is a genetic modifier of *Scn8a* encephalopathy in the mouse. ???

Yu, W, Mulligan, MK, Williams, RW, and Meisler, MH (2022). Correction of the hypomorphic Gabra2 splice site variant in mouse strain C57BL/6J modifies the severity of Scn8a encephalopathy. HGG Adv *3*, 100064.

Zakon, HH (2012). Adaptive evolution of voltage-gated sodium channels: the first 800 million years. Proc Natl Acad Sci U S A *109 Suppl 1*, 10619-10625.

Zaman, T, Helbig, I, Bozovic, IB, DeBrosse, SD, Bergqvist, AC, Wallis, K*, et al.* (2018). Mutations in SCN3A cause early infantile epileptic encephalopathy. Ann Neurol *83*, 703-717.

Zaman, T, Helbig, KL, Clatot, J, Thompson, CH, Kang, SK, Stouffs, K*, et al.* (2020). SCN3A-Related Neurodevelopmental Disorder: A Spectrum of Epilepsy and Brain Malformation. Ann Neurol.

Zhang, Y, Tachtsidis, G, Schob, C, Koko, M, Hedrich, UBS, Lerche, H*, et al.* (2021). KCND2 variants associated with global developmental delay differentially impair Kv4.2 channel gating. Hum Mol Genet *30*, 2300-2314.

Zubovic, L, Baralle, M, and Baralle, FE (2012). Mutually exclusive splicing regulates the Nav 1.6 sodium channel function through a combinatorial mechanism that involves three distinct splicing regulatory elements and their ligands. Nucleic Acids Res *40*, 6255-6269.